Swarm Intelligence based Maximum Power Point Tracking Control Technique for Photovoltaic System under Non-Uniform Environmental Conditions

by

Muhammad Hamza Zafar

A thesis submitted in partial fulfillment for the
degree of Master of Science

in the

Faculty of Engineering

Department of Electrical Engineering

2022

I dedicate this work to my dearest parents and my wife

CERTIFICATE OF APPROVAL

Swarm Intelligence based Maximum Power Point Tracking Control Technique for Photovoltaic System under Non-Uniform Environmental Conditions

by

Muhammad Hamza Zafar

(MEE193005)

THESIS EXAMINING COMMITTEE

S. No.	Examiner	Name	Organization
(a)	External Examiner	Dr. Syed Ali Abbas Kazmi	NUST, Islamabad
(b)	Internal Examiner	Dr. Muhammad Ashraf	CUST, Islamabad
(c)	Supervisor	Dr. Umer Amir Khan	CUST, Islamabad

Dr. Umer Amir Khan
Thesis Supervisor
February 2022

Dr. Noor Muhammad Khan
Head
Dept. of Electrical Engineering
February 2022

Dr. Imtiaz Ahmad Taj
Dean
Faculty of Engineering
February 2022

Author's Declaration

I, **Muhammad Hamza Zafar** hereby state that my MS thesis titled "**Swarm Intelligence based Maximum Power Point Tracking Control Technique for Photovoltaic System under Non-Uniform Environmental Conditions**" is my own work and has not been submitted previously by me for taking any degree from Capital University of Science and Technology, Islamabad or anywhere else in the country/abroad.

At any time if my statement is found to be incorrect even after my graduation, the University has the right to withdraw my MS Degree.

(Muhammad Hamza Zafar)

Registration No: MEE193005

Plagiarism Undertaking

I solemnly declare that research work presented in this thesis titled "**Swarm Intelligence based Maximum Power Point Tracking Control Technique for Photovoltaic System under Non-Uniform Environmental Conditions**" is solely my research work with no significant contribution from any other person. Small contribution/help wherever taken has been dully acknowledged and that complete thesis has been written by me.

I understand the zero tolerance policy of the HEC and Capital University of Science and Technology towards plagiarism. Therefore, I as an author of the above titled thesis declare that no portion of my thesis has been plagiarized and any material used as reference is properly referred/cited.

I undertake that if I am found guilty of any formal plagiarism in the above titled thesis even after award of MS Degree, the University reserves the right to withdraw/revoke my MS degree and that HEC and the University have the right to publish my name on the HEC/University website on which names of students are placed who submitted plagiarized work.

(Muhammad Hamza Zafar)

Registration No: MEE193005

List of Publications

It is certified that following publication(s) have been made out of the research work that has been carried out for this thesis:-

1. **M. H. Zafar**, U. A. Khan, and N. M. Khan, "Hybrid Grey Wolf Optimizer Sine Cosine Algorithm based Maximum Power Point Tracking Control of PV Systems under Uniform Irradiance and Partial Shading Condition," *2021 4th International Conference on Energy Conservation and Efficiency (ICECE)*, 2021.

2. **M. H. Zafar**, U. A. Khan, and N. M. Khan, "A sparrow search optimization algorithm based MPPT control of PV system to harvest energy under uniform and non-uniform irradiance," *2021 International Conference on Emerging Power Technologies (ICEPT)*, 2021.

3. **M. H. Zafar**, U. A. Khan, and N. M. Khan, "Short Term Hybrid PV/Wind Power Forecasting for Smart Grid Application using Feedforward Neural Network (FNN) Trained by a Novel Atomic Orbital Search (AOS) Optimization Algorithm," *2021 6th International Conference on Frontiers of Information Technology (FIT)*, 2021.

(Muhammad Hamza Zafar)

Registration No: MEE193005

Acknowledgement

After being utmost grateful to **Almighty Allah** who gave me help and courage to complete my M.S research work, I would like to express huge gratitude towards the person who is not only my supervisor but also my mentor **Dr. Umer Amir Khan** whose constant support, guidance and true motivation kept me steering in the right direction during my entire research work to get through this demanding and tiresome task.

I pay my deep regards to my friend **Noman Mujeeb Khan** who has helped me a lot in the final formatting of my work.

I would like to show my deepest gratitude and respect to my family, my brother and especially my parents, the ones to whom I owe all the success in my life. No words can express my gratitude to them, but I pray Almighty Allah to bless them and reward them.

A final word to my wife; without you I could have never been able to achieve this work. Your patience and encouragement were always a source of strength for me. You are the shining moon that lightens my life.

(Muhammad Hamza Zafar)

Abstract

The diminishing of conventional energy sources such as fuel, oil, and coal has shifted researchers' focus towards more cost-effective and sustainable energy sources. The conventional energy sources leave the Carbon footprint and Sulphur contents in the atmosphere, which are not only harmful to the environment but also to human health. These issues can be well tackled by the use of renewable energy sources by producing cleaner energy. One of the cleanest sources of energy is solar energy. Solar energy in the form of Photovoltaics offers a wide array of benefits such as having low maintenance cost, no carbon footprint, and being abundant in nature. As compared to wind, geothermal and tidal energy it is free of geological constraints.

Over the last several decades, solar energy has emerged as the most preferable source of renewable energy. Photovoltaic (PV) panels are used to convert solar energy into electricity. PV systems output depends upon the ambient conditions such as temperature and irradiance. Drastically changing weather conditions can affect the PV output. PV system contain multiple PV panels in series and parallel combination to meet the energy demand. Under uniform irradiance on all the panels, PV system have only one global maximum power point (GMPP). However, under non-uniform irradiance level, that is partial shading condition (PSC), multiple local maximum power points (LMPPs) but exist only exists one GMPP. Therefore, the tracking of GMPP is called the maxim power point tracking (MPPT).

The conventional gradient-based MPPT techniques that are, Perturb and observe, incremental conductance performs well under uniform irradiance but falls into the local maxima trap. The meta heuristic optimization algorithm-based MPPT control techniques are presented in the literature. Oscillation at global maxima, high tracking time, less efficiency, low tracked power, and high settling time are the main drawbacks observed in the MPPT techniques. Therefore efficient MPPT technique for PV system is need to present for extraction of maximum power under non-uniform operating conditions.

In this work, a novel hybrid grey wolf optimizer sine-cosine algorithm (HGWOSCA) based MPPT control technique is presented. The proposed technique is compared with grasshopper optimization (GHO), cuckoo search (CS), particle swarm optimization (PSO), particle swarm optimization with gravitational search (PSOGS) and perturb and observe (P&O). Less tracking and settling time, zero oscillations at GMPP, and efficiency enhancement are the improvements observed in the proposed technique.

The proposed technique shows an efficiency that is greater than 99.95% with less than 0.5W oscillation at GMPP and 10% to 40% less tracking time. This technique has also been implemented on a low-cost microcontroller and has been tested on MPPT technique on a PV emulator hardware implementation, which validates the superior performance of the proposed MPPT technique.

Keywords: Photovoltaic (PV), Partial Shading Condition (PSC), Meta Heuristic Algorithms, Hybrid Grey Wolf Optimizer Sine Cosine Algorithm (HGWSOCA), Sparrow Search Optimization (SCA), Statistical Analysis.

Contents

List of Figures

List of Tables

Abbreviations

ABC	Artificial Bee Colony
ACO	Ant Colony Optimization
ANN	Artifical Neural Network
ARV	Adaptive Reference Voltage
CSA	Cuckoo Search Algorithm
FLC	Fuzzy Logic Controller
FOCV	Fractional Open Circuit Voltage
FSCC	Fractional Short Circuit Current
GA	Genetic Algorithm
GHO	Grasshopper Optimization
GMPP	Global Maximum Power Point
GWO	Grey Wolf Optimizer
INC	Incremental Conductance
LMPP	Local Maximum Power Point
MPPT	Maximum Power Point Tracking
PID	Portional Integral Derivative
PSO	Particle Swarm Optimization
PV	Photovoltaic
P&O	Perturb and Observe
SCA	Sine-Cosine Algorithm
SI	Swarm Intelligence
SMC	Sliding Mode Controller
SR	Success Rate

Symbols

α Ideality factor

$\mathbf{d}_i$ Duty cycle

$\mathbf{f}_{sw}$ Switching frequency

$\mathbf{G}_i$ Global best at iteration i

$\mathbf{I}$ Current at output of dc-dc converter

$\mathbf{I}_d$ Current rhough diode

$\mathbf{I}_{mpp}$ Current at maximum power

$\mathbf{I}_o$ Saturtion current in reverse

$\mathbf{I}_{PV}$ Output current of PV cell

$\mathbf{K}$ Boltzmann constant

$\mathbf{N}_P$ Parallel connected PV cells

$\mathbf{N}_S$ Series connected PV cells

$\mathbf{P}_i$ Personal best at iteration i

$\mathbf{P}_{mpp}$ Maximum Power of PV panel

$\mathbf{P}_{PV}$ PV Voltage

$\mathbf{P\&O}$ Perturb and Observe

$\mathbf{q}$ Electron charge

$\mathbf{R}_P$ Resistance in parallel of current source

$\mathbf{R}_S$ Resistance in series of current source

$\mathbf{t}_{sw}$ Switching time period

$\mathbf{X}_i$ Current position of the particle

$\mathbf{V}_{mpp}$ Voltage at maximum power

$\mathbf{V}_T$ PV cell thermal voltage

Chapter 1

Introduction

1.1 Introduction

Energy is the foremost vital acme of human civilization. It plays a principal part in every single activity of living beings. Within the present day period, the economy, agribusiness, transportation, communication, and security are all driven by energy [19]. The fast increment within the human populace and industrialization exponentially expanded the request for energy. This never-ending request has tipped off the adjustment between conventional energy sources like unrefined oil, gas, and coal due to the extreme exhaustion of fossil fuels [20].

The demonstrated hydrocarbon saves should not final the conclusion of this century. This puts energy security at hazard. The created nations have the most elevated per capita utility of energy. Developing energy demands may be a huge indicator of financial advancement and maintainable development in GDP. To meet the request for energy, increasingly hydrocarbons are being burnt. This burning of fuel in commercial control plants, transportation, and houses causes the emanation of nursery gasses. The exhaustion of ozone and the rising global temperature as of now has activated worldwide global warming. The part of renewable energy assets and the optimized utilization of existing assets could be an essential center of the scientific community. The primary objective of renewable energy assets is to make them financially viable. It incorporates the development of unused and

cheap energy assets conjointly expanding the efficiencies of existing innovations to compete with existing non-renewable energy assets.

The utilization of fossil fuels is an unavoidable issue. Large share of energy is being supplied by burning nonrenewable fossil fuels. It has activated a severe impact on the natural balance and could be a major cause of worldwide global warming. An increment in yearly worldwide temperature, and diseases caused by carcinogenic contaminations forces nations to work under the standards of the UN. The measures are being taken to utilize renewable energy sources in all areas of life. The landmark declarations were undertaken in United Nations Framework Convention on Climate Change (UNFCCC) to combat climate change in the "21st Climate Conference" in Paris during the year 2015 [21]. The climate summit in 2019 laid its targets to effectively lock in goals in the Carbon emissions future.

We have been utilizing sun-oriented energy since old times. The beginning of all the energy on the confront of the Soil is atomic fusion happening on the sun. From the ripening of crops, solar drying of food, and modern era PVs, Solar oriented energy plays a significant role. PV panels collect and convert Solar into electrical energy utilizing several key innovative technologies. Its utilization is predominantly in the fields i.e. Electrical Power generation by photovoltaic, heating systems, and concentrated solar power plants. The Photo-electric principle is utilized in PV cells. The heating is achieved by radiation-absorbing materials that hold heat and exchange it to use indoors. Concentrated solar is the modern expansion at utility-scale generation with thermoelectric generators for waste heat recovery.

1.2 PV Cell Technologies

Multiple techniques and methodologies are used to manufacture PV panels. PV cells are building blocks of PV systems. The cell's efficiency is highly dependent upon manufacturing technology. PV fabrication is a sophisticated and complex technology. The efficiency depends upon the materials and their purity. The foundries use materials such as mono-crystalline, poly-crystalline, and amorphous

silicon. The low cost and high power PV cells are the focus of academic research which is going on.
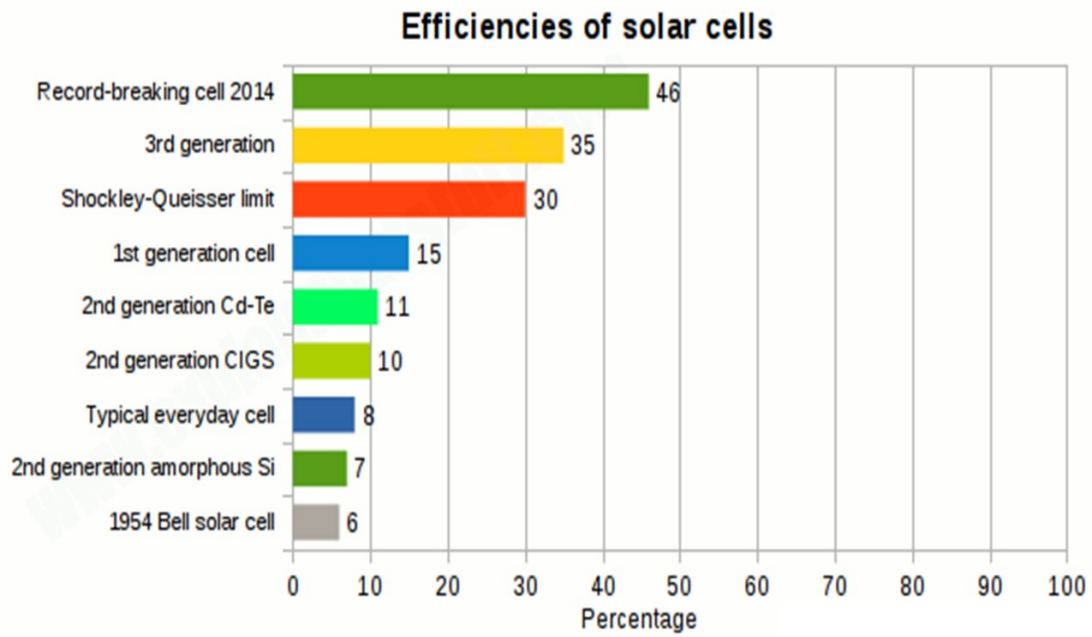
FIGURE 1.1: Comparison of the efficiencies of different photovoltaic technologies in the market [1]

These PV cells have efficiencies of 27.62%, 21.35%, and 13.61% respectively. The highest efficiency in the lab for thin-film technology. For CIGS and CdTe is 23.4% and 21.0% respectively [22]. The new high concentration multi-junction solar cells achieve 47.1% efficiency. The concentrated solar technology can achieve 38.9% efficiency. Multiple layer cells and multi-junction cells exhibit up to 43% efficiency [23]. Multi-junction cells are costly to produce. Germanium is used for manufacturing which is a rare element. So there is a tradeoff between cost, efficiency, and power. The largest producers of PV cells are China, Japan, South Korea, Malaysia, Germany, India, and the USA. Figure 1.1 gives a comparison of PV cell efficiencies for different technologies. This comparison shows how the efficiencies of different solar cells varies over the year. The record breaking cell was developed in 2014 with 46 percent efficiency. The goal is to develop the solar cells which converts the solar energy into electrical energy with high efficiency. This is really the challenge for the material scientists to develop these solar cells. So there is a tradeoff between cost, efficiency, and power. The largest producers of PV cells are China, Japan, South Korea, Malaysia, Germany, India, and the USA.

1.3 Photovoltaic System

The energy production capability of the PV system is dependent upon the solar energy received by that system. Therefore, any kind of shading will reduce energy production. PV systems can experience shading due to nearby buildings, trees, cloudy weather, and dust upon them or mountains if panels are installed in the fields with mountains nearby. In any case, shading will impact the efficiency of the solar systems. Since solar panels are connected in series, any shading on any panel will force the PV panels, including the shaded ones, to carry the same current [24]. Consequently, the shaded panels might get reversed biased and may act as a source and will draw power which will rapidly minimize the yield of the PV systems and because of the nonlinear property of PV systems, the P-V & I-V characteristic curves of PV system shows nonlinear behavior. These I-V & P-V curves can be generated by varying resistance from zero to infinity. These curves contain multiple peaks with one global maximum peak.
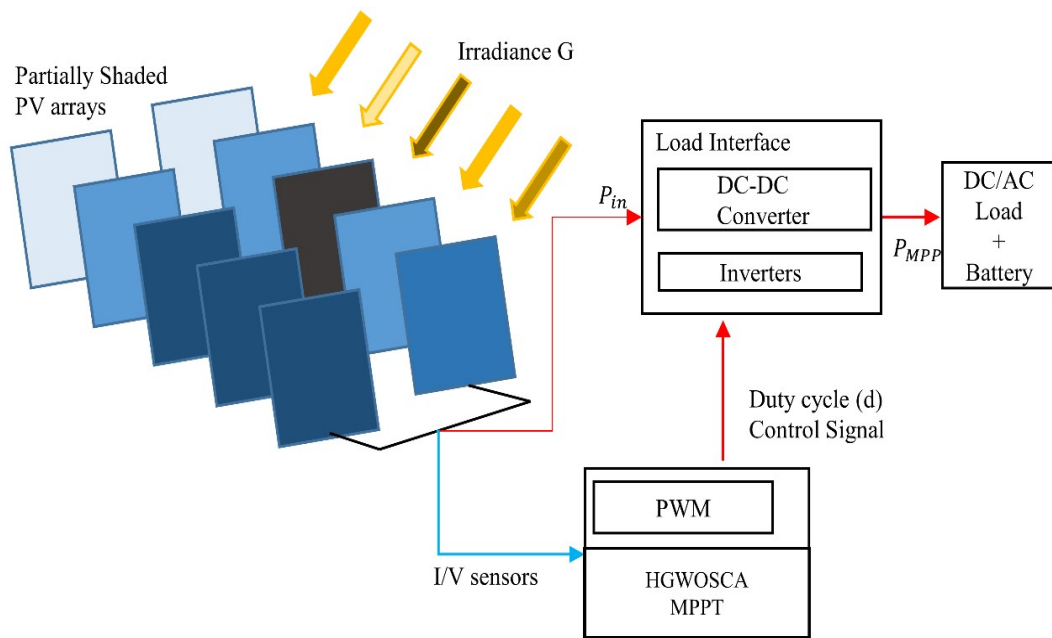
FIGURE 1.2: Components of the photovoltaic system contains PV arrays, converter, control technique, and load [2]

PV system comprises PV arrays, DC converter, control, and sensor peripherals as shown in Figure 1.2. The controlled output of the PV system is adjusted using current and voltage feedback through sensors. Here MPPT controls the Boost

converter switching using duty cycle as control variable generated by MPPT technique. Moreover, a driver circuit is connected to a DC converter whose functionality is to compensate for the low power of the microcontroller. To guarantee smooth enactment of the PV system, MPPT control action needs to be updated continuously.

There exists a single operating point under certain ambient conditions. That operating point is known as a maximum power point (MPP) which has a certain value of current and voltage. This MPP is the point at which the solar panel operates thus proving the max net power, which brings into account the MPPT whose aim is towards the harnessing of maximum power. The utilization of MPPT control in a PV system is an important and efficient method to obtain maximum output power. PV system presented in Figure 1.2 is usually used to perform MPPT techniques.

1.4 Conventional Maximum Power Point Tracking Techniques

In literature, numerous MPPT techniques have been introduced and every technique have its own merits and demerits. Some well-known conventional MPPT techniques include Fractional Short Circuit Current (FSCC), perturb and observe (P&O) besides with modified P&O, hill climbing (HC), incremental conductance (IC), modified incremental conductance, and Fractional Open Circuit Voltage (FOCV) [25]. These techniques are effective and have efficiency under uniform irradiance but fails under non-uniform irradiance. The major drawbacks of the conventional MPPT techniques are that they have continuous oscillations and they lose their tracking direction under variable temperature and climate. Moreover, these methods might not differentiate between global maxima (GM) and local maxima (LM). To minimize the said oscillations, steps size needs to be varied, however little change in the step size slows down the convergence and increases

the tracking time. This trade-off between convergence and tracking time gives these algorithms a bad reputation when it comes to partial shading (PS) [26]. Under PS, the output is power severely reduced causing major power loss to the load.

1.5 Machine Learning based Techniques

With a rise in artificial intelligence (AI), a few AI-based MPPT techniques are surfacing such as artificial neural networks (ANNs), fuzzy logic (FL), and Neuro-Fuzzy Hybrid-ANN [27]. AI offers some appropriate solutions to the problems caused by rapidly changing ambient conditions and climate. Even though these algorithms are extremely smart and provide very high efficiency in their performance, they require a huge amount of data to extensively train them which gives rise to the cost and computational complexity, and time [28].

1.6 Soft Computing based Techniques

In order to overcome the problems mentioned previously, a meta-heuristic approach has been adopted [29] i.e. soft computing methods known as bio-inspired algorithms such as particle swarm optimization (PSO), PSO-gravity search (PSOGS), Ant colony optimization (ACO), cuckoo search (CS), Moth flame optimization (MFO), grey wolf optimization (GWO), genetic algorithm (GA), dragonfly optimization (DFO), Gross Hopper Optimization (GHO) and Pattern Search (PS) have been proven to be much effective to optimize power. The performance of these algorithms again depends upon several elements such as computation time, number of iterations, population size, etc. PSO is an algorithm that provides the solution to the problem where a point in n-dimensional space may offer a better solution [30]. This algorithm utilizes several agents, where each agent is responsible for exchanging information that is obtained in a respective process. Here, each agent is referred to as a particle whose task is to follow another particle that

is performing best as well as traverse ahead to those conditions that are found by the particle itself. This causes each particle to evolve to an optimal solution. However, there is a high probability that PSO particles traverse the same scope that was searched by the previous particles.

In CS, random values are allocated to Levy flight which causes undesired fluctuations in the control signal [30]. Now, the problem is, the small size of the searching population can enhance this defect. The computational power and convergence time at GM will be severely impacted if a sizeable figure of population particles is resorted to. Similarly, other algorithms provide a solution to the problem of contingent oscillations around GM. The grasshopper optimization (GHO) effectively tracks GM but there are oscillations due to small decrement in parameter 'c'. Therefore it causes the power to settle at GM slowly.

Most of the bio-inspired techniques workaround to overcome the problems caused by PS, and they do locate MPP in uniform or non-uniform cases. However, they come across some definite issues with respect to PV applications [31]. One of the problems they encounter is time-varying GM positions on the P-V curves. The problem is that most of the time they track the first GM and are stuck there. Another problem faced by these algorithms is that since quite a number of variables are used in these soft computing techniques, they give rise to random power oscillations in the steady state. Few bio-inspired MPPT techniques fail to follow the GM under complex PS and get stuck at LM. This paper will try to solve these problems using smart and robust techniques.

1.7 Thesis Contribution

Observing all these mentioned shortfalls of existing bio-inspired techniques, a new meta-heuristic technique HGWOSCA is implemented for tracking MPP in PV systems. This algorithm utilizes the best features and characteristics of GWO and SCA. Characteristics of HGWSCA are mentioned as follows:

- Implementation of Novel Hybrid Grey Wolf Optimizer Sine Cosine Algorithm (HGWOSCA) based Maximum Power Point Tracking (MPPT) Technique.

- Testing under varying irradiance, Partial Shading Condition (PSC), and especially in complex-PSC (CPSC).

- Achieves up to 99.9% power tracking efficiency with less than 200 ms tracking time and less than 300 ms settling time.

- Extracts 10% more energy as compared to competing techniques

1.8   Thesis Overview

Chapter 1 presents the need for renewable energy, the benefits of PV systems, and the effect of partial shading on the PV system with a basic purpose of maximum power point tracking techniques presented in the literature.

Chapter 2 of this thesis presents the literature review in which different types of PV systems equivalent diode models are explained. Afterward, the explanation of different MPPT techniques, i.e. conventional, intelligent, and swarm intelligence based, is presented. This chapter also contains an explanation of different types of DC-DC converters used for MPPT applications. Research gap analysis and problem statement are highlighted in light of the literature survey.

Chapter 3 is utilized to present the proposed technique with detailed mathematical modeling. The working of the proposed technique under PSC and CPSC is elaborated.

Chapter 4 of this thesis work presents the results and discussion section in which four different scenarios are used for comparison. These four cases are fast varying irradiance, partial shading condition-1, partial shading condition-2, and complex partial shading condition. The Comparison is made with Cuckoo search algorithm (CSA), Grasshopper optimization (GHO), particle swarm optimization with gravitational search (PSOGS), and particle swarm optimization (PSO). MPPT rating

of all competing techniques, statistical analysis, qualitative analysis, and experimental verification is done to highlight the significance of the proposed control technique.

Chapter 5 presents the conclusion section with the future work. This section concludes that the proposed technique shows better performance as compared to the comparing MPPT techniques.

1.9 Chapter Summary

This chapter highlights the quickly changing trends from conventional energy sources to renewable energy sources. The benefits of PV systems are discussed and the partial shading (PS) effects on the performance of PV systems are examined to justify the necessities of sophisticated maximum power point tracking (MPPT) control technique. The conventional MPPT techniques fail to perform under PS but intelligent MPPT techniques specially Swarm intelligence (SI) techniques are effective under this multi-solution nonlinear monotonic control problem. Shortfalls of SI-based techniques in literature are studied and as a solution a novel hybrid SI-based MPPT technique is presented for extraction of maximum power under all dynamic operating conditions.

Chapter 2

Literature Review

In this chapter, different models of PV cells are discussed. The single diode model, double model, and triple diode model are presented in the literature. All the efforts made to model the PV cell are for the accurate estimation of non-linear P-V and I-V curves.

The effect of partial shading on the P-V and I-V characteristics curves are examined. Since the PV panels are made of PN junction, therefore the diode effect can be seen in I-V curve. PV cell behaves as a constant current source with an anti-parallel diode to instigate diode effect in I-V curve. This is known as an ideal model of PV cell. The problem with the ideal model is that it does not account for the non-linearity due to environmental conditions. So the practical models of PV cell are explained.

2.1   Single Diode Model

PV panel behaves like a current source when the light falls on it. The current generator by PV panel on irradiance is photon current (I_{ph}). Ideal diode model is shown in Figure 2.1. In which there is an anti-parallel diode which is connected with current source [32]. The output current for the ideal diode model is presented in Equation 2.1.

$$I = I_{pvh} - I_o = I_{pvh} - I_s \times e^{\left(\frac{V}{\eta N_s V_T}\right)} \tag{2.1}$$

Where I_{pvh} is photon current generated due to solar irradiance, I_o the diode current, I_s is a diode saturation current, N_s is the number of series-connected cells, V_T is the thermal voltage.
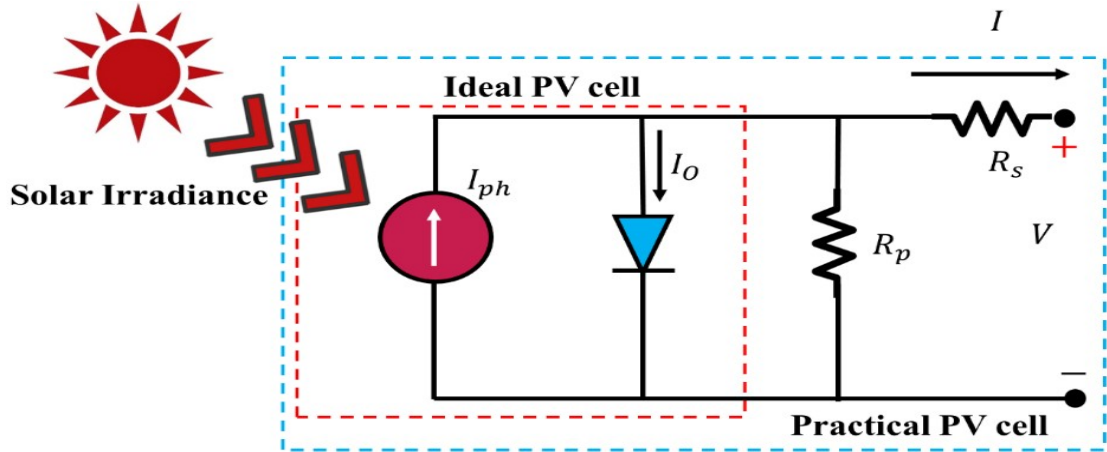
FIGURE 2.1: Single diode model of the photovoltaic cell contain anti-parallel diode, series and shunt resistors [3]

$$I = I_{pvh} - I_s \times exp^{\left(\frac{V + R_s I}{\eta N_s V_T}\right)} - \frac{V + R_s I}{R_p} \tag{2.2}$$

$$V_T = \frac{N_s K T}{q} \tag{2.3}$$

Where R_s and R_p are the series and parallel connected resistances, T is the temperature and q is the charge of the electron. V and I are the output voltage and output current respectively. The ideal diode model does not account for the non-linearity of the I-V and P-V curves on the curve knee. Therefore, the practical model is presented in Figure 2.1 which contains the series resistance R_s and shunt resistance R_p. The mathematical modeling of the practical single diode model is presented by Equation 2.2. The effect of R_s and R_p can be seen in Equation 2.2. The single diode model is a very simple design to model I-V and P-V curves of PV cells. The description of the symbols for the PV cell is presented in Table 2.1.

TABLE 2.1: Symbols and description of parameters of the PV cell

Symbol	Description
I	Current at output of dc-dc converter
V	Voltage at output of dc-dc converter
$\mathbf{I}_{PV}$	Output current of PV cell
$\mathbf{I}_d$	Current through diode
$\mathbf{R}_s$	Resistance in series of current source
$\mathbf{R}_p$	Resistance in parallel of current source
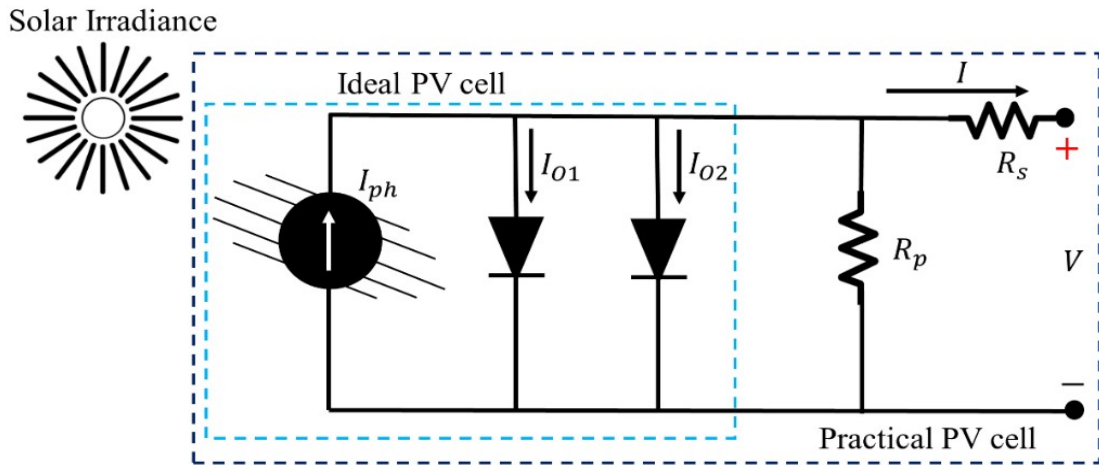
FIGURE 2.2: Double Diode Model of photovoltaic cell

2.2 Double Diode Model

In literature another model is presented that efficiently model the PV cell is a double diode model [33]. In this model, two diodes are added in parallel to the current source as shown in Figure 2.2. For the accurate modeling of the PV cell, five parameters are needed to be estimated, that is R_s, R_p, I_{ph}, I_{O1}, I_{O2}. The series/parallel resistances added for practical model, which effect the variation of output current and voltage. The mathematical model of the double diode model is presented in Equation 2.4, which shows the relation of output current with the diode currents. The diode currents are subtracted from the photon current.

$$I = I_{pvh} - I_{O1} - I_{O2} \tag{2.4}$$

Where I_{O1} and I_{O2} are the diode currents for diode 1 and diode 2 respectively. I_{s1} and I_{s2} are the saturation currents for diode 1 and diode 2 respectively.

2.3 Triple Diode Model

To model the non-linearity of I-V and P-V curves, the triple diode model is presented in the literature [34]. The current source has three anti-parallel diodes with series and shunt resistance is the practical triple diode model as shown in Figure 2.3. The mathematical model of the tipple diode model is presented in Equation 2.5. The diode currents are subtratced from the photon current to get the output current. Practical diode model contains series and parallel resistors to model the parameters of PV cell.
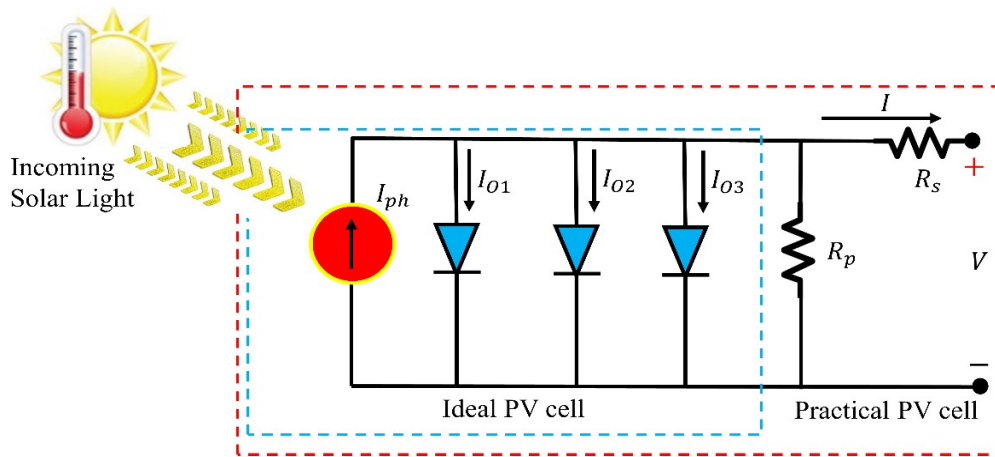
FIGURE 2.3: Triple Diode Model of photovoltaic cell [4]

$$I = I_{pvh} - I_{O1} - I_{O2} - I_{O3} \tag{2.5}$$

Where I_{o3} is the third diode current and I_{s3} is the third diode saturation current. R_p is the shunt resistance in the triple diode model. I and V is the output voltage and current respectively. R_s and R_p are the series and parallel resistances.

2.4   Characteristic of PV Cell

In this section, I-V and P-V characteristics of the PV cell are discussed. Also, the effect of dynamic environmental conditions on I-V and P-V curves is discussed. PV parameters are explained which alter the electrical characteristics of PV system.

2.4.1   I-V and P-V Characteristics

I-V and P-V curves of the PV module with the explanation of the different regions are shown in Figure 2.4. Since PV cell is made of PN junction and generates current when the light strikes. I-V curve can be obtained by varying load resistance at the output of the PV module [35]. First make it short circuit at the output means load resistance is zero. In this scenario, the maximum current will flow which is known as short circuit current.
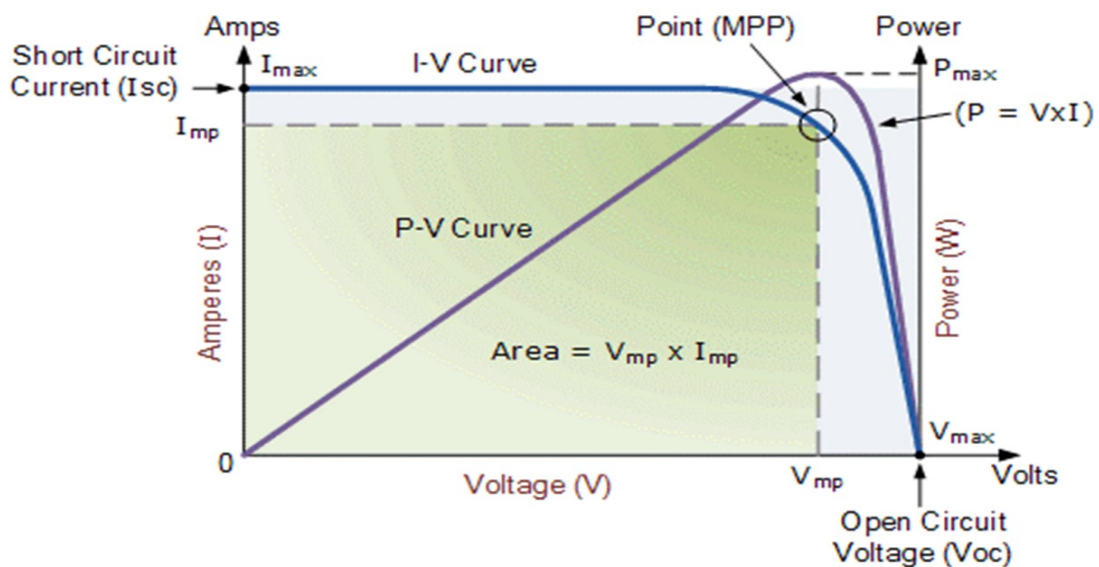
FIGURE 2.4: IV and PV curve with the elaboration of different regions in the curves [5]

After that, resistance is modified from zero to maximum value which makes the output of the panel an open circuit. At this point, we will get zero current but maximum voltage which is called open-circuit voltage. Clearly, it is seen that the I-V curve is nothing but the superposition of characteristics of the current source

and diode at parallel. There are some important regions in I-V and P-V curves that are:

- Constant current region

- Constant voltage region

- Knee region region

2.4.2   Effect of Series and Parallel Modules

In order to get high power multiple modules are required to be added in series/-parallel combination in series combination total voltages of the panel increase but to increase the current, we need to add the PV panels in parallel connection.
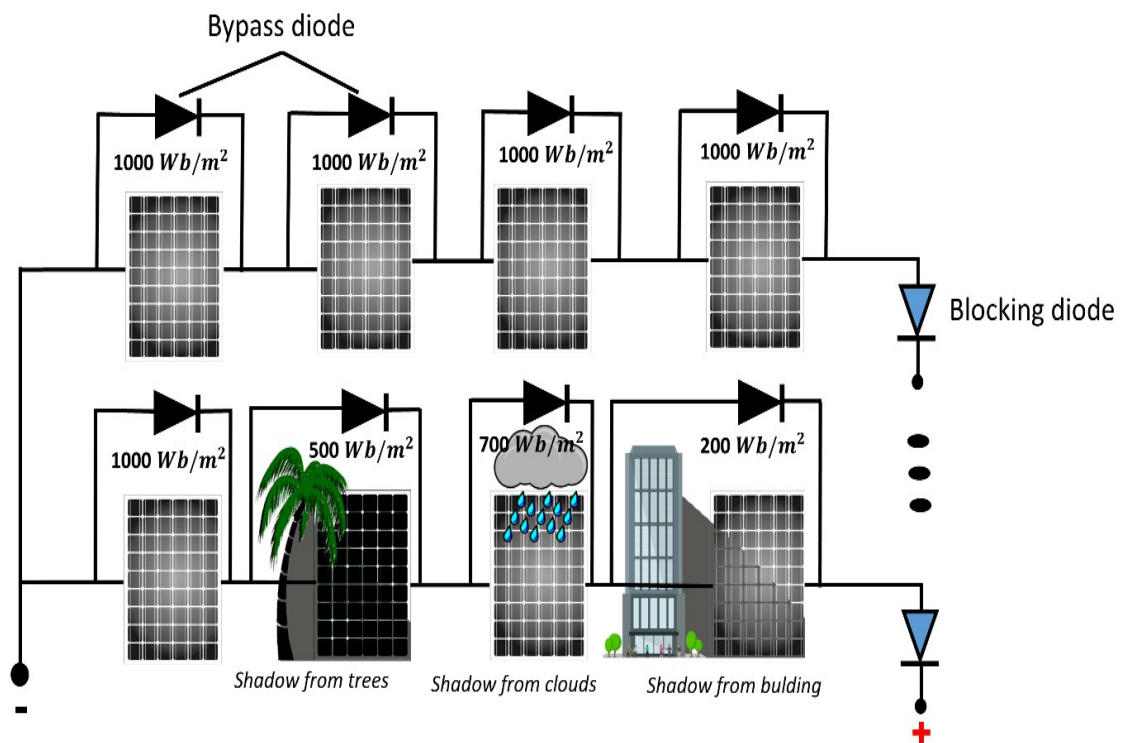
FIGURE 2.5: Series/Parallel connected photovoltaic panels which are under uniform and non-uniform irradiance causing partial shading condition

The PV modules connected Series and Parallel combination with different operating conditions are shown in Figure 2.5. The effect of the dynamic environmental conditions can cause a change in I-V and P-V curves [36]. PV system needs to

operate at maximum power point even under dynamic environmental conditions, which is the task of MPPT controller.

2.4.3   Description of PV parameter

There are different parameters that affect the power extraction of PV modules. The description of these parameters is shown in Figure 2.6. These parameters are listed and explained below

- **Open circuit voltage ($\mathbf{V}_{oc}$):** When the output load is infinity then voltage appears at the load is called V_{oc} open-circuit voltage.

- **Short circuit voltage ($\mathbf{I}_{sc}$):** When the output load is zero then the current through the load is maximum called I_{sc} short circuit current.

- **Maximum power point (MPPT):** The point of operation at which maximum power is delivered to the load by PV panel is called maximum power point. The tracking of this MPP is called maximum power point tracking (MPPT). MPP is the multiplication of V_{mpp} and I_{mpp}.

- **Efficiency (η):** the efficiency of PV cell depends upon the properties of the material. N is the ratio f practical and theoretical power. Therefore it is highly dependent upon the type of cell. Typically its value is between 9-22%.

  The PV module used for the simulation is "SunPower SPR-320E-WHT-D". The electrical characteristic of the PV panel is shown in Table 2.2. These parameters are taken from the PV module in MATLAB 2018a/Simulink. The maximum power of the PV panel is 320 W. So, combination of 4 panels will increase the power upto 1280 W. PV panels needs to operate Vmpp and Impp defined in Table 2.2 under uniform irradiance.

TABLE 2.2: Electrical Characteristic of SunPower SPR-320E-WHT-D

Parameters	Values
Power at MPP (Pmp)	320 W
Maximum Voltage (Vmpp)	54.7 V
Maximum Current (Impp)	5.49 A
Current at short circuit (Isc)	5.87 A
Voltage at open circuit (Voc)	64 V
Peak Efficiency	19.62%
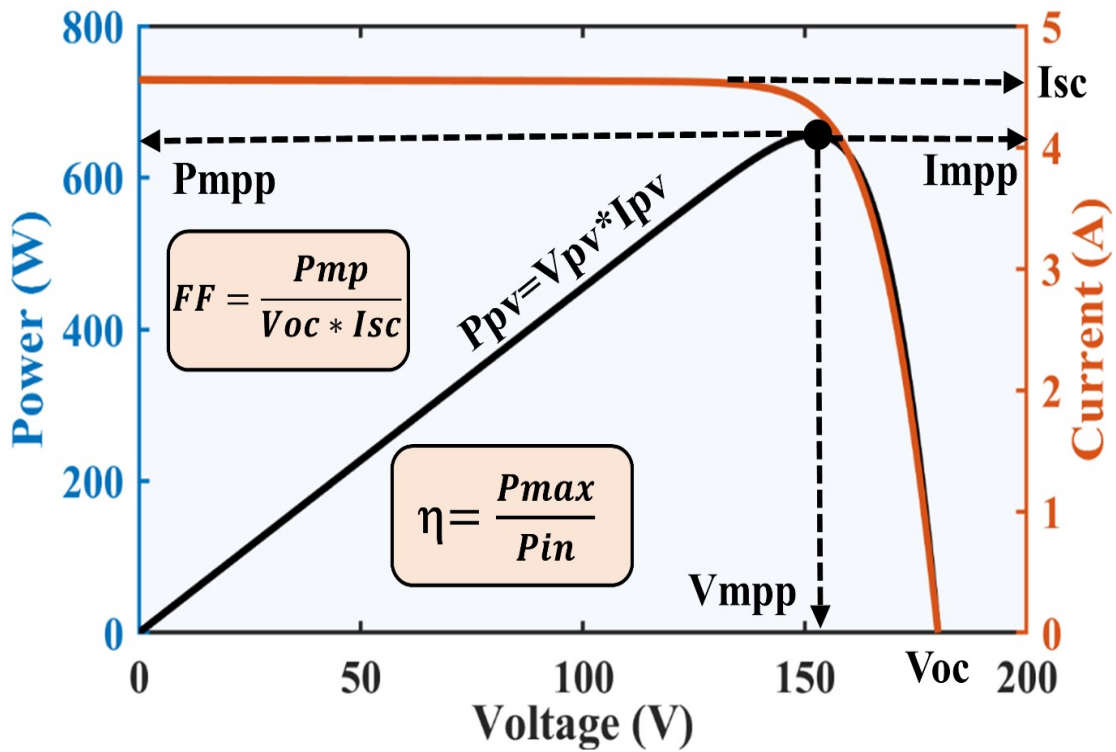
FIGURE 2.6: Description of PV parameter in IV and PV curve [6].

2.4.4   Effect of Varying Temperature and Irradiance

At STC, when the temperature is kept constant and variation occurs in the irradiance then the change in MPP also occurs as shown in Figure 2.7. However, the change in irradiance does not significantly affect the voltage but varies the current as shown in Figure 2.8. Since the power is nothing but the product of voltage

and current, therefore the change in power is directly proportional to the change in irradiance. The effect of the irradiance on I-V and P-V curves can be seen in Figure 2.7 and Figure 2.8, respectively.
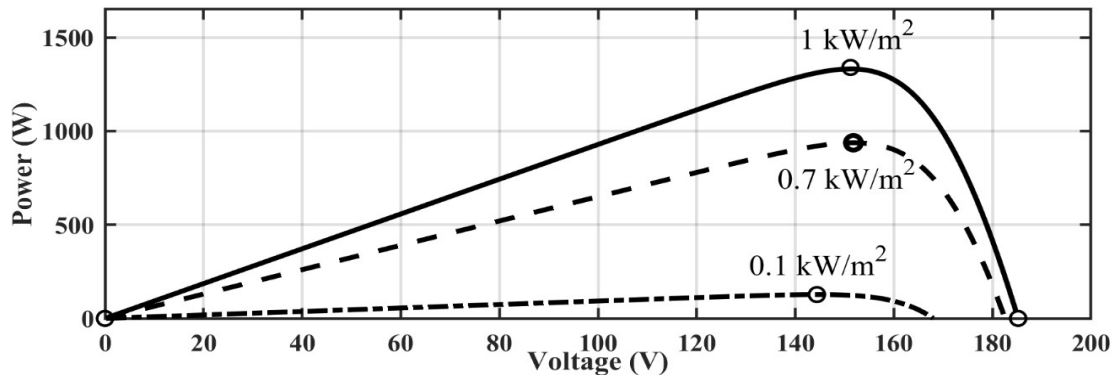
FIGURE 2.7: Effects of different irradiance levels on PV curve under uniform irradiance condition [7].
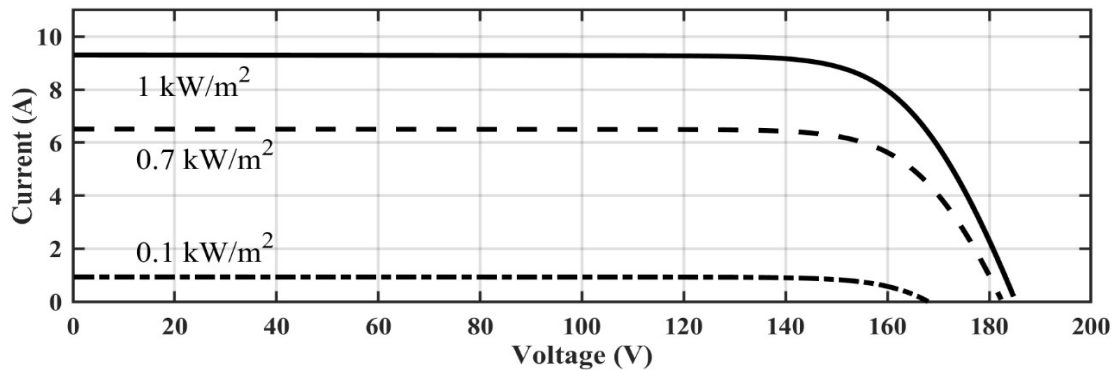
FIGURE 2.8: Effects of different irradiance levels on IV curve under uniform irradiance condition [7].

The output power of PV module is dependent on irradiance and temperature. When irradiance is kept constant at STC and temperature increases then the power of PV panel will decrease [37]. As shown in Figure 2.9. The panel temperature and power are inversely proportional. From Figure 2.10 it is verified that change in temperature has a minor effect on current but has a greater impact on voltage. This change in temperature of changes the MPPT on the PV curve. There the change in temperature affects the performance of PV module.
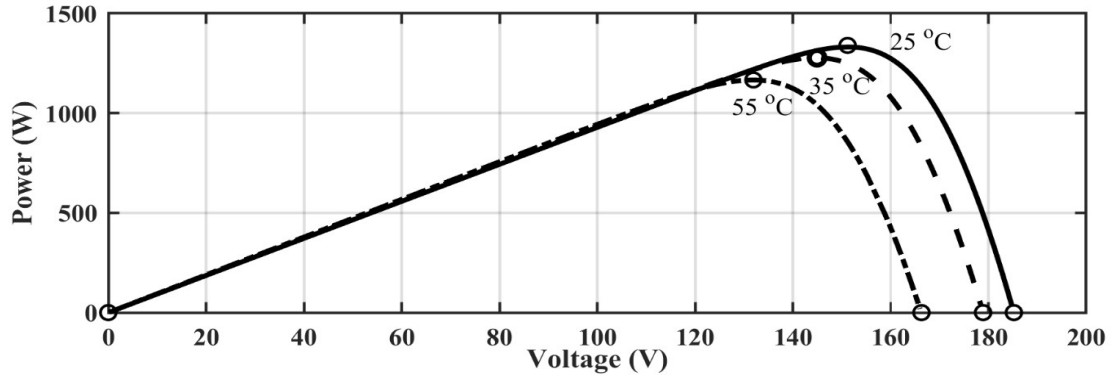
FIGURE 2.9: Effects of different temperature levels on PV curve under uniform irradiance condition [7].
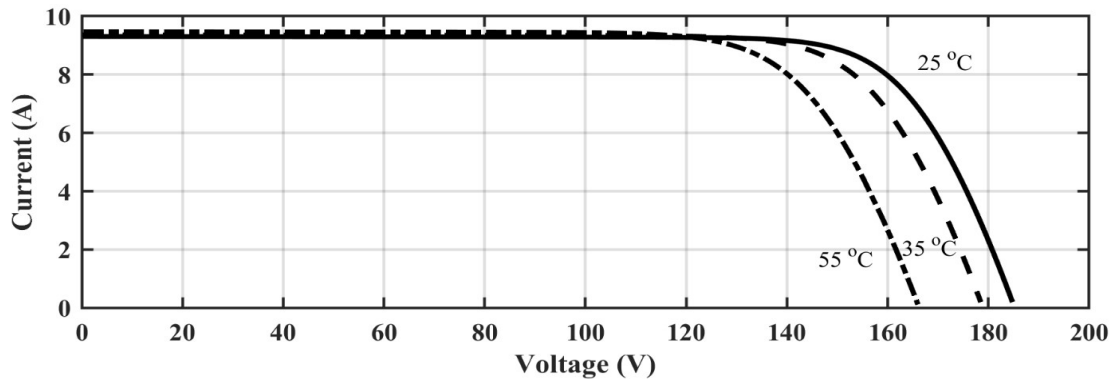
FIGURE 2.10: Effects of different temperature levels on IV curve under uniform irradiance condition [7].

2.4.5 Effect of Partial Shading Condition

For the large power production, multiple panels are connected in series/parallel configurations. The 4x1 string of PV modules is shown in Figure 2.5. It is not possible that every PV module receive an equal amount of irradiance. This intensity level can vary due to nearby building shadow, clouds, and dust, etc. as shown in Figure 2.5. This effect in PV panels is called partial shading effect. The module which doesn't receive equal irradiance becomes least productive, and extra power is lost in the PV panel which causes the hot spot effect [38]. Due to this, the PV panel could damage permanently. In order to avoid this, an alternative path is provided for the current through bypass diode which is parallel with the PV module. Due to this bypass diode, the IV and PV curves become non-linear as shown in Figure 2.11 (c). The conventional MPPT techniques cannot extract

the maximum power from this non-linear behavior. As shown in Figure 2.11 (d). there is only single global maximum and multiple local peaks. Intelligent MPPT control techniques are required for the extraction of global maximum power point (GMPP).
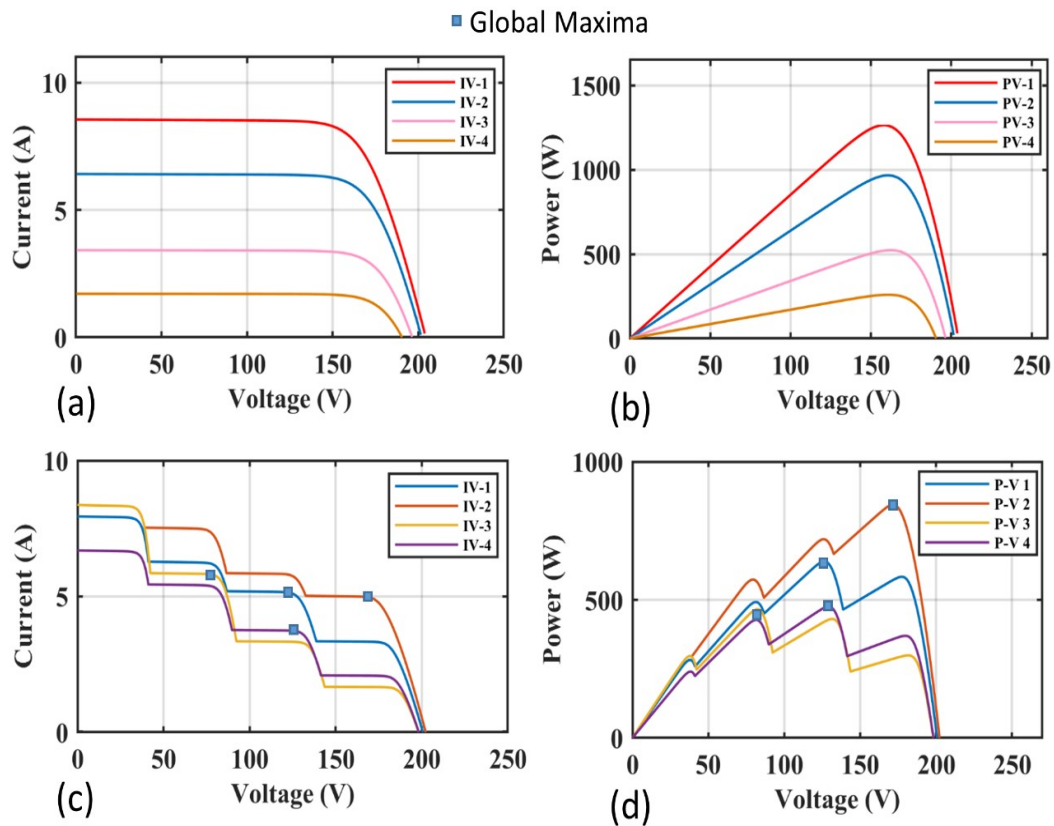
FIGURE 2.11: (a) IV curve at varying irradiance under uniform condition (b) PV curve at varying irradiance under uniform condition (c) IV curve under non-uniform irradiance (d) PV curve under non-uniform irradiance [8].

2.5 PV System and its Components

The standalone PV system as shown in Figure 2.12 consists of these components [39].

- PV module

- Boost converter (DC-DC converter)

- MPPT control
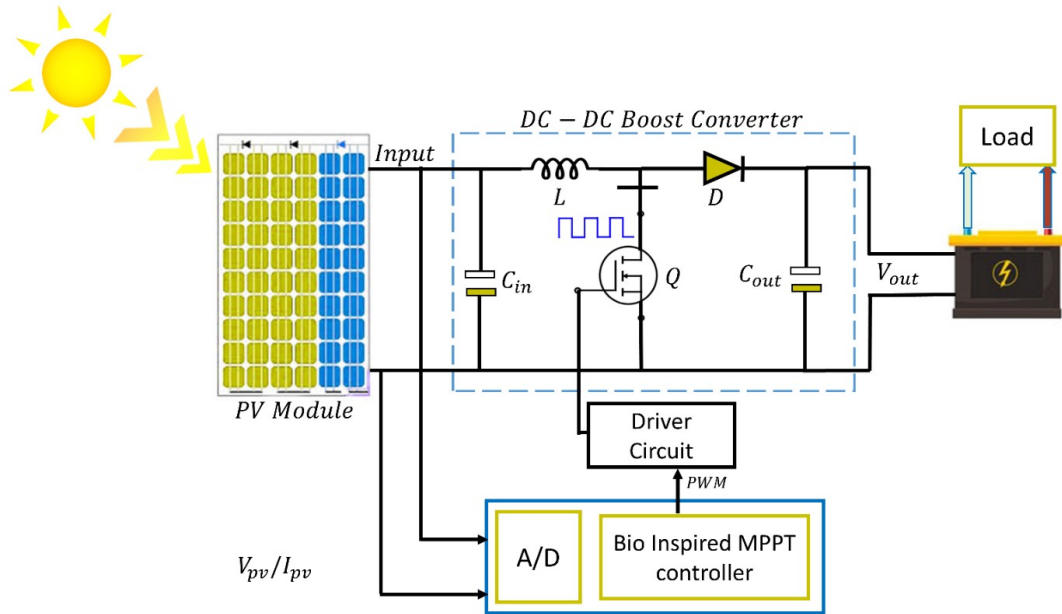
FIGURE 2.12: Components of the photovoltaic system contains PV arrays, converter, control technique and load [9].

The boost converter behaves as an interface between load and PV panel whose duty cycle is controlled by the MPPT controller current and voltage sensors are used to read the PV current and voltage.

These parameters are fed into MPPT controller which calculates PV power using the product of current and voltage sensor readings. The stabilized output power depends upon the efficient design of boost converter components, that is, inductor, capacitors, frequency of switching. The microcontroller generates a PWM signal given to the MOSFET driver and controls the voltage of the PV panel. The complete design of the boost converter for the MPPT applications is explained in the next section.

2.6 DC Boost Converter

DC to DC boost converter acts as an interface because the PV panel generates DC output and DC power is delivered to the load. Many DC-DC converter topologies are presented in the literature [40]. For MPPT application, DC-DC boost

converter is selected. As the name suggests, the output of the voltage converter is higher than the input voltage. Due to the higher voltage at the output, the low power is dissipated in the form of heat. The schematic diagram of the boost converter is shown in Figure 2.13. In this study for the simulation and practical implementation, a boost converter has been used. Because the resistance of the boost converter varies directly with the duty cycle. The effect of the duty cycle change in the output voltage with respect to input voltage is shown in Equation 2.6.
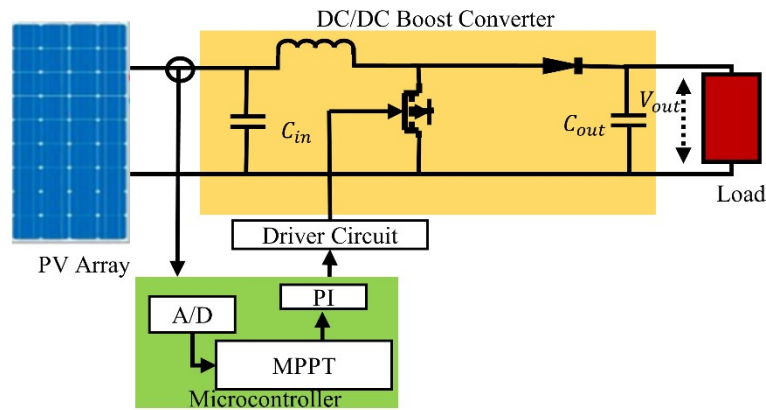
FIGURE 2.13: Implementation of maximum power point tracking control using boost converter [9].

$$D = T_{on}/T_{sw} \tag{2.6}$$

Where D is the duty cycle of the converter, Ton is the ON time of the duty cycle, Tsw is the switching time also called time period and Toff is the LOW signal time of the duty cycle.

2.6.1 Mathematical Modeling of Boost Converter

The mathematical modeling of boost converter explains the working and effect of components design on putout. The output voltage is dependent upon the variation in duty cycle, which varies between 0-100%. The input capacitor (C_{in}) is dependent upon switching frequency and current ripples but the output capacitor (C_{out}) depends upon the duty cycle.

The important component design is the inductor whose value depends upon the PV voltages [41]. The inductor controls the current ripples at the output. The design of all the components depends upon the following equations

$$C_{out} = (I_o D)/(8V_d f_{sw}) \tag{2.7}$$

$$L = (V_{PV} D)/(2I_d f_{sw}) \tag{2.8}$$

Where I_d and V_d are the ripples of current and voltage. The switching frequency is represented by f_{sw} and L represents the inductance of the inductor. Vpv is the input voltage of the converter which is actually the output of PV.

2.7 Boost converter application in MPPT

Since the PV system is different from the conventional energy sources because we cannot store energy like other sources, such as hydropower, chemical energy, therefore continuous extraction of power is required by interfacing DC-DC converter between panel and resistive load. For the maximum power extraction from the solar module, the maximum power transfer theorem is needed to apply which states that the maximum power will be delivered to the load if the mismatch between load resistance and source resistance is zero[33].

Now, if the load resistance at the PV panel is kept at maximum power then the change in environmental conditions will affect the operating point and the maximum power will stop delivering to the load. Therefore, the resistance of the load and boost converter will change in the duty cycle and be maintained at that value where maximum power is delivered to the load. This load variation capability provided by the boost converter is very effective.

Therefore, the change in resistance is dependent on the change in duty cycle when R is kept constant. By any change in the load resistance and environmental conditions will cater to the MPPT control technique by continuously monitoring the power of the PV panel.

The equivalent resistance of boost converter [42] can be calculated using Equation 2.9 presented below:

$$L = R_{eq} = V_o/I_o = (V(1-D)^2)/I_o = R(1-D)^2 \qquad (2.9)$$

Req is the equivalent resistance of the converter which is the division of the output voltage Vo to the output current Io and R is the load resistance.

The design parameters used in this study are presented in Table 2.3.

TABLE 2.3: Design Parameters of DC Boost Converter

Parameter symbol	description	value
L	Inductor	1.2 mH
C$_o$	Output capacitance	70 mF
C$_{IN}$	Input capacitance	70 mF
D$_{mpp}$	Duty cycle at MPP	0.69 at STC
R	Load resistance	50Ω
f	Operating frequency	8-10 KHz

2.8   Buck Converter

Another type of DC-DC converter is the buck converter which is also known as a chopper circuit [43]. The input voltage of this converter is greater than the output voltage by the relation as presented in Equation 2.10.

$$V_{out} = D(V_{in}) \qquad (2.10)$$

Where Vout is the voltage at output, duty cycle is D and input voltage is Vin. The basic operation of buck converter is to step down the voltage. In the positive half

of the cycle, the switch s1 is on, which delivers the current to the load inductor L but in the negative cycle on only the inductor and the output capacitor deliver the power to the load. Due to low voltage and high current at the output, the heat losses rise in this converter. The design of the inductor, input capacitor, and output capacitor for buck converter depend upon the following Equation2.11 and Equation 2.12 [44].

$$C_{in} = I/(8V_d f_{sw}) \tag{2.11}$$

$$C_{out} = (I - D)/8L(f_{sw})N_{out} \tag{2.12}$$

$$L = (V_{out}(1 - D))/(f_{sw}I) \tag{2.13}$$

Cin is the input capacitance, Cout is the output capacitance, L is the inductance, Vout is the output voltage, fsw is the switching frequency, D is the duty cycle.
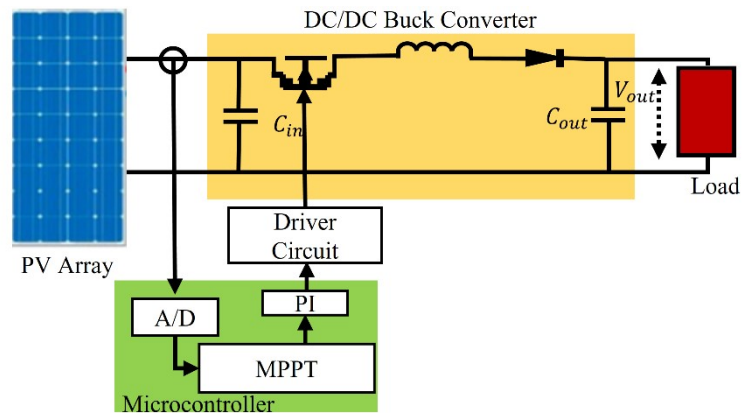
FIGURE 2.14: Implementation of maximum power point tracking control using buck converter [10].

The selection of MOSFET and diode depends upon the voltage and current across these switches. Figure 2.14 shows the schematic of buck converter. The voltage and current is the input for the MPPT controller while the output is the duty cycle fed to the buck converter. Driver circuit is used between the MPPT controller and swtich to drive the MOSFET. The variation of the duty cycle cause the change in overall resistance and changes the operating point.

2.9   Buck-boost Converter

In buck or boost converter, voltages step down or step up at the output. The technique is presented in which we can step up or step down voltages using only one circuit is called buck-boost converter [45]. The relation of input and output voltage with respect to duty cycle is presented in Equation 2.14.

$$V_{out} = D/(1-D)(V_{in}) \tag{2.14}$$

Where Vout is the voltage at output, duty cycle is D and input voltage is Vin.

For the duty cycle greater than 0.5 the circuit behaves as the boost converter and the duty cycle less than 0.5, the circuit behaves as buck- converter. One of the drawback of buck-boost converter is the output voltage is negative as compared to the buck and boost converter.
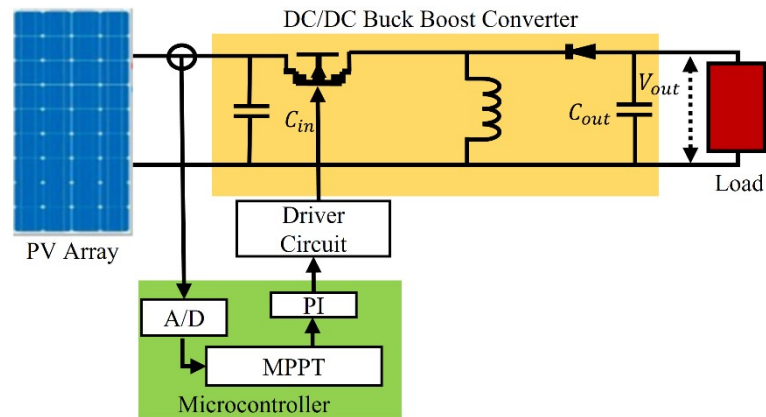
FIGURE 2.15: Implementation of maximum power point tracking control using buck-boost converter [11].

Cout is the output capacitance, inductor is L, duty cycle is D, switching time is Tsw, Vout is the output voltage and V_{out} is the ripple voltage. Figure 2.15 shows the schematic of buck-boost converter.

For the positive cycle, MOSFET charges the inductor due to reverse biasing of the diode. For the negative cycle the inductor discharge across the load in the opposite direction which causes the output to the negative design of inductor, input capacitor and output capacitor can be done by the following equations.

$$C_{out} = (V_{out}DT_{sw})/2V_{out} \qquad (2.15)$$

$$L = (V_{out}DT_{sw})/2V_{out} \qquad (2.16)$$

2.10   Cuk Converter

Cuk converter is the modified version of the buck-boost converter [46]. Cuk converter has a high impedance due to the capacitor C_f. The design of inductor, input capacitor, output capacitor, and integrating capacitor is presented by the following equations.

$$V_{out} = D/(1 - D)(V_{in}) \qquad (2.17)$$

$$C_{out} = (I_{out}DT_{sw})/V_{out} \qquad (2.18)$$

$$L_1 = DV_in/(I_lf_{sw}) \qquad (2.19)$$

$$L_2 = ((1 - D)V_{out})/(I_{out}f_{sw}) \qquad (2.20)$$

$$C_f = I_{out}/WV_{out} \qquad (2.21)$$

Where Vout is the output voltage, Cout is the output capacitance, L1 and L2 are the input and output inductors, Cf is the middle capacitor, D is the duty cycle, Vin is the input voltage, Tsw is the switching time, V_{out} is the output voltage ripples, I_{out} is the output current ripples.

Due to high impudence and less resistance variation by duty cycle, Cuk converter is not an optimal converter for MPPT control. The circuit diagram of Cuk converter is shown in Figure 2.16.
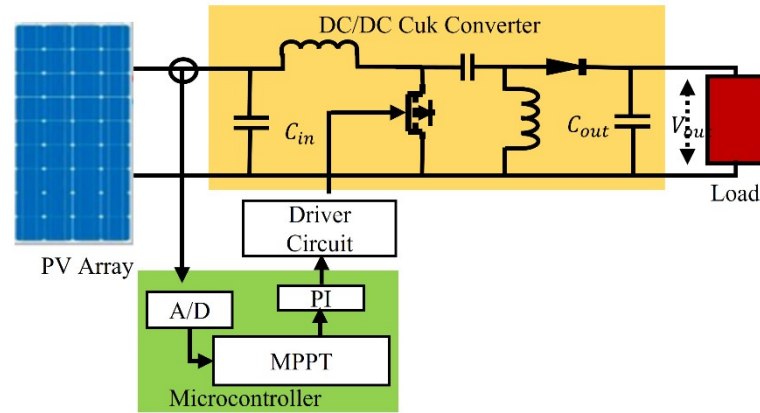
FIGURE 2.16: Implementation of maximum power point tracking control using Cuk converter [12].
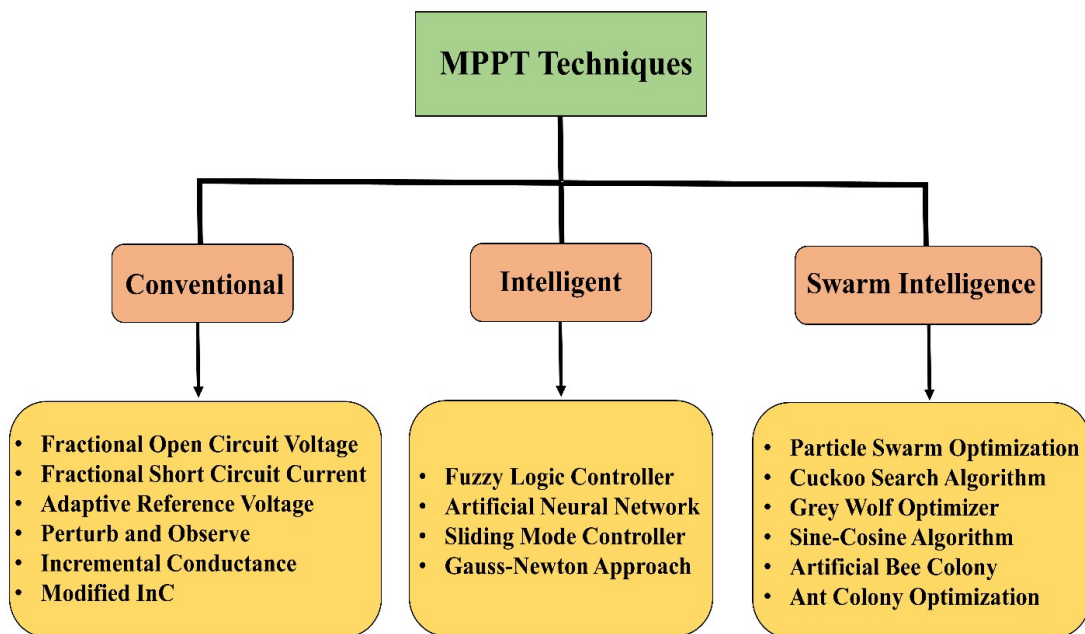
FIGURE 2.17: Classifications of different maximum power point tracking techniques which includes conventional, intelligent, and swarm intelligence based control techniques [13].

2.11 Maximum Power Point Tracking Techniques

Under the dynamic environmental conditions, that is, non-uniform irradiance and temperature PV systems fall into partial shading. Under PSC only one GMPP with multiple LMPPS's. Therefore, the maximum power point tracking control is required to extract the maximum power and get the high efficiency from PV

system. The effectiveness of MPPT techniques can be verified by tracking and settling time required, tracked power, hardware required for the implementation. In this study, different MPPT techniques are studied under these classifications.

- Conventional MPPT

- Intelligent MPPT

- Swarm Intelligent MPPT

The classification of all these MPPT techniques is presented in Figure 2.17.

The conventional MPPT techniques includes fractional short circuit (FSCC)[47], fractional open circuit voltage (FOCV) [48], perturb and observe (P&O) [49], incremental conductance(INC) [50], hill climbing (HC) [51], modified incremental conductance (Mod INC) [52] , lookup table method [53] and ripple correlation control (RCC). Advantages of these techniques are their low complexity for the implementation required less time to track GMPP and very efficient under uniform irradiance and temperature. However, the disadvantage is there are oscillations at GMPP which causes power loss. Also, under PSC when multiple peaks occur in P-V curve then conventional techniques could not differentiate between GMPP and stuck at LMPP causing extensive power loss and degrading the efficiency of the PV system.

Intelligent MPPT techniques include Artificial neural network (ANN) [54], fuzzy logic control (FLC) [55], Hybrid MPPT techniques and sliding mode control (SMC) [56] based control techniques. These techniques are highly efficient which can track GMPP which high accuracy and in very less tracking time. Under varying environmental conditions these techniques also perform with very high accuracy. The real problems with these techniques are the requirement of large data samples for the training and high computation cost.

Another class of MPPT controllers that use meta-heuristic optimization algorithms is called swarm intelligence-based MPPT control. These MPPT control techniques

use optimization algorithms which include particle swarm optimization (PSO) [57], grey wolf optimization (GWO) [58], whale optimization algorithm (WOA) [59], cuckoo search algorithm (CSA) [60], grasshopper optimization (GHO) [61], flower pollination algorithm (FPA) [62], low computation cost, high efficiency and medium time required for the MPPT are the main advantages of these MPPT control techniques. These control techniques can effectively differentiate between GMPP and LMPP and extracts the maximum power. In this work, a hybrid grey wolf optimizer with a sine-cosine algorithm (HGWOSCA) is presented for the MPPT control technique.

2.12   Conventional MPPT Techniques

In this sub-section, conventional MPPT techniques are presented and explained in brief. These techniques are shown below:

- Fractional open circuit voltage

- Perturb and observe

- Incremental conductance

- Adaptive reference voltage

- Fractional short circuit current

- Modified incremental conductance

2.12.1   Fractional Open Circuit Voltage (FOCV)

Fractional open circuit voltage is an approximation-based technique. In this technique, a pilot PV cell of the same type of PV module used in PV system is employed whose open-circuit voltage is monitored every time. We assume that the same irradiance and temperature condition is applied to pilot cell. The maximum power point of PV module in PV system can be calculated using the Equation 2.22 [48].

$$V_{mpp} = KV_{oc} \tag{2.22}$$

Where V_{oc} is the voltage when panel is open, V_{mpp} is MPP voltage and k is scaling factor whose value is between 0.7-0.8 and PID is the Proportional-integral-differential controller. The block diagram of the implementation of FOCV is shown in Figure 2.18.
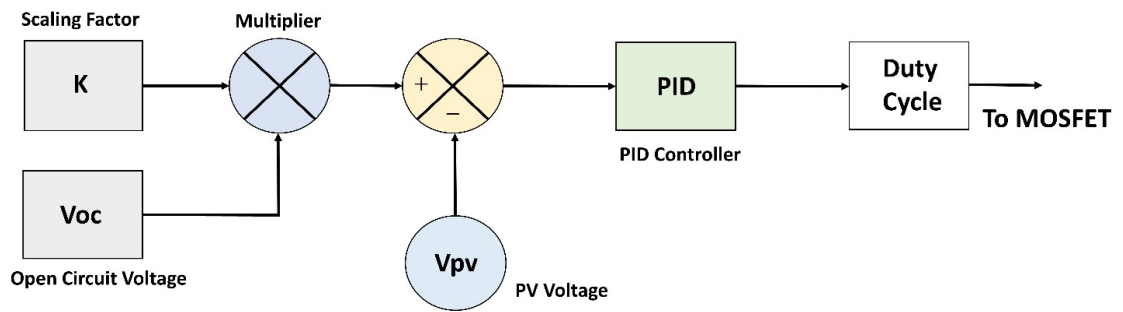
FIGURE 2.18: Block Diagram for implementation of fractional open circuit voltage based MPPT control [13]

The advantage of FOCV is very simple technique for implementation. The maximum power point tracking techniques can be implemented using the digital-analog circuit. No costly hardware is required for implementation. The disadvantage is that it is based on approximation of V_{oc} which is very inefficient and requires pilot cell which needs to be operating under the same conditions. Also, these techniques fail under PSC. Due to falling into local maxima under PSC causes the power loss. So, this technique is not effective for MPPT control.

2.12.2   Fractional Short Circuit Current (FSCC)

This technique is similar to FOCV. Since MPP contains both I_{mpp} and V_{mpp} so, in this technique I_{mpp} is taken into account in the place of V_{mpp}. So the short circuit current is measured of the pilot cell and multiplied by the factor k and fed into PI controller which maintains the required duty cycle can be calculated using Equation 2.23 [47]. The generic control diagram of FSCC is shown in Figure 2.19.

$$I_{mpp} = KI_{sc} \qquad (2.23)$$

Where I$_{mpp}$ is the maximum power point current, k is the multiplication factor and Isc is the short circuit current.
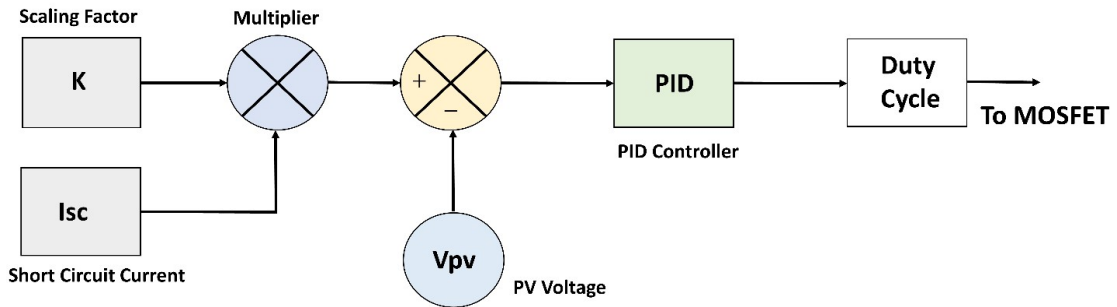
FIGURE 2.19: Block Diagram for implementation of fractional short circuit current based MPPT control [13]

Like FOCV, FSCC is also very simple technique for implementation. No complex hardware is required for FSCC. But same like FOCV, FSCC, also have an approximation which does not track GMPP effectively. Also fails to track GMPP under partial shading condition.

2.12.3   Perturb and Observe Algorithm (P&O)

Perturb and observe is one of the simplest algorithm to implement on any microcontroller. Voltage and current sensors are required to calculate the PV power after sampling time. As the name suggests, perturbation is made on power which decides the next perturbation of duty cycle. As shown in Figure 2.20. The duty cycle is changed and the previous power is compared with the next power. If the current power is higher than the previous power, then still increase the duty cycle and if the current power is less then the previous power is decreased the duty cycle. This process will continue and P&O will continuously track GMPP. The mathematical formulation of P&O is shown in Equation 2.24 to Equation 2.26.

$$dP_{PV}/dV_{PV} = 0 = MPP \qquad (2.24)$$

$$dP_{PV}/dV_{PV} > 0 \, left \, side \, of \, MPP \tag{2.25}$$

$$dP_{PV}/dV_{PV} < 0 \, right \, side \, of \, MPP \tag{2.26}$$

Where dP_{pv} is the differential PV power and dV_{pv} is the differential PV voltage.
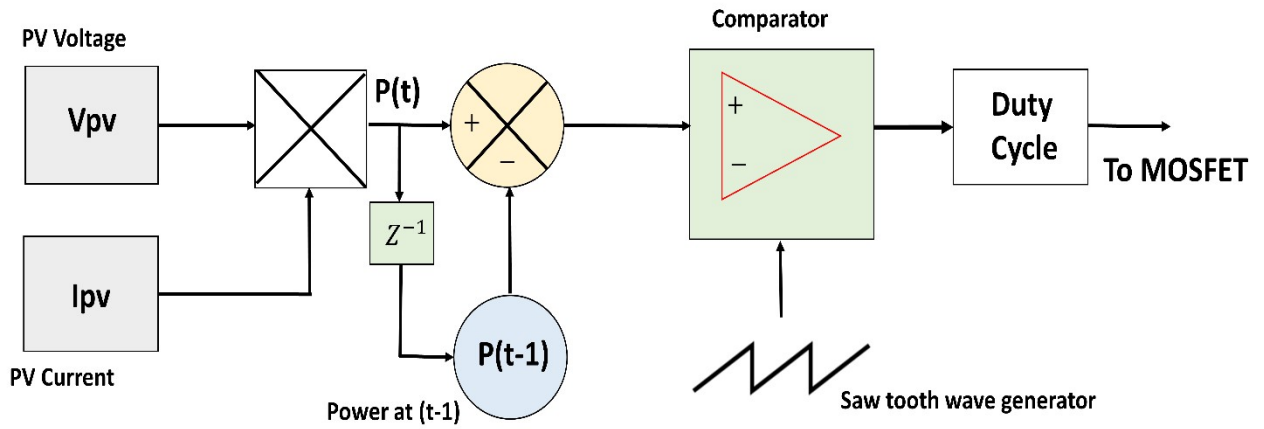
FIGURE 2.20: Block Diagram for implementation of perturb and based MPPT control

The implementation of P&O as shown in the flow chart in Figure 2.21 is also dependent upon the change in voltage of PV module. The problem with P&O is that continuous oscillations occur at GMPP and under PSC, P&O is stuck into the local minima. As presented in the literature under uniform irradiance GMPP with greater than 98% efficiency. Vpv is the PV voltage, Ipv is the PV current, P(t) is the instantaneous power, P(t-1) is the power at time t-1.

In the flow chart, V(i) and I(i) are the instantaneous voltage and current respectively, V(i-1) and I(i-1) are the voltage and current at the previous step, dP and dV is the measured change in power and voltage respectively. The D represents the duty cycle and ΔD is representing the change in the duty cycle.

Perturb and observe is one of the simplest algorithm to implement on any microcontroller. Voltage and current sensors are required to calculate the PV power after sampling time. As the name suggests, perturbation is made on power which decides the next perturbation of duty cycle. The problem with P&O is that continuous oscillations.
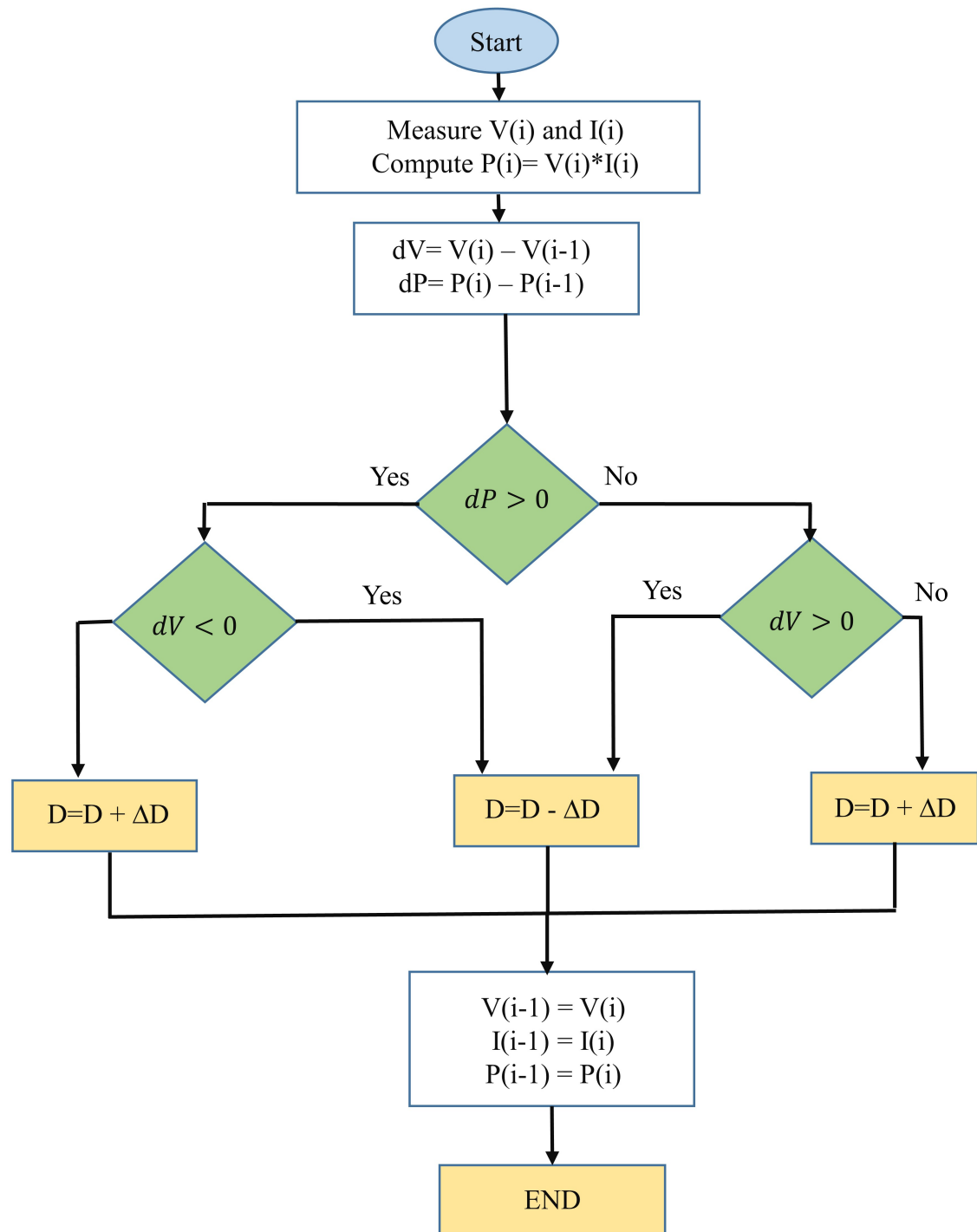
FIGURE 2.21: Flow Chart of the Perturb and Observe Scheme for MPPT technique

2.12.4 Incremental Conductance

The slope of a PV array power is zero at MPP and this is the basic concept behind INC in order to rack the GMPP under uniform irradiance. INC uses slope of power

curve to tack the GM rather than power value in P&O which makes incremental conductance better than P&O. The flow chart shown in Figure 2.22 explains the working of INC. As we know, the maximum power is defined by Equation (2.27).

$$P_{Mpp} = V_{MPP} x I_{MPP} \tag{2.27}$$

$$P = V x I \tag{2.28}$$

$$dP/dV = I + d/dV \, x V \tag{2.29}$$

Where Pmpp is the power at maximum power, Vmpp is the voltage at maximum power, Impp is the current at maximum power, dP is the differential power, dV is the differential voltage.

In the Figure 2.22 flow chart, V(i) and I(i) are the instantaneous voltage and current respectively, V(i-1) and I(i-1) are the voltage and current at previous step, dP and dV is the measured change in power and voltage respectively. The "D" represents the duty cycle and ΔD is representing the change in duty cycle. I and V are the instantaneous current and voltage. he slope of a PV array power is zero at MPP and this is the basic concept behind INC in order to rack the GMPP under uniform irradiance. INC uses slope of power curve to tack the GM

$$dI/dV = -I/V \tag{2.30}$$

dI/dV is called incremental conductance. Thus we can track the MPP by using incremental conductance of P-V curve.

PV module is forced to operate at Vref and which is equal to VMPP at MPP. As MPP is reached, unless the change in power occurs due to environmental changes, which causes the change in MPP, convergences, the Speed of INC depends upon the increments or decrements in Vref. Larger increments lead to fast tracking but cause more oscillations at GM which leads to power loss.
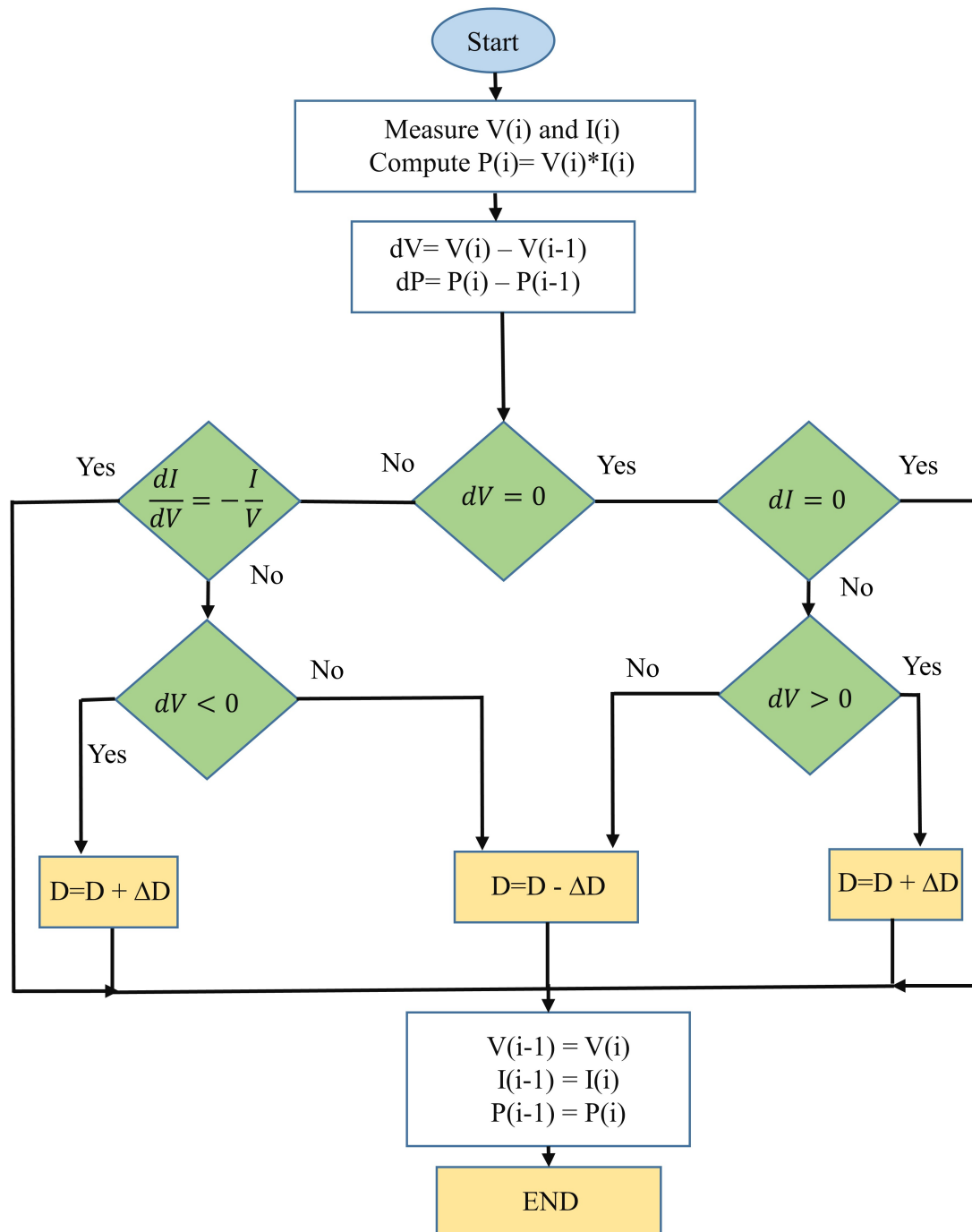
FIGURE 2.22: Flow Chart of the incremental conductance Scheme for Maximum power point tracking technique

2.12.5 Modified INC

Modified INC presented is used to avoid mathematical divisions used in conventional INC making the algorithm simpler. So this motivated the use of low cost microcontroller MPPT. Modified equations are shown as

$$((V x dI) + (I x dV))/(dV x V) = 0 \tag{2.31}$$

$$((V x dI) + (I x dV))/(dV x V) > 0 \tag{2.32}$$

Where V and I are the instantaneous voltage and current respectively, dI and dV are the differential voltage and current respectively.

Equation 2.31 is used to define the MPP and Equation 2.32 represents operating point at left and right of MPP respectively.

dV x V can be avoided from the previous Equation 2.31 which removes the division operators in calculation.

$$(V x dI) + (I x dV) = 0 \tag{2.33}$$

$$(V x dI) + (I x dV) > 0 \, and \, \Delta V > 0 \tag{2.34}$$

$$(V x dI) + (I x dV) > 0 \, and \, dV < 0 \tag{2.35}$$

$$(V x dI) + (I x dV) < 0 \, and \, dV > 0 \tag{2.36}$$

$$(V x dI) + (I x dV) < 0 \, and \, dV < 0 \tag{2.37}$$

The structure of modified incremental conductance is shown in Figure 2.23. We can see that only arithmetic and logical operator are used to track the MPP and after detection of MPP in Equation 2.37 no more perturbs are observed.

In the above mentioned flow chart, V(i) and I(i) are the instantaneous voltage and current respectively, V(i-1) and I(i-1) are the voltage and current at previous step, dP and dV is the measured change in power and voltage respectively. The "D" represents the duty cycle and ΔD is representing the change in duty cycle. I and V are the instantaneous current and voltage. The change in duty cycle is produce after specific time and check the power and calculate the conductance. This conductance will define the next change in duty cycle.

FIGURE 2.23: Flow Chart of the modified incremental conductance Scheme for MPPT technique

2.12.6   Adaptive Reference Voltage (ARV)

Unlike all other conventional MPPT techniques, adaptive reference voltage uses environmental parameters to track the maximum power. These parameters include irradiance and temperature.

Therefore extra sensors for irradiance and temperature measurement is required which definitely increases the hardware implementation cost but this will be compensated by the efficiency achieved by ARV. This technique is very effective under changing weather conditions unlike FOCV, FSCC techniques, These irradiance and temperature conditi ons will generate the reference voltage for MPPT which is then fed to PI controller for tracking of MPP [63]. The generic diagram of ARV based MPPT techniques is shown in Figure 2.24.
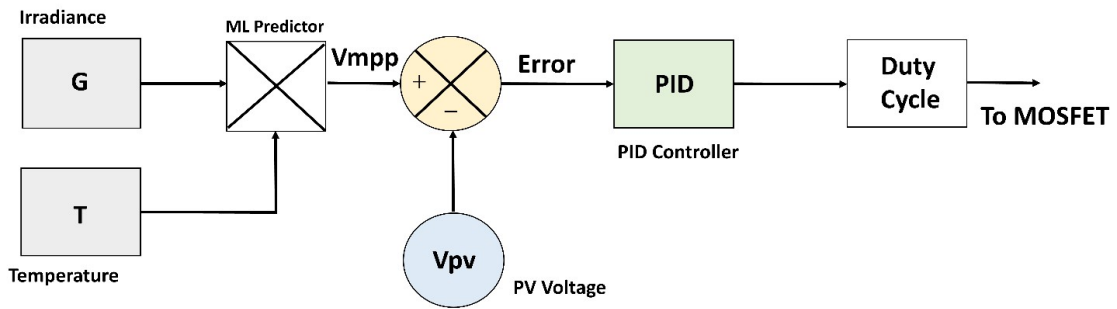
FIGURE 2.24: Block Diagram for Implementation of ARV Technique

In the above presented block diagram, G is the irradiance, T is the temperature Vmpp is the voltage at maximum power, Vpv is the PV voltage.

As presented in the literature, the FOCV and FSCC technique perform with equal efficiency at 99.7% at the irradiance 1000 w/m^2 but FOCV and FSCC techniques reduce its efficiency when irradiance reaches 400 w/m^2. The efficiency achieved is 98% but ARV still performs with $\geq$99% efficiency at some irradiance level.

2.12.7 Performance evaluation of classical techniques for MPPT

In this section, the comparison is also between conventional MPPT techniques in Table 2.4. which shows the comparison in the form of advantages, disadvantages

and the applications. The biggest problem with the conventional techniques occurs during PSC when these techniques are unable to track GMPP and loss too much power.

TABLE 2.4: Comparative Analysis of Conventional MPPT Techniques

Tech	Advantage	Disadvantage	Application
FOCV	Best application when temperature vary very low	Approximation to cause power loss under PSC	Stand-alone
FSCC	Very simple low hardware cost	Periodic measurement of ISC is required and high power loss under PSC	Stand-alone
P&O	Very simple implementation with high efficiency under dynamic weather condition	High oscillations at GMPP and couldn't differentiate between LMPP and GMPP	Stand-alone
INC	Low oscillations at GMPP as compared to P&O and achieves high efficiency	Required costly hardware due to variable step control	Stand-alone
MOD-INC	Very little oscillations with low execution time	Hardware implementation is costly	Stand-alone
ARV	Very low tracking time with very few oscillations	Due to addition G&T sensors hardware is costly	Stand-alone

2.13   Intelligent MPPT Techniques

In this section, intelligent MPPT control techniques are presented and discussed in brief. The discussed techniques are listed below which are going to explain in this section.

- Fuzzy Logic Controller based MPPT

- Artificial Neural Network based MPPT

- Sting mode controller based MPPT

- Gauss-Newton approach based MPPT

2.13.1 Artificial Neural Network

With the development of artificial intelligence, a new field emerges which is deep learning (DL) [64]. Artificial neural network (ANN) basically uses the concept of neurons in the brain. ANN with the single hidden layer is shown in Figure 2.25. ANN typically consists of three layers, that is, input, hidden and output layer. The first layer takes inputs and pass them to the next layer.

]
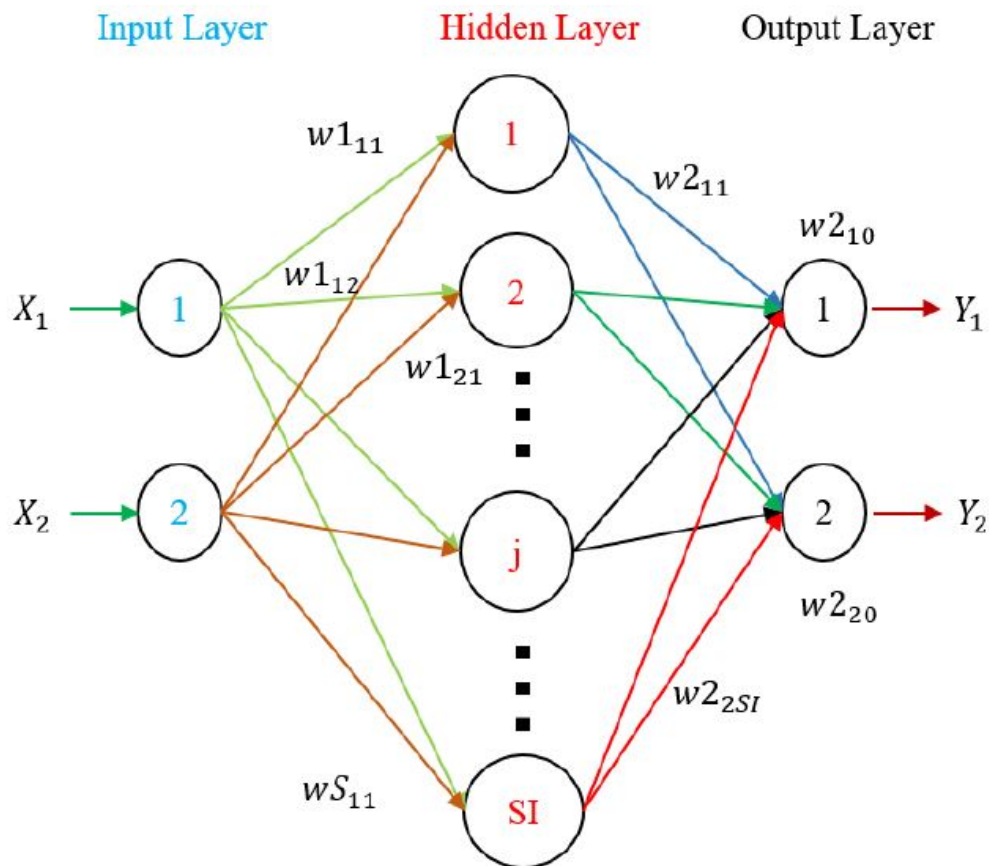
FIGURE 2.25: Three Layer Structure of ANN with Single Hidden Layer, Input layer and output layer [14].

The weights and biases connected define the relation of previous layer with the net layer. The weights connected between input and hidden layers is w_ij. The second layer is called hidden layer which originally map the input with output using the activation function. The weights connected between the hidden layer and output layer and it contains activation function or not, depends upon the application. There are two important factors in ANN [65].

- Learning method

- Activation method

The updation of weights and biases in ANN depending upon the predicted output is called learning of ANN for effective performance of ANN during the training and testing of model, a good learning technique is needs to be opted.

Another important thing in ANN is the selection of activation function for ANN. This selection is mainly dependent upon whether the problem is classification or regression. There are different types of activation functions, that is, RELU, sigmoid, radial basis function [66].

Another method is to use IV curve. The I_pv and V_pv is fed to ANN with duty cycle as the output. In this method, the dataset is generated with any conventional or swarm intelligence-based MPPT technique [67]. As discussed above the input features of this dataset is I_pv and V_pv and the class is the duty cycle d. Then with proper learning method and activation function ANN gets trained on the given dataset and generated model is employed to track the MPP. This type of MPPT control technique is presented in Figure 3.10. The inputs to ANN are the output voltage and current sensor and the output of ANN is directly fed to fed to the MOSFET driver circuit. Another technique is employed in which general regression neural network is trained by the fruit fly optimization algorithm [7].

2.13.2 Fuzzy Logic Controller (FLC)

To extract maximum from PV systems MPPT control technique needs to be efficient and can extract maximum energy under dynamic environmental conditions. For this MPPT controller PV panels needs to be modeled into the mathematical form. This modeling is easy under uniform irradiance but very difficult to model under PSC. So the intelligent MPPT techniques are presented in the literature which achieves high efficiency without knowing the mathematical model of PV

system because MPPT tracking depends upon fuzzy. Advantages of using FLC controller for MPPT are

- Doesn't require exact modeling of PV

- Controller design is totally dependent upon human

- Typically FLC controller design contains three steps which are [68]:

- Fuzzification

- Fuzzy rules

- De-fuzzification

The block diagram of different steps in FLC based MPPT controller for PV system is shown in Figure 2.26.
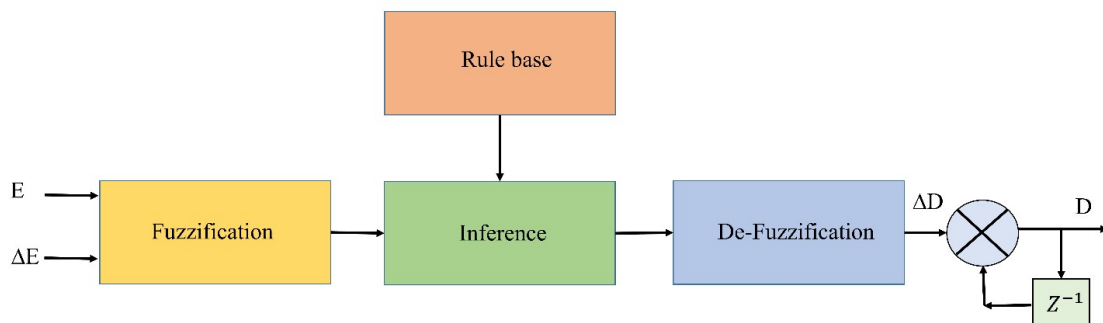
FIGURE 2.26: Block Diagram of Different Steps for Fuzzy logic based MPPT controller

In the first step is fuzzification in which PV parameter inputs are transformed in linguistic variables. Then fuzzy rules which are "if then" are designed by humans for the mapping of inputs and output of PV system.

In the last de-fuzzification is done which is nothing but invert of fuzzification. The fuzzification process and membership function are shown in Figure 2.27. In this step, mathematical relation is used to acquire crisp inputs. For the computation of this process following methods are utilized

- Membership function

- Centroid method

- Weighted average method
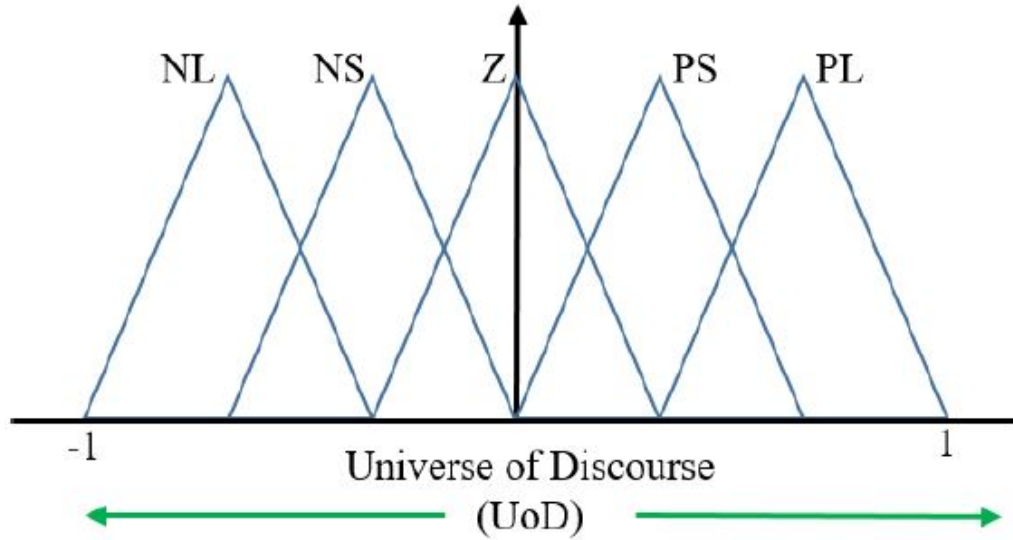
FIGURE 2.27: Process of Fuzzification and Membership Functions

FLC controller working depends upon the continuous variation of duty cycle d of the converter with the change in error which is modeled in Equation 2.38.

$$Error(n) = \{P/\{V \tag{2.38}$$

$$(V_{PV}(n)I_{PV}(n) - V_{PV}(n-1)I_{PV}(n-1))/(V_{PV}(n) - V_{PV}(n-1)) \tag{2.39}$$

Where Vpv(n) and Ipv(n) are the instantaneous voltage and current respectively, Vpv(n-1) and Ipv(n-1) are the previous values of the voltage and current respectively. P and V are the differential power and voltage.

Now the duty cycle is changed contours varying the d by focusing on error while tracking the V_ref reference voltage of PV with V_{mpp}. In this change in error is also taken into account which is

$$dE(n) = Error(n) - Error(n-1) \tag{2.40}$$

In literature it is proven that FLC performs with high efficiency even under dynamic weather conditions [69].

2.13.3 Sliding Mode Controller (SMC)

For any type of controller, tracking process is very important. This process needs to be very effective for the unforeseen disturbances or abruptly happening changes. So, without effecting the efficiency a sophisticated intelligent SMC based techniques are presented. This technique controls the DC-DC converter by sensing the current DC link capacitor.

In SMC control, there are typically modes of operation.

- Approaching mode

- Sliding mode

In SMC control, important thing is to choose a sliding surface [70]. This selection is totally dependent upon the application. This strategy (non-linear method) is employed to control non-linear parameter of system. Biggest advantage of this technique is that it doesn't require information/knowledge about the PV panel.

This SMC control technique effectively track GMPP with less tracking time and very low oscillation produced by the boost converter. These advantages are more observed when connected with the grid.

$$S = (dP_PV)/(dV_PV) = I_PV + V_PV(dI_PV)/(dV_PV) \tag{2.41}$$

where S represents the calculation of the exact value of PV voltage, dI_PV, dP_PV, and dV_PV are the differential current, differential power and differential voltage respectively. The flow chart for implementation of SMC control for MPPT application is shown in Figure 2.28.
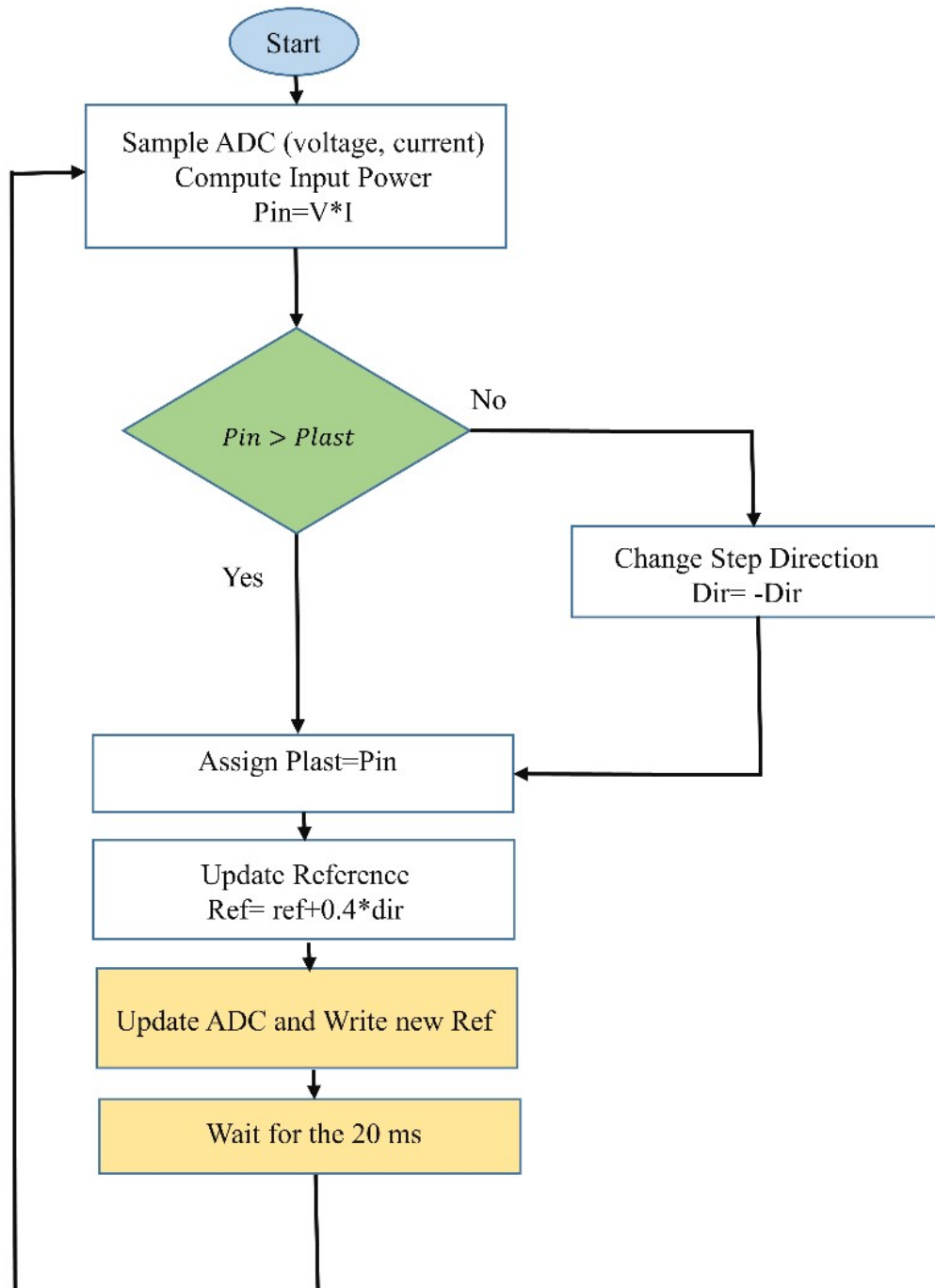
FIGURE 2.28: Flow Chart for Implementation of Sliding mode control based MPPT Control

2.13.4 Gauss Newton Based MPPT

Gauss newton method is also an intelligent MPPT technique, theoretically which have higher efficiency [71]. The main advantage of this method is that no need of computing the second derivatives. So these kinds of techniques effectively reduces

the computation cost. Trade-off is required between the number of iteration vs the computation cost. The main purpose of this technique is to disintegrate fitness function f(x) which can be modeled using Equation 2.42 to Equation 2.44 [72].

$$m_i = y_i - r(t_i, x)(y_i, t_i)i = 1, 2, \ldots, P \tag{2.42}$$

$$f(x) = 1/2P((y_i - r(t_i, x))^2 \tag{2.43}$$

$$l = e((m_i)^2) \tag{2.44}$$

2.13.5 Performance of Evaluation of Intelligent MPPT Techniques

Intelligent machine learning based MPPT techniques are very efficient and achieve high efficiency under dynamic atmospheric conditions but a large dataset is required for training and MPPT techniques are system dependent with high computation cost. The comparison of intelligent MPPT techniques is presented in Table 2.5, in which merits, de-merits and applications are defined.

2.14 Optimization Algorithm or Swarm Intelligence Based MPPT

Meta-heuristic optimization algorithm or swarm intelligence based algorithm used behavior of animals or swarm to solve complex optimization problems. In recent decades these optimization algorithm used as MPPT control technique which can effectively track the GMPP under dynamic environmental conditions using exploration and exploitation strategy by updating the duty cycle. In this section different SI-based MPPT based techniques are discussed and at the end evaluation comparison is made. The SI based MPPT techniques discussed are listed below

- Particle swarm optimization (PSO)

TABLE 2.5: Comparative Analysis of Intelligent MPPT Techniques

Tech	Merits	De-Merits	Application
ANN MPPT	Able to track MPP under PSC with efficiency and less time once it is trained	Large dataset is required to train ANN and also it depends upon system	Grid-Interface
FLC MPPT	Mathematical model is not required and shows few oscillations to track GMPP	Required tuning of membership function control rules and scaling factor	Grid-Interface
SMC MPPT	Due to perfection in mathematical model is very precise for tracking GMPP	Needs to effectively tune sliding surface to MPPT control	Grid-Interface
Guass Newton MPPT	Accurate tracking of GMPP with no PV system information	Very complex calculations are required	Grid-Interface

- Grow wolf optimizer (GWO)

- Cuckoo search optimization (CSO)

- Sine cosine algorithm (CSO)

- Artificial bee colony (ABC)

- Grass Hopper Optimization (GHO)

- Genetic algorithm (GA)

- Ant colony optimization (ACO)

2.14.1 Particle Swarm Optimization (PSO)

Particle swarm optimization (PSO) is the optimization algorithm used for solving complex engineering problems [73]. This algorithm basically uses the concept of

swarm intelligence. Its working is inspired by the behavior of flocking birds and shaolin fish. These flock of birds (particles) search for the food (global best) in specific area (search space) and the birds update their position in search of flood according to the bird who finds the food. This method is applied on engineering problems where particles update position and velocity using the current best and global best position PSO has very vast applications in engineering problems. The mathematical model of PSO is presented in Equation 2.45 and Equation 2.46.

$$X(i+1) = X(i) + V(i) \tag{2.45}$$

$$V(i) = W(V(i)) + C_1 r_1 (P_{best} - X(i)) + C_2 r_2 (G_{best} - X(i)) \tag{2.46}$$

where x(i) is the current position x(i+1) is the next position. V(i) is the velocity. w is the weight, C_1, and C_2 are the controlling parameters and r_1 and r_2 are random numbers. P_best and G_best are the personal best and global best respectively.

PSO is used to track MPP in PV systems with good efficiency. In MPPT applications, position of duty cycle is going to be updated using the PSO algorithm. Firstly, the particles or duty cycles are initialized in the search space, that is, between 0-100% duty ratio. Then power is checked at every particle which is called as fitness of the duty cycle. By using the best fitness check the global best particle with the help of personal best positions of particles. Then velocity is calculated using Equation 2.46 and updated using the duty cycles using Equation 2.45. The flow chart for the implementation of PSO as MPPT is shown in Figure 2.29.

In literature, PSO is implemented as MPPT in PV system. Also, there are different variants of PSO are also proposed for tracking GMPP with high efficiency [74].

Due to random numbers in velocity vector, oscillations are caused even after achieving the GMPP which causes the power loss. The effort is made to reduce the oscillation by improvising the PSO and achieving good efficiency. Another technique is presented which combines the PSO with INC.

This hybrid technique achieves a high efficiency of >98.5% with IS tracking time during the initial stage [75]. Another effort is made to implement PSO on low-cost controller and comparison is made. Simulation results are also presented with the hardware results. Therefore, this shows that reasonable efficiency can be achieved by implementing MPPT control technique on the low-cost hardware.
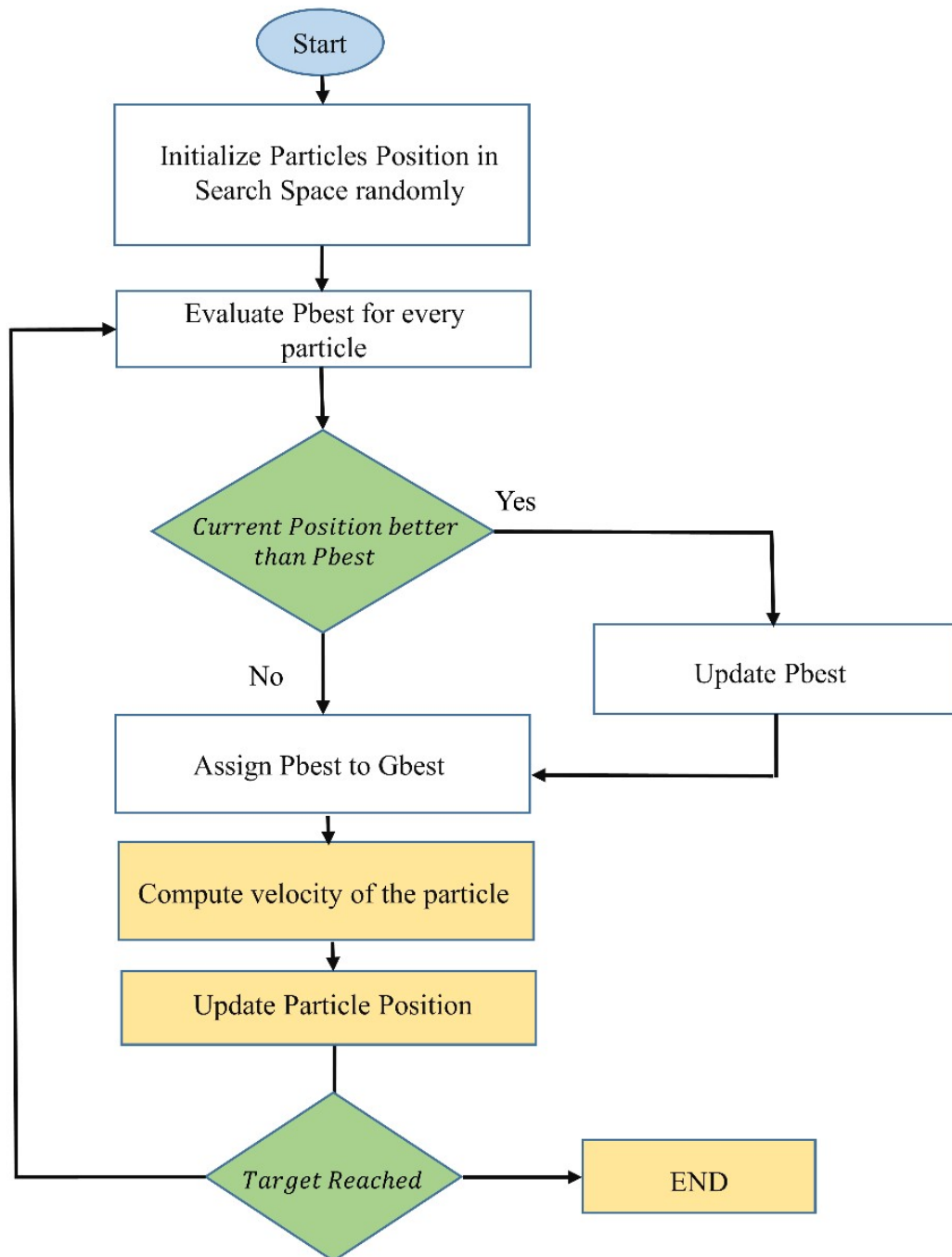
FIGURE 2.29: Flow chart of PSO Algorithm for MPPT Control

2.14.2   Cuckoo Search Algorithm (CSA)

This algorithm is inspired by the reproduction behavior of cuckoo bird is taken to solve optimization problem [76]. Cuckoo bird lay eggs on other birds' nests by finding the feasible nest and drops the eggs of other children. CSA uses levy flight function in order to space, basically, the updating of particle position using the swarm intelligence which contains direction and velocity. Also, the movement is restricted using the weight w. The particle position is updating mathematically as

$$X_{(i+1)} = X_i + \text{ff} levy(\breve{}) \tag{2.47}$$

$$levy(\breve{}) = l^{(} - \breve{}) \tag{2.48}$$

Where x_(i+1)and x_i is the updated and current position, λ is the variance, l is length of the flight and α is used to control the step length which can be calculated as

$$\text{ff} = \text{ff}_o(x_j^t + x_i^t) \tag{2.49}$$

Where α_o is the fixed step length constant, x_i^t and x_j^t are two different positions of the particle selected randomly.

In literature, CSA is used with different variations, that is, adaptive cuckoo search [77], which tracks the GMPP in PV system with high efficiency and takes less time as compared to PSO.

2.14.3   Ant Colony Optimization (ACO)

ACO algorithm is inspired by the living behavior of ants in which they move in search of fold/ ACO [78], mainly there are three steps used which are

- Greedy search

- Positive feedback

- Distributed computing

Greedy search algorithm helps ACO find more optimal solutions and enhances the effectiveness of the algorithm. The detection of best optimal solution can be guaranteed using the positive feedback mechanism to avoid the pre-mature convergence in ACO, distributed computing is used. In this algorithm for MPPT control, multiple parameters are needed to be selected by the users which are

- Number of Ants (population)

- Solution of archive size (K)

- Convergence constant (ε)

- Search space locality (R)

In literature. ACO is compared with the classic methods and this comparison shows that ACO performs better as compared to other MPPT techniques. The hybrid MPPT technique [79], that is , ACO-P&O is presented with high efficiency and high convergence speed. Under all environmental conditions.

2.14.4   Artificial Bee Colony (ABC)

ABC is another meta-heuristic optimization algorithm which use the cooperation of bees to find the food [80]. Basically, the bees live in colonies where they divide themselves in groups to find food. The bees are divided into three groups

- Employed Bees

- Outlook bees

- Scouts

Employed bees search for the food and the outlook bees choose food source while awaiting in hives. The initial random solution in ABC is assigned by using following Equation 2.50:

$$X_i = X_{min} + rand()(X_{max} - X_{min}) \tag{2.50}$$

where X_{min} is the minimum value of solution, X_{max} is the maximum value of solution, X_i is the current position of the particle and rand() is the random number between 0 and 1. The updating of new solution by employed bee can be modeled using Equation 2.51.

$$V_i = X_i + r_i(X_i - X_k) \tag{2.51}$$

Where V_i is the velocity vector, φ_i is the weight vector, X_i and X_j are the two randomly selected particles from the search space.

The employed bees share information with outlook using probability equation

$$P_i = fit_i x SN fit_i) \tag{2.52}$$

Where fit_i is the fitness value of the ith particle and Pi is the mean fitness of the particle i. In literature, ABC is presented and compared with PSO and P&O. ABC achieves the efficiency of 99.99% with 4.234s. The efficiency of ABC decreases with the dynamic changing environmental condition. Hybrid ABC-ANFIS [81] technique presented which tracks the GMPP very effectively but the implementation is cost of this technique is high.

2.14.5 Genetic Algorithm (GA)

The genetic algorithm basically works on the principle of biological evolution of human [82]. In this method, particles have high fitness basically have higher chance of reproduction,. Initially the random solution are created then the fitness

of every solution is calculated. On high fitness solution following three techniques are applied

- Selection

- Crossover

- Mutation
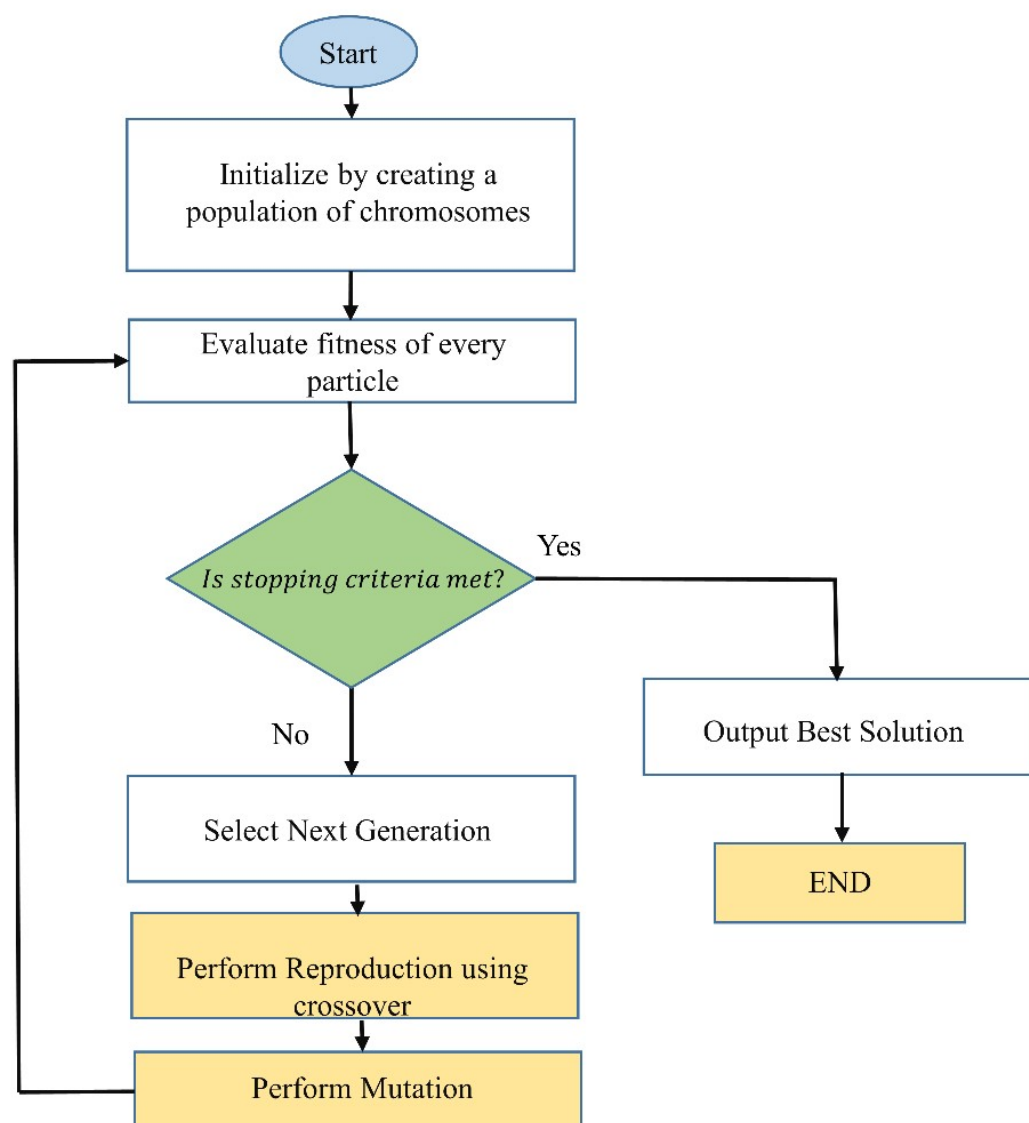
FIGURE 2.30: Flow Chart for GA based MPPT Control [15].

So, GA works on the survival of the fittest. GA optimizes the function with low speed but achieves high efficiency. Also, high computation power is required for the implementation of GA. The flow chart for the GA is shown in Figure 2.30.

Chromosomes are initialized which could be voltage or duty cycle. Than the power, that is, fitness is calculated. After that the mutation and crossover method is applied which generates new solutions and again calculate the fitness of solution and replace with old ones. In literature GA is used to train the ANN and fuzzy logic controller and implemented as MPPT control but these techniques required high dataset with high computational cost [83]. Another way is used in which GA is combined with P&O which reduces the time taken by MPPT technique with decent efficiency.

2.14.6   Grasshopper Optimization (GHO)

GHO is a swarm intelligence based optimization algorithm[83], which mimics the life cycle of grasshopper which consists of two cycles as shown in Figure 2.31.

- Nymph cycle

- Adult cycle

Nymph cycle is basically related to the exploration phase. This is necessary to have a balance between exploration/exploitation phase, the updating of particle position is presented in Equation 2.53.

$$X_i = S_i + G_i + A_i \tag{2.53}$$

where S_i is the social interaction, X_i is the particle position, A_i is the effect of the wind and G_i is the factor of gravity. In order to apply the randomness and control, the movement of particles, weights are applied and Equation 2.54 is the modified form of Eq 2.53

$$X_i = w_1 S_i + w_2 G_i + w_3 A_i \tag{2.54}$$

where w_1, w_2, and w_3 are the weights This also shows that the particles will re-initialize and all this optimization process will restart which significant, change in power occurs due to change in environment condition. These weight vectors are applied to control the movement of particle in the search space for global solution.
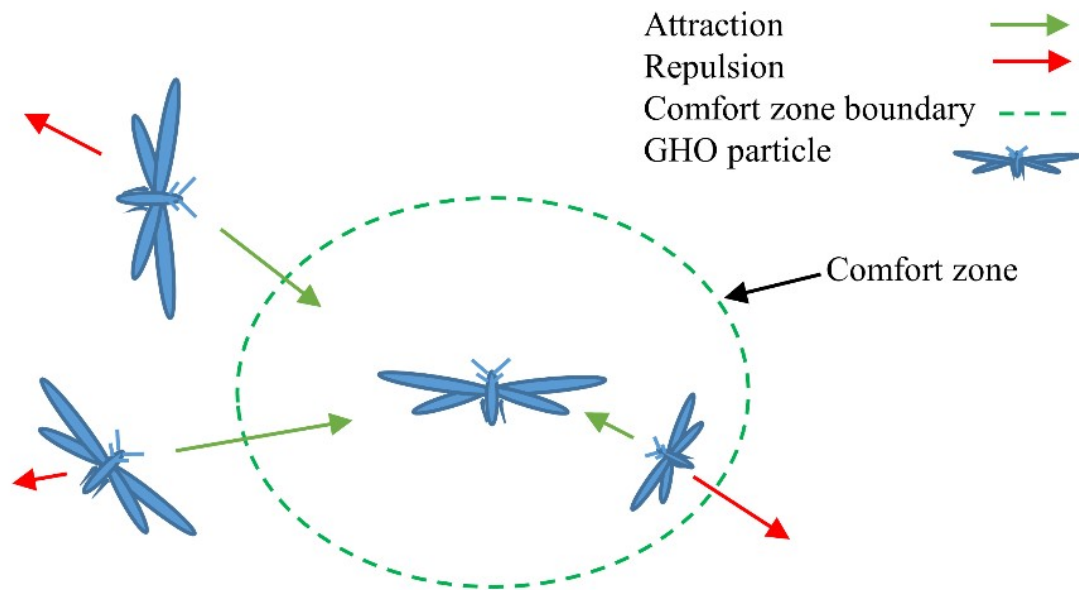
FIGURE 2.31: GHO Structure for the Particle Position Updation [16].

In literature, GHO is used with search and skip for MPPT control technique. It presents that GHO achieves up to 99.5% efficiency under various environmental conditions with up to 400ms for settling at GMPP. The techniuque is compared with PSO, P&O, DFO, ABC and shows significant efficiency improvement.

2.14.7 Comparative Analysis

SI based MPPT techniques effectively track GMPP under various environmental conditions and low cost hardware required but the high settling time cause power loss. The competitive analysis of SI based MPPT techniques is presented in Table. 2.6.

TABLE 2.6: Comparative Analysis of Swarm Intelligence Based MPPT Control Techniques

Technique	Summary
Genetic Algorithm (GA)	In this paper, MPPT controller is implemented on varying irradiance. GA-ANN is used to predict step size of INC-based MPPT. · MPP detection is offered under constant irradiance. · Fail to track MPP under non-uniform irradiance.
Particle Swarm Optimization (PSO)	· Improved version of PSO algorithm is implemented for MPPT. · Testing is performed under PSC to track MPP. · Achieves power traking efficuency > 99%.
Artificial Bee Colony (ABC)	· Hybrid ABC and P\&O combined MPPT technique is presented. · Efficiency achieved larger than 99.5% under PSC. · Did not incorporate complex shading condition.
Grey Wolf Optimizer (GWO)	· Improved GWO MPPT technique is implemented. · Achieves 98.54% power efficiency with 240 ms tracking time under PSC.
Grasshopper optimization (GHO)	· GHO based MPPT technique is implemented. · Testing is performed under varying irradiance and PSC. · Under complex shading, this technique achieves 99.5% efficiency.

2.15 Gap Analysis

Conventional energy sources are not a suitable option to meet the increasing energy demand due to high carbon footprints, which severely damage the environment. Therefore, solar energy is one of the solutions for clean energy due to no carbon footprint and its abundant nature.

For high-energy production, multiple solar panels are required in series/parallel combinations. However, due to dynamic environmental conditions, i.e. non-uniform irradiance and temperature on the solar panels, the photovoltaic system

falls into the category of partial shading condition, which causes a non-linear PV curve. This non-linear PV curve has multiple local maxima's and only one global maxima. PV system therefore needs to operate at this global maximum in order to deliver maximum power. Sophisticated control techniques are required to track the global maxima and this tracking of maximum power is called maximum power point tracking (MPPT).

Conventional MPPT techniques i.e. P&O, INC, Mod-INC show low efficiency under partial shading conditions due to trapping in local maxima, which decreases the efficiency of the PV system. Intelligent MPPT techniques or Machine learning-based MPPT techniques have high efficiency but these techniques require a large amount of data for training and testing the model. In addition, these techniques are system-dependent which means we need to train and test the model again whenever the PV system changes. Swarm intelligence (SI) based MPPT techniques are the viable solution for the extraction of maximum power under partial shading conditions but high tracking time, slow convergence time, low tracking efficiency, low tracked power, and extracted energy are the drawbacks observed. Hence, novel swarm intelligence-based MPPT techniques are required to fill this gap.

2.16 Problem Statement

Selection of maximum power point tracking control technique depends upon the tracking time, settling time, tracking efficiency, energy extraction, and implementation cost. MPPT control techniques presented in the literature show high tracking and settling time, low tracking efficiency with high implementation cost. Therefore, to overcome these drawbacks, a novel swarm intelligence-based MPPT control technique is needed for implementation. Exploration and exploitation phases are important parts in swarm intelligence based techniques. In exploration phase, particles search for the global maxima in whole search space and in exploitation phase, particles settles at the global maxima. Therefore, proposed

MPPT control technique should have an effective exploration and exploitation phase to locate the global maximum power point with high accuracy and minimum oscillations at global maxima.

Hybrid grey wolf optimizer sine cosine algorithm (HGWOSCA) is a swarm intelligence-based MPPT technique presented in this work, which has effective exploration and exploitation phases with fewer random numbers for position updation of particles and only one tuning parameter. Characteristics of both grey wolf optimizer and sine cosine algorithm make HGWOSCA an effective MPPT control technique. Also, HGWOSCA has very low complexity for the implementation on a low-cost microcontroller.

2.17   Chapter Summary

In this chapter, first the different modelling techniques of the PV panel are explained which includes Single diode model, double diode model and triple diode model. Single diode model is very easy to implement due to usage of single diode but this model doesn't cater the all non-linarites of IV and PV curves. These drawbacks compensated by the double diode model but more precise representation of IV and PV curve is done by triple diode model. Then the effect of temperature variation and irradiance variation on I-V and P-V curve is observed which shows that the change in environmental conditions effect the PV power. Under uniform irradiance and temperature only one global maxima is observed in P-V curve. The nonlinearity of I-V and P-V curves becomes more complex when the panels are exposed to different irradiance which causes hotspot effects and generates multiple peaks in P-V curve. Due to these multiple peaks, PV doesn't operate at maximum Power point. MPPT controller is required which extracts the maximum power from the PV and always makes it operate at MPP. Different types of converters are used for the implementation of MPPT control which includes Buck converter, boost converter, Buck-boost converter and cuk converter. But change in resistance of the boost converter is directly proportional to the change in duty

cycle which makes it better suitable for the MPPT controller. So, Boost converter is used in this study for the implementation of MPPT controller.

In this chapter, a comprehensive review of the MPPT techniques are presented. Conventional MPPT techniques include Fractional Open Circuit Voltage FOCV, Fractional Short Circuit Current FSCC, Perturb and Observe P&O, Incremental Conductance INC, Modified Incremental Inductance Mod-INC and Adaptive Reference Voltage. Conventional MPPT techniques perform better under uniform irradiance conditions. Perturb and Observe is one of the simplest technique which tracks the MPP with high efficiency. It is very easy to implement on the low cost microcontroller. The hovering of the operating point around MPP is the drawback of the P&O. The INC and Mod-INC reduces the ripples at the MPP. But under partial shading condition, conventional MPPT techniques doesn't perform well and unable to differentiate between GMPP and LMPP. Intelligent MPPT techniques are presented which includes Artificial Neural Network (ANN), Sliding Mode controller (SMC) and Fuzzy Logic Controller (FLC). Bio-inspired meta heuristic optimization algorithms are implemented for the MPPT which performs with higher efficiency and takes less computational power for MPPT implementation.

Chapter 3

Proposed Technique(s) and Implementation

This chapter deals with the mathematical model and characteristics of the PV system components in detail. The purpose of this section is to discuss the hardware components and proposed machine learning algorithm, optimization algorithm, and PV system integration as MPPT control.

3.1 Grey Wolf Optimizer

Another bio inspired algorithm based on population for solution of optimization problems is Grey Wolf Optimizer [17]. The working model of GWO is shown in Figure 3.1. The inspiration of this algorithm is the social hierarchy ad leadership qualities of grey wolfs.

Alpha is in charge for decision making in hunting. Beta supports the alpha in commanding other pack actions. Omega is usually called the scapegoat and the last one permissible to eat. Wolf will be called delta, if it is not alpha, beta, or omega, which is superior to omega but they have to submit to alpha and beta. Group hunting is another spellbinding grey wolves behavior. The main phases of hunting include encircling, hunting, attacking, and searching for prey. The mathematical modeling of these phases is explained.

61
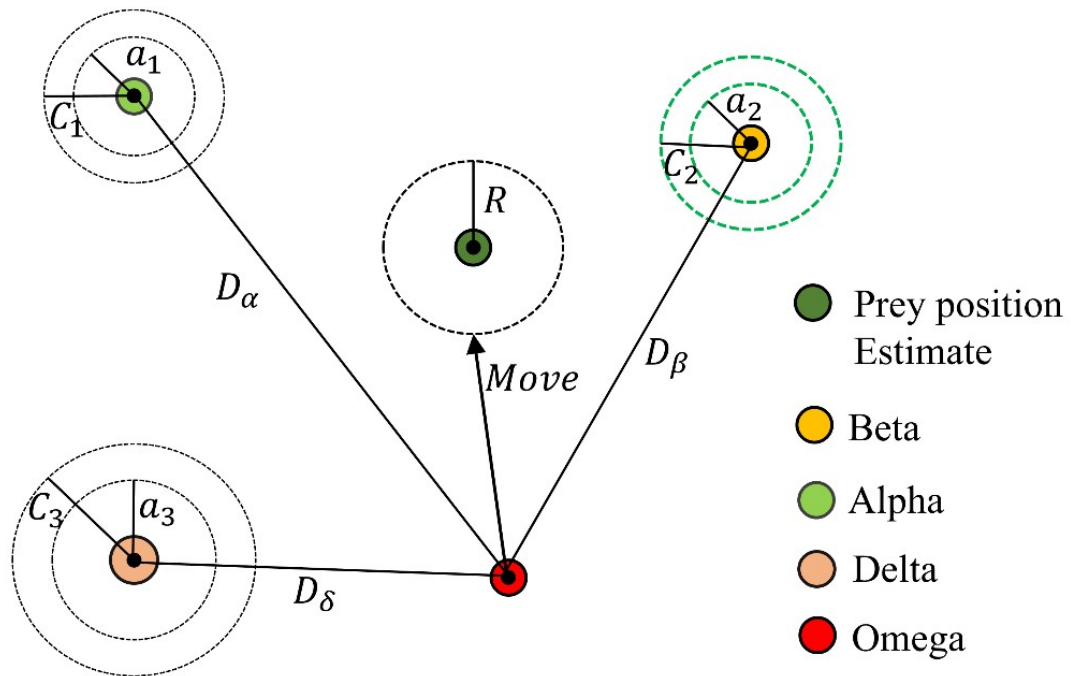
FIGURE 3.1: Particle Position Updation in Grey Wolf Optimzer in pursuit of Prey [17].
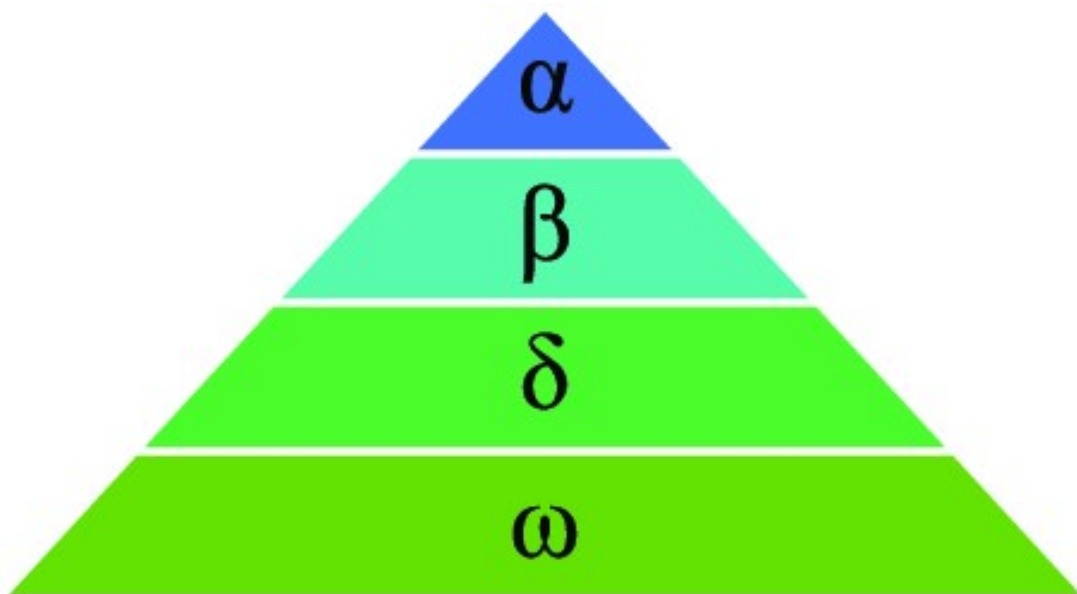
FIGURE 3.2: Leadership Hierarchy of Grey Wolfs followed for hunting and living

3.1.1 Social Hierarchy

To mathematically represent the social hierarchy, fitness of population required. The top three fittest solutions will be ranked as alpha (α), beta (β) and delta (δ)

whereas the rest of solutions will be considered as omega (Ω).

3.1.2 Encircling Prey

Equation 3.1 and Equation 3.2 are presented to model the encircling behavior of wolves.

$$D = (CxX_p(t) - X(t)) \tag{3.1}$$

$$X(t+1) = X_p(t) - AxD \tag{3.2}$$

Where current iteration is represented by t, A and C are the coefficients. Xp representing position of the prey and position of grey wolf represented by x. D is the distance parameter, A and C are calculated by Equation 3.3 and Equation **??**:

$$A = 2ar_1 - a \tag{3.3}$$

$$C = 2r_2 \tag{3.4}$$

Where 'a' is linearly reduced from 2 to 0 over the iterations and r1, r2 are random numbers between 1-0. Leadership hierarchy has four categories in pack namely alpha, beta, delta and omega as shown in Figure 3.2. Symbolically represented as α, β, δ and Ω respectively.

3.1.3 Hunting

We accept that alpha, beta and delta have a fitter understanding about the probable prey's location. In mathematical modeling of hunting behavior we are obliged

that the other search agents are to update their positions according to the position of best search agents by the following equations:

$$D_a = (C_1 x X_a - X) \tag{3.5}$$

$$D_b = (C_2 x X_b - X) \tag{3.6}$$

$$D_c = (C_3 x X_c - X) \tag{3.7}$$

$$X_1 = (X_a - A_1 x D_a) \tag{3.8}$$

$$X_2 = (X_b - A_2 x D_b) \tag{3.9}$$

$$X_3 = (X_c - A_3 x D_c) \tag{3.10}$$

$$X(t+1) = (X_1 + X_2 + X_3)/3 \tag{3.11}$$

Where a b and c are alpha, beta and delta positions assigned on fitness bases. C1, C2, C3, A1, A2, A3 are the coefficients, X_1, X_2, X_3 are the positions of the particles whose value is going to be updated.

3.1.4   Attacking Prey (Exploitation)

Grey wolves will bombard the prey when they finish hunting and this happens when the prey stops moving. To model the approaching prey, value of 'a' decreases with iterations. With this the range of fluctuation of 'A' will also decrease. Note that 'A' represents the random number in interval [-2a, 2a]. So the values which will decide the upcoming location of search agent which can be anywhere between its current position and location of the prey. So if —A—<1, this forces the wolves to attack towards the prey.

3.1.5   Search for Prey (Exploration)

In exploration phase, wolves split from each other to hunt the prey and converge to attack the prey. As described above, the values of 'A' occurs between +1 and

-1. If —A—>1, this forces the wolves to diverge from the prey to hopefully find a better a prey.

3.2 Sine Cosine Algorithm

Newly proposed sine cosine functions based algorithm for exploration and exploitation phases in optimization problems presented by Mirjalili is called sine cosine algorithm (SCA) [84], For the creation of different random solutions and fluctuations towards or outwards the optimal solution, SCA is used. The basic mathematical model of SCA is:

$$X(t+1) = X + r_1 x sin\}(r_2)x(r_3x(l-x)) \tag{3.12}$$

$$X(t+1) = X + r_1 x cos(r_2)x(r_3x(l-x)) \tag{3.13}$$

Where X is the current position, r1, r2 and r3 are the random values in [0, 1] and 'l' is the optimal solution.

In optimization algorithms, generally, there are two phases, that is, exploration and exploitation. In sine-cosine algorithm as name suggests, sine and cosine functions are utilized for the updating of particle position. The mathematical model of sine-cosine algorithm is presented below:

$$X(t+1) = X_i + asin\}(r_1)(r_2G_i - X_i)r_3 < 0.5 \tag{3.14}$$

Where G_i is the global best solution, α is the factor which is decreasing over the iteration, r1,r2 and r3 are the random numbers between [1,0]. Alpha can be calculated as

$$a = 1 - iter/(max\}_i ter) \tag{3.15}$$

where iter means the current iteration, $max\}_i ter$ means the maximum number f iterations. The structure of the Sine Cosine Algorithm for the particle position updation is shown in Figure 3.3.

In literature, modified sine-cosine algorithm is used for maximum power point tracking of grid-connected PV systems. High efficiency, low cost of implementation and high tracking speed are the merits reported for SCA [85].
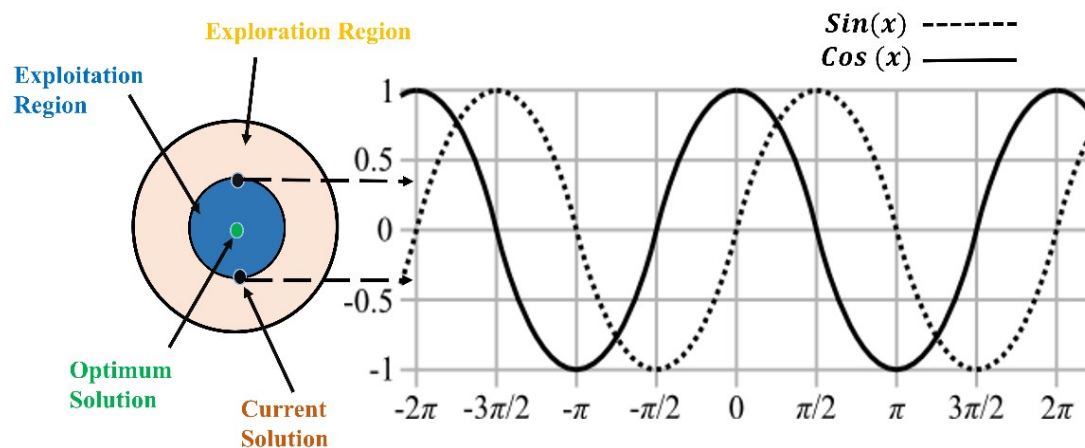
FIGURE 3.3: Structure of Sine-Cosine Algorithm for Updation of Particle Position

3.3 Hybrid Grey Wolf Optimizer Sine Cosine Algorithm (HGWOSCA)

Not fitting for highly complex functions and getting trapped in the local maxima are the fragility of the other well-known optimization techniques. In order to

overcome these flaws and increase the searching capability, new algorithm, which is the hybrid version of GWO and SCA is proposed [86]. The flow chart of the presented HGWOSCA is shown in Figure 3.4. In this variant sine cosine algorithm is used to improve movement of alpha agent in GWO.

The intention here is to enhance the global convergence, exploration and exploitation performances. In this HGWOSCA, the convergence, accuracy, speed and position of alpha agents has been enhanced. This SCA-based movement of alpha will balance the exploration and exploitation process represented in Equation 3.16 and Equation 3.17. The remaining operation of GWO is the same.

3.4 Implementation of HGWOSCA as MMPT

For extraction of maximum power, the particles i.e. duty cycle in this case, are initialized over the whole space Dmin and Dmax. The duty cycle is the current position of the individual. Alpha, beta, and delta positions are Dα, Dβ and Dδ. The pseudocode of HGWOSCA based MPPT is shown in Figure 3.5.

HGWOSCA is reinitialized when a considerable change of operating conditions takes place. Variations in weather conditions are detected as the relative change of power over-passes the threshold.

$$X(t+1) = X_i + asin\}(r_1)(r_2G_i - X_i)r_3 < 0.5 \tag{3.16}$$

$$X_1 = (X_a - A_1xD_a) \tag{3.17}$$

Where r1, r2, r3 are the random numbers in [0,1], C1, A are the coefficient, X_1, X_a, D_a, are the particle position, position of alpha particle and distance from prey of alpha particle respectively. The intention here is to enhance the global convergence, exploration and exploitation performances.

3.5   Re-initialization Strategy

With the change of irradiance, temperature or load the operating point of the PV panel will deviate and also the power of the panel will change. Therefore, the algorithm should be that much robust to tackle this change in the system. Whenever these changes occur, keep track of the power and measure the percentage change in power using Equation 3.18.

$$(P_{PVnew} - P_{PVlast})/P_{PVlast}) = P\_PV(\%) \tag{3.18}$$

where PPV is the power threshold, PPVnew, PPVlast are the new PV power and PV power taken previously. The considerable change triggers the re-initialization of HGWOSCA method.

At first step, initialize the particles randomly on the search space and set the maximum number of iterations for the control technique. This initialization must be between 0 and 1 for the case of duty cycle. Then the next step is to calculate the power of every duty cycle, which is called the fitness value of every particle. In our case the fitness function is the power of the duty cycle. On the basis of calculation of the fitness, the top three particles named Alpha, Beta and Delta are selected. Since, HGWOSCA follow the hierarchy of the GWO so, the top three ranked particles are selected for the position updation. The global best solution is forwarded to the boost converter for the power tracking.

After that, update the position of the particles using equation, which is dependent upon the values of all the particles and the top three particles. This particle position updation will take the current duty cycle near to the global best solution in extraction of global maxima. Than next step is the updation of "A" and "C".

In next step update the values of the alpha, beta and delta which is mathematically modeled above. After that update the values X1, X2, and X3 which are going to be used for the updation of the particle position for duty cycle. If the change in power occurs due to irradiance or temperature variation, then the detection mechanism is used which is done using the formula above mentioned.

FIGURE 3.4: Flow chart of proposed technique

In next step update the values of the alpha, beta and delta which is mathematically modeled above. After that update the values X1, X2, and X3 which are going to be used for the updation of the particle position for duty cycle. At the end check for the termination criteria if the termination criteria are met then we have to stop the tracking and send the global best that is alpha position to the boost converter and the converter will settle at the global maxim.

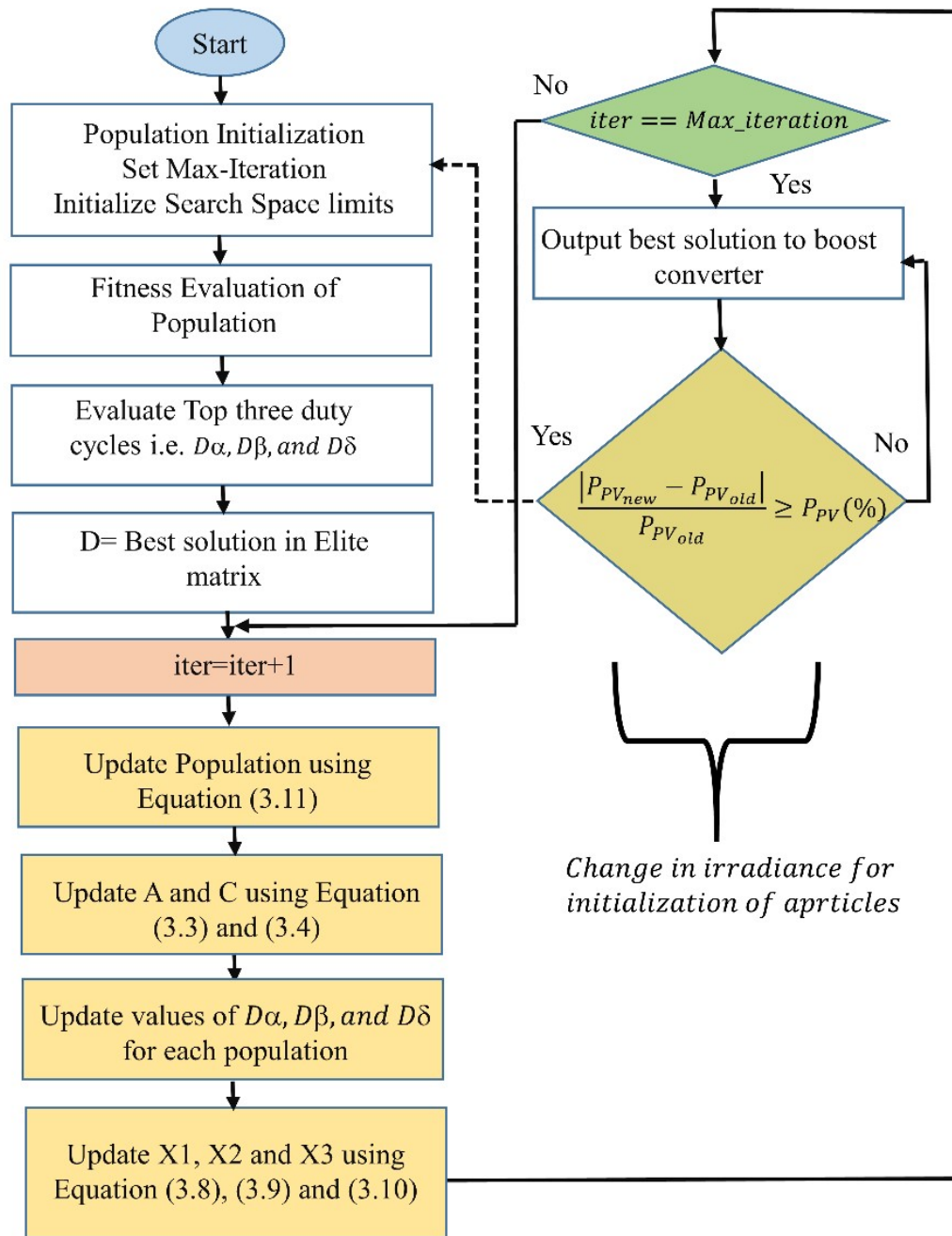If the change in power occurs due to irradiance or temperature variation, then the detection mechanism is used which is done using the formula above mentioned. When the change in power detected after the settling of duty cycle, this means now the Re-initialization is need to be done for again tracking of MPP. Again the particles will be randomly assigned and the exploration and exploitation phase will again start.

> **initialize** the population d_i (i=1, 2,..., N)
>
> Initialize A, a and C
> Calculate the fitness of each agent
> Evaluate d_α, d_β and d_δ
> **while** (T<iter_max)
>   **for** each search agent (i=1: 1, 2,..., N)
>   update particles position
>   **end for**
> update A & C
> update D_β and D_δ
> update D_α
> update x_1, x_2, x_3,
> T=T+1
> **end while**
> **Return** d_α

FIGURE 3.5: Pseudo code of proposed technique

3.6 Tracking mechanism of HGWOSCA

Tracking mechanism of HGWOSCA is shown in Figure 3.6. Using the curves of the output voltage and duty cycle. Top right curve shows the PV curve in PS condition which has 3 LM's and 1 GM. Four particles P1, P2, P3, and P4 represent the population which is randomly initialized in the whole search area.

In every iteration, the position is updated and the particles are shown on P-V curve with different colors. Power is calculated against every particle which is the fitness of each particle and other particles position is updated based upon the particles position.

In PSO, position of every particle is updated using the Pbest and Gbest values. In HGWOSCA, top 3 particles with best fitness play an important role for the

position update. Large fluctuations in the voltage are observed due to updating of particle position with large value of A and these particle positions are the duty cycle which is the control variable of the boost converter which changes the voltage vigorously.

In first 60ms, high increase in voltage is observed due to the high explorative behavior of HGWOSCA controlled. Till 150ms, the explorative behavior can be observed. P2 encounters LM2 at 90ms and when the particles are stuck at LM, its movement becomes minimum. LM trap cannot break until other particles are found at global best and then all particles again start to converge towards the global maxima causing large fluctuations in the voltage and power as created by P2 when moving towards GM, found by P3 as shown in Figure3.6 (C).

(a) Power fluctuations of HGWOSCA
(b) Summary of movement of HGWOSCA during
    the exploration phase
(c) Reference voltage computed by HGWOSCA
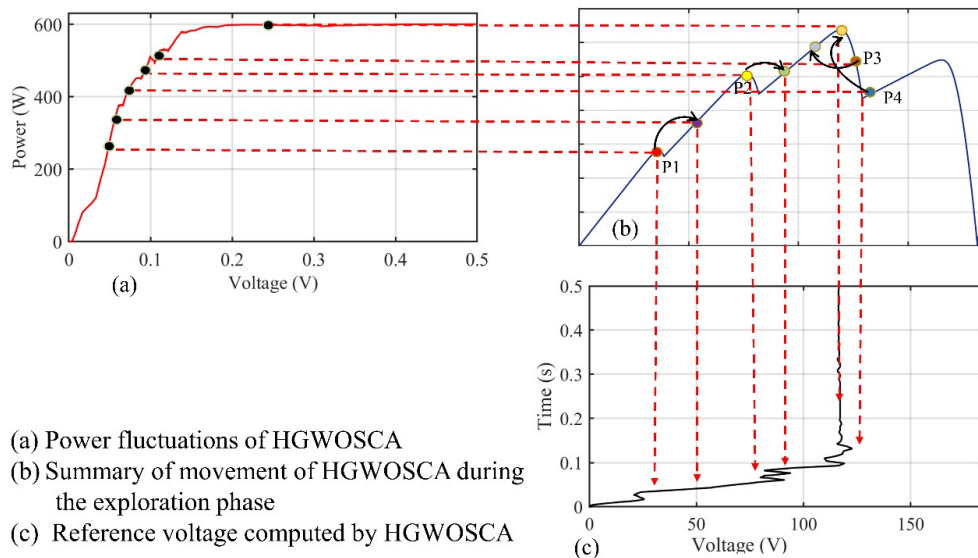
FIGURE 3.6: The tracking formation of HGWOSCA in partial shading conditions on P-V curve

All particles start to converge towards GM after 120ms. Meanwhile, P4 finds a new best and a surge is again detected at 120ms. LM is encountered again due to overtaking of P3 from P4. During the breaking of LM3, a voltage spike is observed at 150ms and GM is found between 150ms-160ms and all particles converge at GM. As the factor A becomes small over the iterations, the oscillations at GM are reduced significantly and the mechanism settles at GM. Searching mechanism
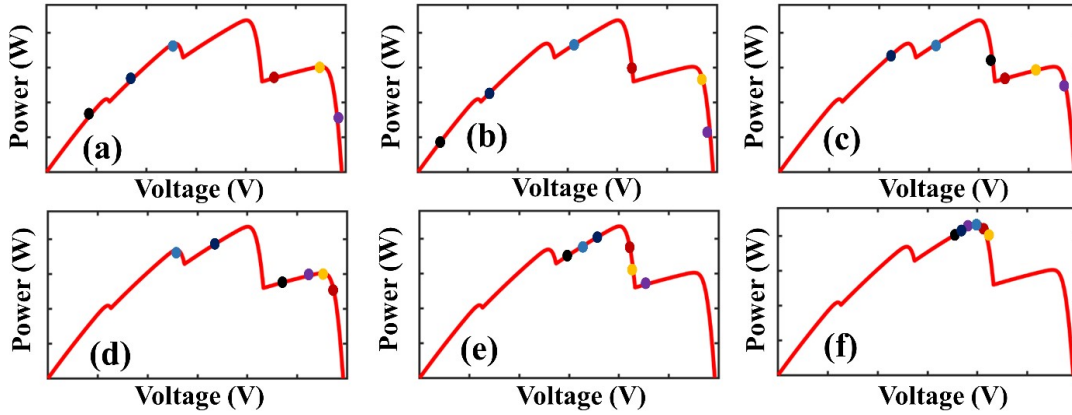
FIGURE 3.7: Movement of particles for proposed technique during extraction of global optimum solution

of HGWOSCA is further elaborated in Figure 3.7. Exploitations become effective after number of iterations which is perfect for the efficiency and oscillations reduction. The operating points lie on P-V curves and I-V curves. Iterative process to track GM under PS is shown in Figure 3.7. In Figure 3.7(a) initialization occurs. In Figure 3.7(b) and 3.7(c) best solution is tracked which is LM3. Figure 3.7(d) and Figure 3.7(e) represent the breaking of the LM3 track and finally, the true GM is tracked successfully in Figure 3.7(f).

3.7 HGWOSCA Under Complex Partial Shading

When large numbers of PV modules undergo partial shading, several closely linked peaks are formed. This type of shading is known as complex partial shading which has already been discussed in case 4. Cluster is the collection of above mentioned local peaks and Cluster Head Maxima (CHM) is a unique point in every cluster.

In Figure 3.8, CPS condition is shown and it can be seen that there are two clusters. Cluster-1 exists in left half plane of P-V curve which contains three MPPs. From left - right LM power is 738.3W, 901.4 W and 892.6 W which is the head maxima of cluster 1 whereas, in cluster 2, there are three MPPs. Powers from left to right are 896.6W, 918.2 W and 851.5W. CHM occurs at the center which is also the

global maxima which is just 17 W less from cluster 1 and also has a close value with other MPPs in cluster 2.
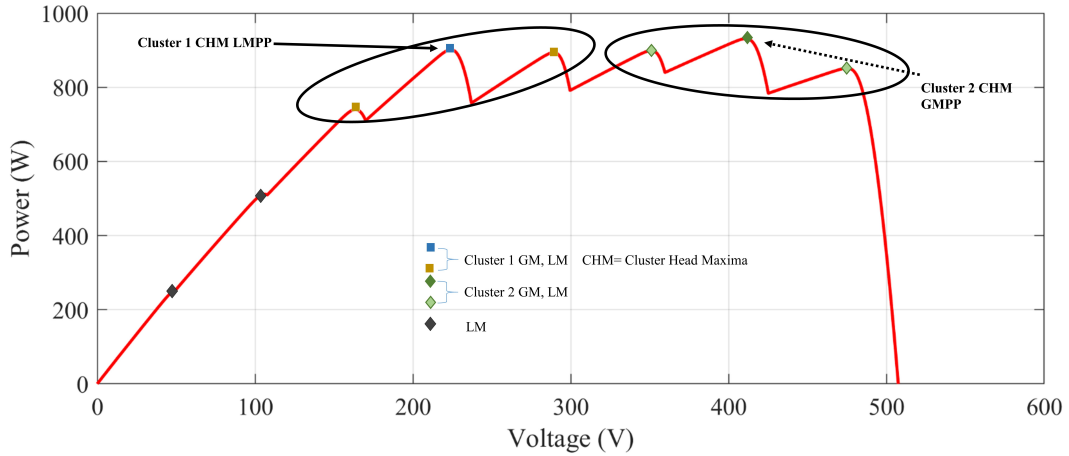

FIGURE 3.8: Cluster Formation of multiple peaks in complex partial shading scenario with two cluster heads

In the last iterations, velocity vectors deliberately retard the movement of the particles. For better convergence and less oscillations, in the last iterative cycles slower movement of particles is suitable. Around 6% power loss occurs in complex partial shading due to undetected GM. The loss becomes prominent due to non-proper tuning of swarm based intelligence techniques. These techniques are effective when the GM is in the center but the problem develops superior as the GMPP is tilted from center. Using of large number of particles is a common approach used to overcome the latter issue however this approach raises the resources to compute the social interaction. Therefore reduced ranged applications, complexity and cost are the side effects. HGWOSCA effectively deals with these issues by increasing the exploration phase and has a slow movement as the iterations increase in order to reduce the oscillations and get GMPP effectively.

3.8 Chapter Summary

In this chapter, proposed MPPT technique, which is the fusion of two meta-heuristic algorithms i.e. grey wolf optimizer and sine cosine algorithm, is explained. The hybrid grey wolf optimizer sine cosine algorithm have the best merits of both algorithms. Then the implementation of HGWOSCA is presented as

MPPT control and explained the working of proposed technique under partial shading condition. HGWOSCA takes less time to track and settle at GMPP with higher efficiency. The working of MPPT technique is also needed to be checked under complex partial shading condition.

Chapter 4

Results and Discussions

In this section 4, different cases have been presented which represents the operating conditions of PV panel. The descriptive structure of the setup implemented for the MPPT control is presented in Figure 4.1. Simulation setup for MPPT control based on Bio-inspired MPPT technique is shown in Figure 4.2, which is simulated using MATLAB/SIMULINK 2018a.

- Performance of HGWOSCA is compared with PSO, PSOGS, CS, P&O, and GHO by simulating four cases.

- Case 1 represents the fast varying conditions. Case 2 and 3 represents the partial shading conditions. Complex partial shading condition is presented in Case 4.

- Table 4.5 represents the detailed performance analysis.

- The specifications of the components used for the simulations are presented in Table 4.1.

Due to high switching frequency of the boost converter, the design value of the inductor and capacitor is low which reduces the size of the circuit and makes less hardware for the implementation. The PV module used is having maximum power of 300 W and load resistance selected for the MPPT implementation is 70 ohms.
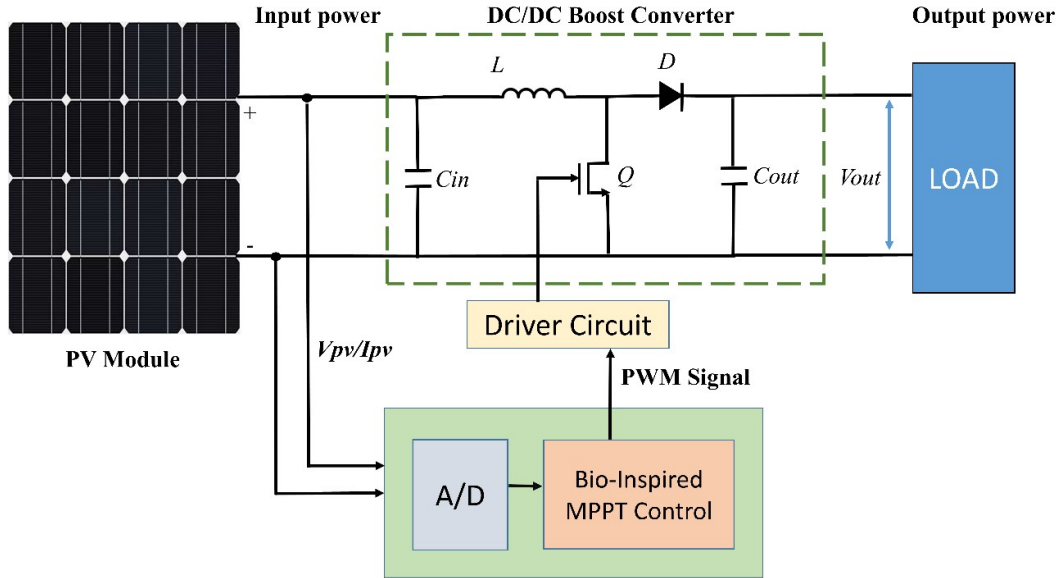
FIGURE 4.1: Descriptive Diagram of Simulation Setup Implemented in MAT-LAB Simulink

TABLE 4.1: Components specifications used for the simulation

Components	Values
Panel Power	320 W
Inductor	1.4 mH
Capacitor at input, Cin	10 uF
Capacitor at output, Cout	470 uF
Frequency of switching, f	50 kHz
Resistive load, RL	70 Ω

4.1 Evaluation Criteria of MPPT Techniques

To evaluate the performance of MPPT techniques, evaluation criteria is defined below:
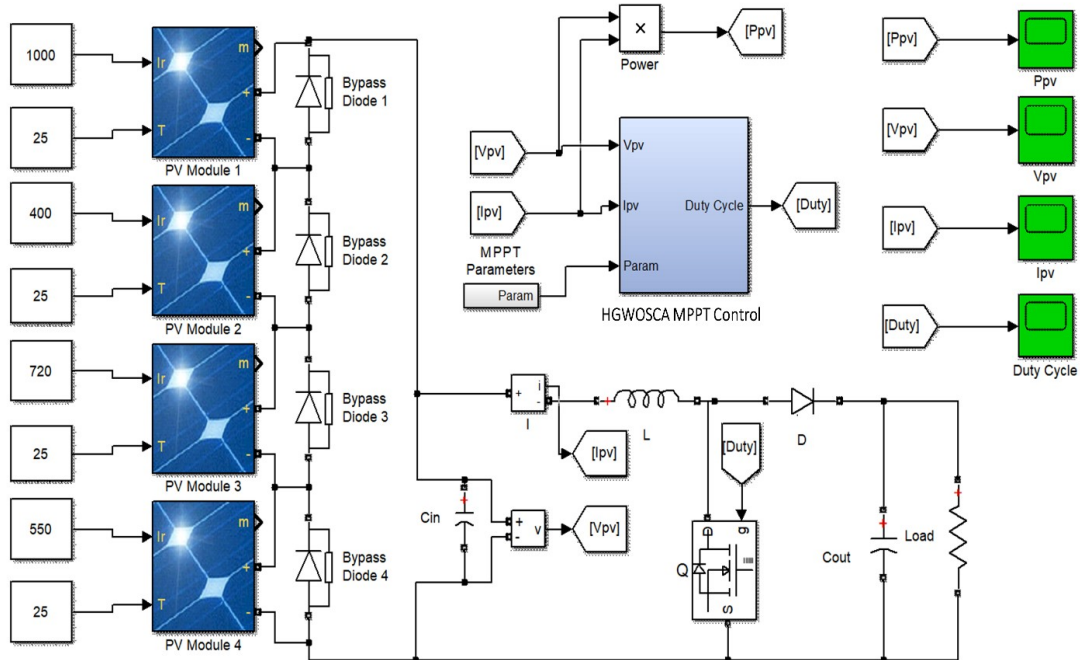
FIGURE 4.2: Simulation Setup of Bio-Inspired based MPPT Control of PV System

- Oscillations at GMPP, Power tracked, tracking time, settling time and power efficiency are the terms used for comparative analysis.

- Tracking time is the time required to track the global maximum power point. Low tracking time will lead to high efficiency and less power loss.

- Settling time is the time required to settle at the global maximum power point with no oscillations. Less settling time also leads to the higher efficiency of PV system.

- Tracked Power is the power at which the MPPT technique is settled which defines the tracking efficiency of the PV system. For MPPT technique it needs to be maximum.

- Robustness and sensitivity of MPPT techniques can be validated using the statistical analysis i.e. Root mean square error (RMSE), Mean absolute error (MAE), relative error (RE).

TABLE 4.2: Irradiance pattern for cases 1, 2 and 3

Cases	Irradiances G (kW/m2) of each PV module				Pmax (Watts)
	PV1	*PV2*	*PV3*	*PV4*	
Case 1: Varying	1,0.35,0.75	1,0.35,0.75	1,0.35,0.75	1,0.35,0.75	1,280,257,957
Case 2: PS-1	0.35	0.8	0.5	0.24	335
Case 3: PS-2	0.9	0.69	0.8	0.5	702

4.2 Case 1: Fast Changing Irradiance

4.2.1 Test Scenario for Case 1:

Under uniform irradiance, PV panels obtain same irradiances but irradiance intensity change over the time known as rapidly changing irradiance. Case 1 shown in Table 4.2 encapsulates the behavior of MPPT techniques in fast varying irradiance and test pattern. The changing irradiance with the maximum power is shown in Figure 4.3. The PV curves for the change in irradiance in case 1 is shown in Figure 4.4. The maximum power point is also mentioned in P-V curve which needs to track by the MPPT technique.

4.2.2 Case 1 Results

In Case 1 irradiance is changing and the re-initialization of the particles occurs after every 2 seconds due to change in power and algorithms restart and again track the power. The variation of the duty cycle for tracking of power. The duty cycles are evaluated and fitness values are calculated during the exploration and exploitation phase. HGWOSCA MPPT technique is effective in both the exploration and
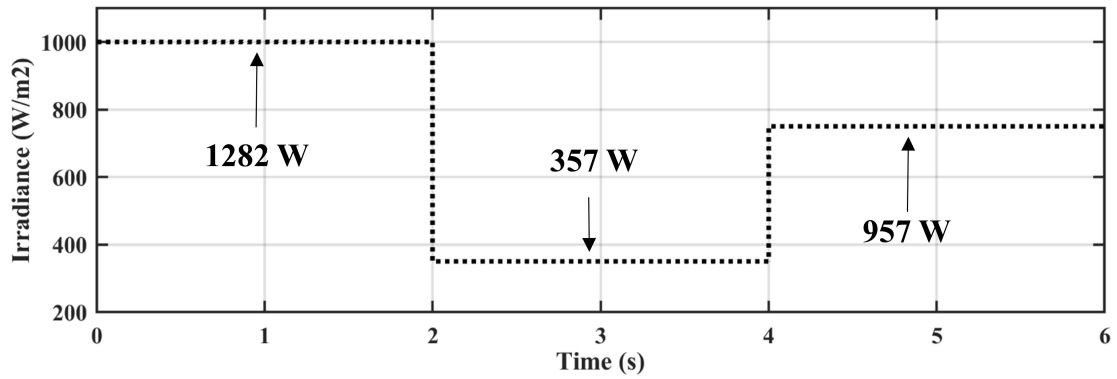
FIGURE 4.3: Irradiance pattern for PV panels for case 1 with maximum power at every changing irradiance
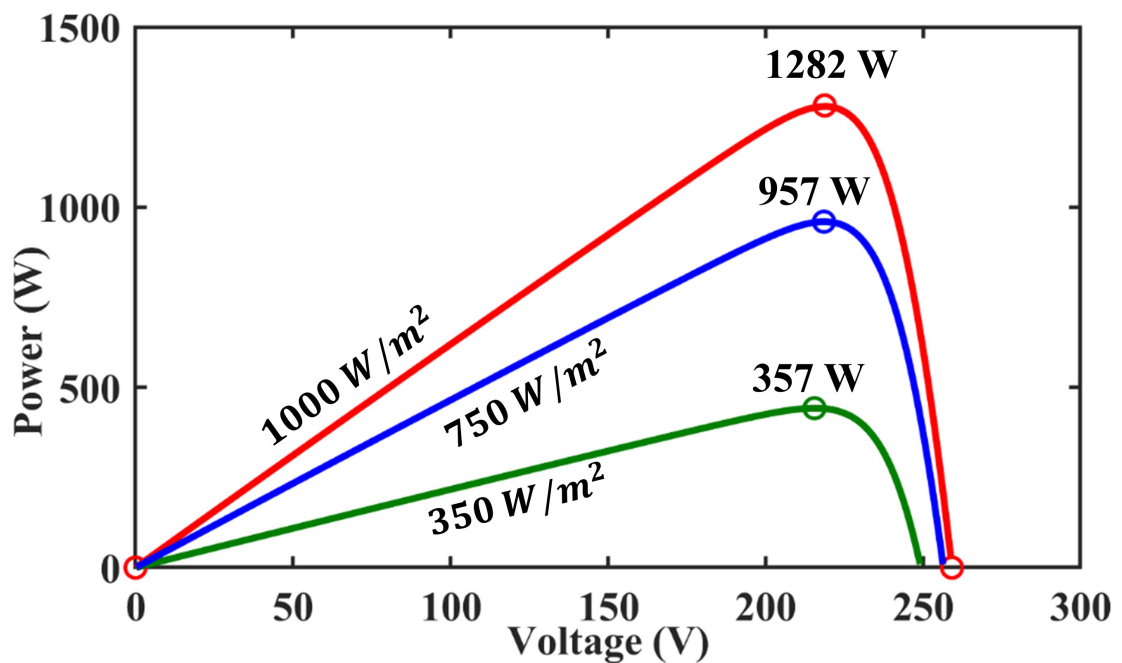
FIGURE 4.4: PV curves for different irradiance levels in case 1

exploitation phase and extracts maximum power as compared to other techniques. HGWOSCA have good capability of exploration and exploitation phases, which cause effective tracking of GMPP under dynamic irradiance variation conditions. The HGWOSCA tracks the global maxima in less than 0.2 seconds and have high tracking efficiency. Figure 4.5 (a) shows the tracking of power under case 1 by HGWOSCA and Figure 4.5 (b) shows the variation of duty cycle for case 1. The evaluation parameter achieved by the HGWOSCA is shown in Figure 4.6.

Integration of Sine-Cosine algorithm in GWO makes exploration capability very high, which helps to locate the GM very efficiently. Over the iterations, the parameter "a" decreases, which works as exploitation, phase, and reduces the movement

of the particles. Over the iterations, the particles will start converging to the global maxima and settles at GM. The average maximum power in case 1 is 1282 W and the power tracked by the HGWOSCA is 1280 W which shows the high efficiency of the HGWOSCA under varying conditions.

The effectiveness of the proposed technique can be verified by the tracking and settling time. The tracking time is 0.16 seconds and the settling time is 0.24 seconds. This proposes that the HGWOSCA is best suitable for MPPT applications.
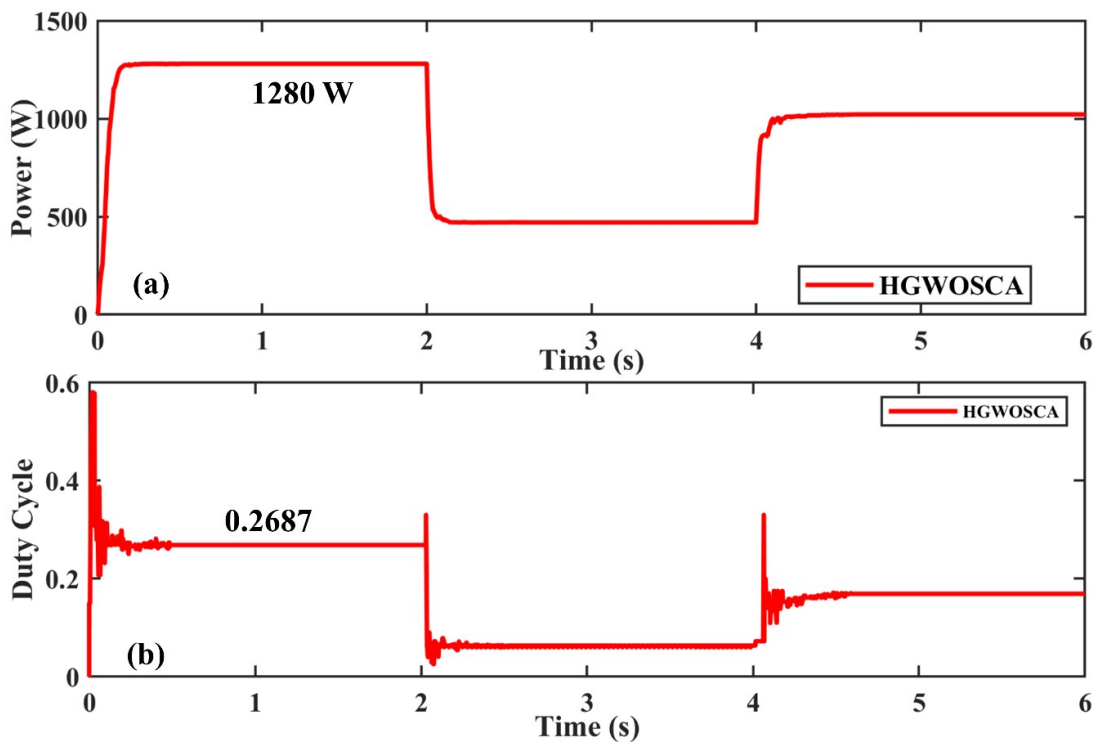
FIGURE 4.5: (a) Power Tracking of HGWOSCA in Case 1 (b) Duty Cycle Variation of HGWOSCA in Case 1

GHO has the capability to effectively track GM under varying conditions but the oscillations after tracking of GM are the main problems, which cause the low efficiency. The re-initialization occurs after every 2 seconds. Power tracked by the GHO under case 1 is shown in Figure 4.7 (a) and duty cycle variation by GHO under case 1 is shown in Figure 4.7 (b). The extraction of the energy is also an important parameter, which depends upon the extraction of power over time. Therefore, high power extraction leads to higher energy extraction from the PV system.

FIGURE 4.6: Evaluation parameters of HGWOSCA in case 1

Parameter "c" in GHO causes oscillations, which reduces average power and efficiency. The effective tuning of parameter "c" is the biggest problem in GHO, It has to be done very precisely for effective tracking. The average power tracked by the GHO is 829.7 W, which is low as compared to HGWOSCA. The track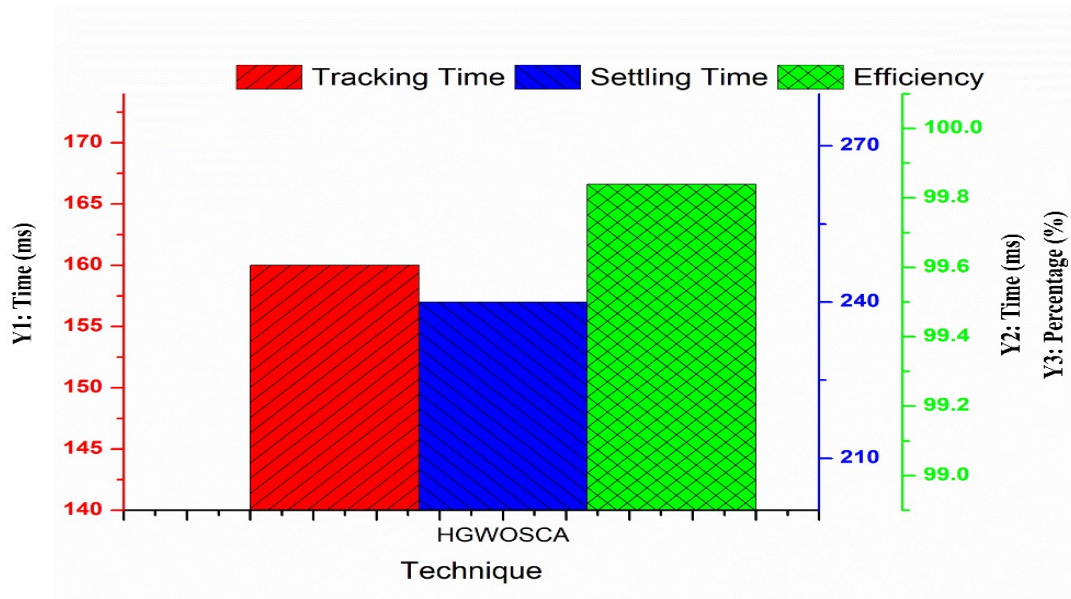ing time of the GHO is 0.19 seconds and the settling time of the GHO is 0.35 seconds. The tracking and settling time are high as compared to HGWOSCA, which causes the low efficiency of the GHO as compared to HGWOSCA. The evaluation parameters achieved by GHO are presented in Figure 4.8.

Particle swarm optimization with gravitational search (PSOGS) is another technique that is implemented for the MPPT application. The PSOGS have low oscillations as compared to GHO but have low tracking efficiency due to restricted movement of the particle due to gravitational effect. The power tracked by PSOGS is shown in Figure 4.9 (a) and the duty cycle variation of PSOGS under varying irradiance condition is shown in Figure 4.9 (b).

After every 2 seconds, the particles are initialized and the particle updation occurs due to PSOGS algorithm but the oscillations are very low. The average power tracked by the PSOGS is 829.6 W, which is less than GHO and HGWOSCA.

FIGURE 4.7: (a) Power Tracking of GHO in Case 1 under varying irradiance
(b) Duty Cycle Variation of GHO in Case 1 under varying irradiance
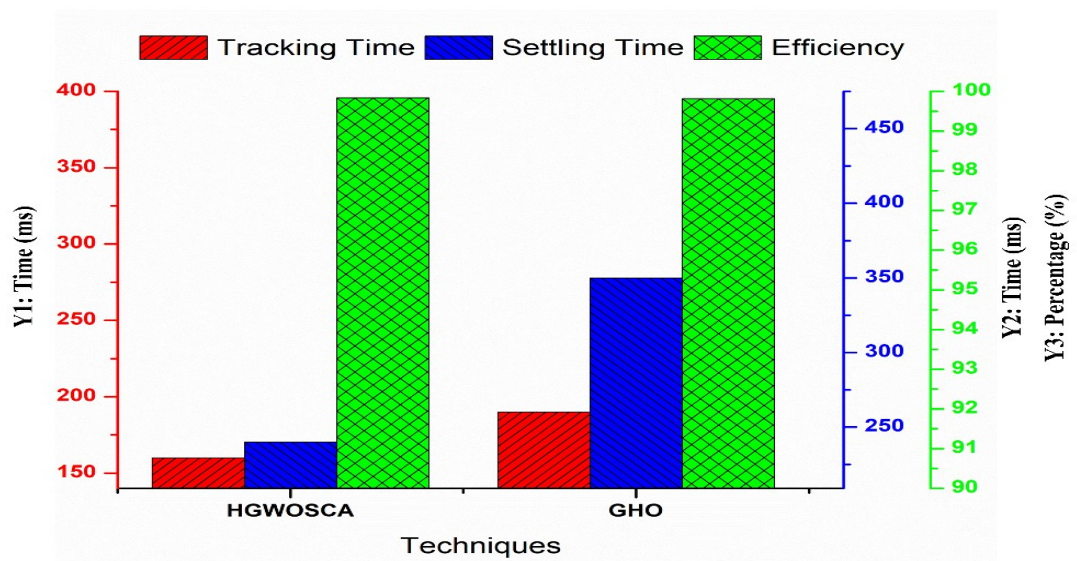
FIGURE 4.8: Evaluation Parameter of GHO for Case 1

The tracking time and settling time are the 0.21 seconds and 0.35 seconds respectively. The oscillations of PSOGS after tracking of GM is very low due to high exploitation behavior. The tracking time, settling time and efficiency achieved by the PSOGS is shown in Figure 4.10.

PSOGS is the variant of the PSO algorithm, which shows better results as compared to CSA and PSO. In addition, the extraction of energy is less as compared to GHO and HGWOSCA.

FIGURE 4.9: (a) Power Tracking of PSOGS in Case 1 under varying irradiance (b) Duty Cycle Variation of PSOGS in Case 1 under varying irradiance

FIGURE 4.10: Evaluation Parameter of PSOGS for Case 1

Levy flight function is one of the random walks, which are used in the optimization algorithm. Cuckoo search uses the levy flight function for updation of particles
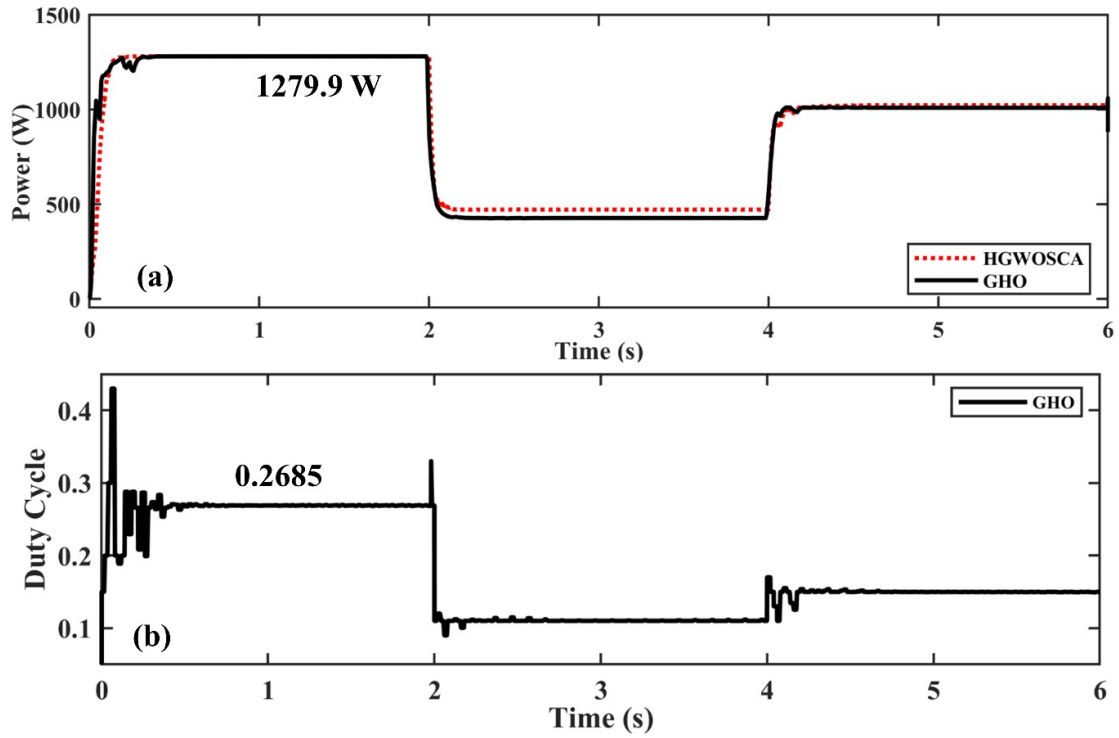
FIGURE 4.11: (a) Power Tracking of CSA in Case 1 under varying irradiance
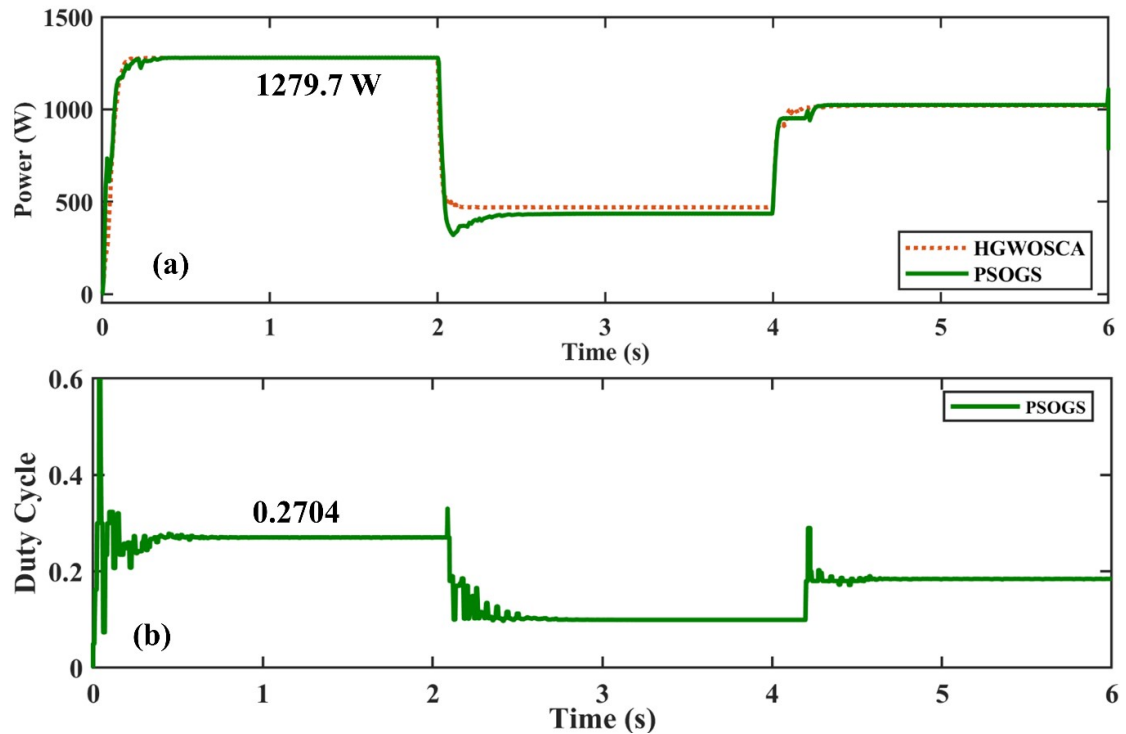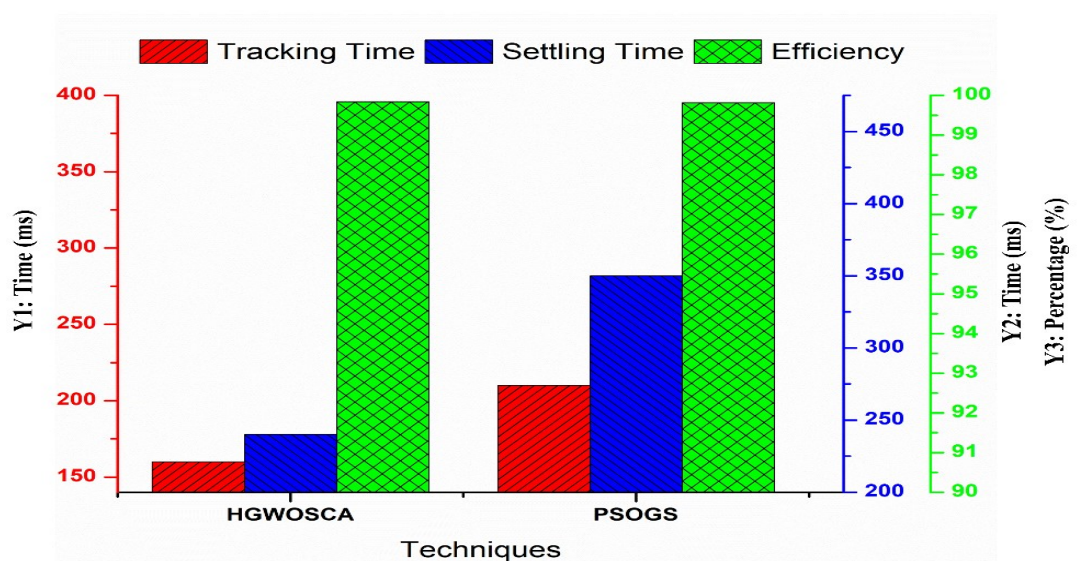(b) Duty Cycle Variation of CSA in Case 1 under varying irradiance

position. Due to this levy flight function the particles are moving even after the exploitation phase. Due to this oscillations can be observed after tracking of GM and the efficiency of the CS based MPPT technique is reduced.

Power tracking capability of CSA is shown in Figure 4.11 (a) and the variation of the duty cycle is shown in Figure 4.11 (b). The power tracked by the CSA is 1278 W which is less as compared to GHO, HGWOSCA, and PSOGS. The average time taken to track and settle at GM is 0.35 seconds and 0.55 seconds respectively. The high settling time validates that the CSA uses the levy flight function for updation of particles position.

The evaluation parameters achieved by the CSA MPPT technique are presented in Figure 4.12 which validates that the efficiency achieved by the CSA is lower than HGWOSCA and has high settling and tracking time as compared to HGWOSCA.

Particle swarm optimization uses the behavior of birds flock to locate the global maxima in the optimization problem. The position updation of the particles in PSO depends upon the velocity vector used which has random numbers embedded. The parameters C1 and C2 are also required to tune for the specified applications.
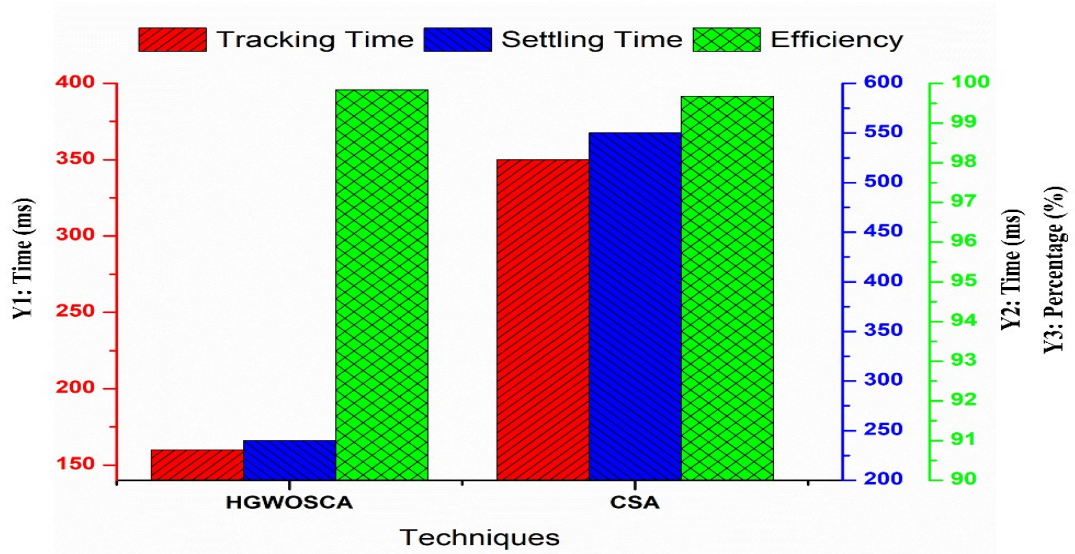
FIGURE 4.12: Evaluation parameters of CSA in case 1

PSO is one of the first swarm optimization algorithms presented that's why it is used for the comparison.

Particle swarm optimization algorithm shows high oscillations due to random numbers in velocity vector and the weight factor is used to control the movement of particles. Figure 4.13(a) shows the power tracking of PSO under case 1 and Figure 4.13(b) shows duty cycle variation of PSO for case 1. The tracking time and settling time achieved by PSO are 0.32 s and 0.45 s respectively. The efficiency achieved by PSO is 99.72 %. These evaluation parameters are shown in Figure 4.14.

HGWOSCA settles 35% faster at GM which shows that it is robust. HGWOSCA reduces the oscillations at GM, which in turn increases the efficiency and helps in saving power. P&O congregates at GM but doesn't settle at GM, rather it keeps on oscillating around 40 W which decreases its efficiency.
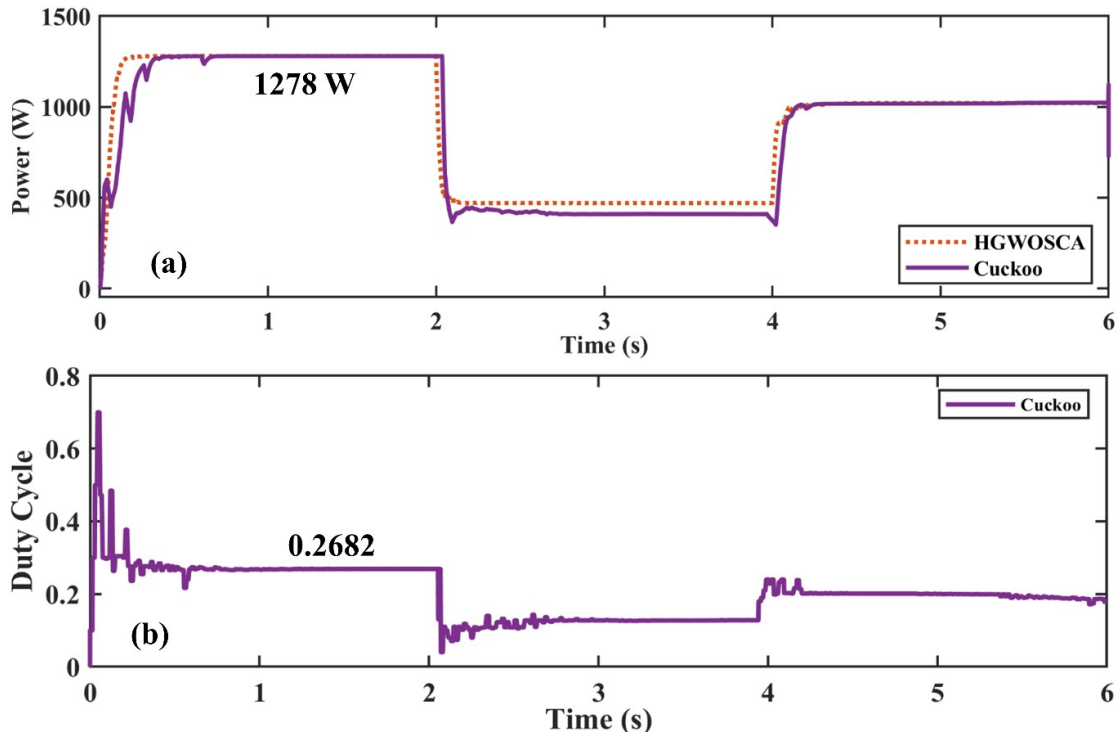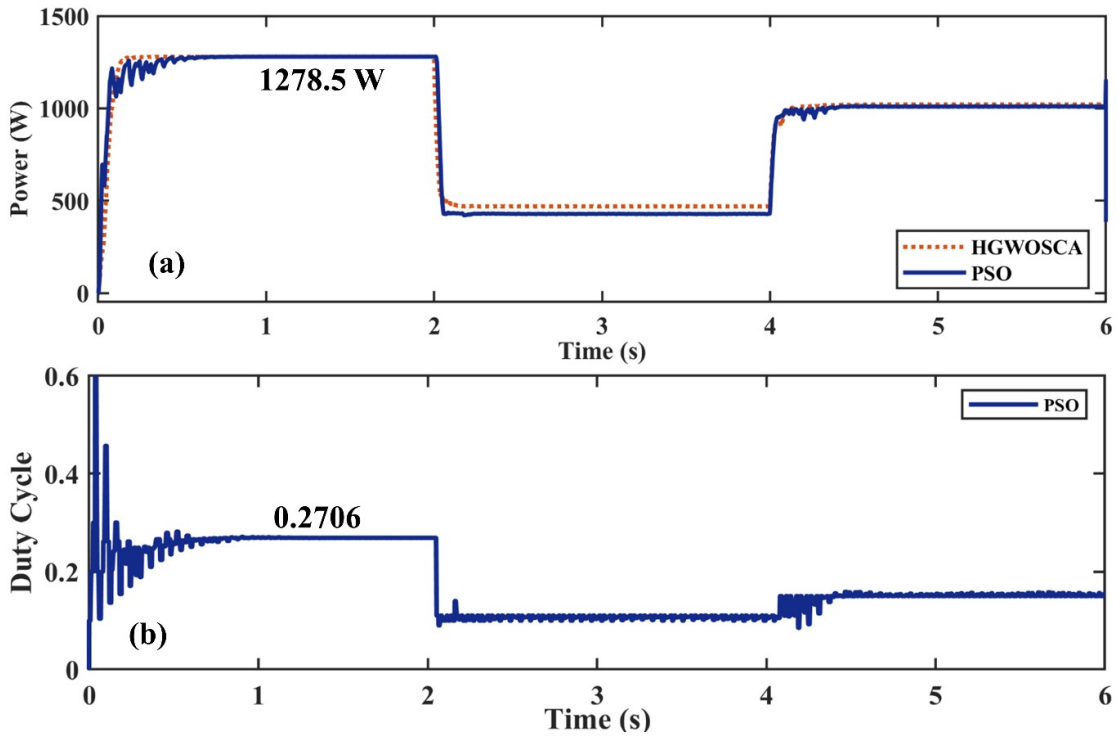
FIGURE 4.13: (a) Power Tracking of PSO in Case 1 under varying irradiance
(b) Duty Cycle Variation of PSO in Case 1 under varying irradiance
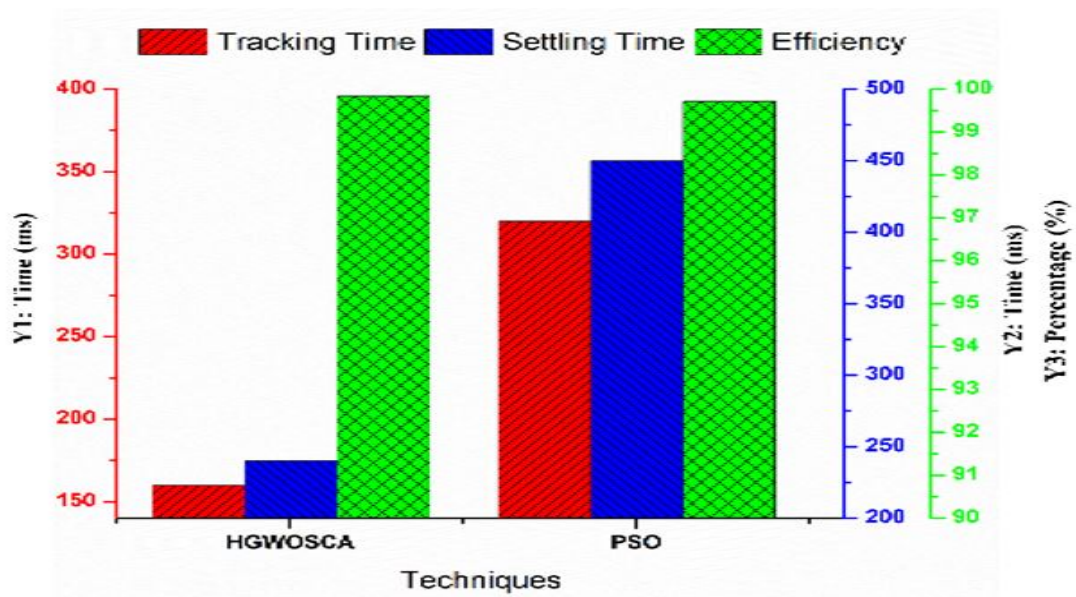
FIGURE 4.14: Evaluation parameter of PSO in case 1

4.2.3   Comparative Analysis Case 1

Power achieved by HGWOSCA is 1280 W, which is highest as compared to 1279.9 W, 1279.7 W, 1278 W, 1278.5 W, 1257 W of GHO, PSOGS, CS, PSO and P&O respectively.

HGWOSCA achieved the highest efficiency of 99.84%, whereas other techniques offered the efficiency of 99.82%, 99.81%, 99.68%, 99.72% and 98.04% for GHO, PSOGS, CS, PSO and P&O respectively.

To gauge the performance of fast varying irradiance, the average value is suited the best. The average power achieved by HGWOSCA, GHO, PSOGS, CS, PSO and P&O are 924.3 W, 912.33 W, 911.66 W, 903.3 W, 902.66 W and 909.33 W. This shows that HGWOSCA achieved 12-15 W more power than others.

The overall efficiency achieved by HGWOSCA, GHO, PSOGS, CS, PSO and P&O is 99.17%, 97.88%, 97.56%, 97.78%, 96.92% and 96.81% respectively. Therefore, these techniques can be ranked as HGWOSCA > GHO > PSOGS > CS > PSO > P&O. Tracking time of HGWOSCA, GHO, PSOGS, CS, PSO and P&O is 0.16s, 0.19s, 0.21s, 0.35s, 0.32s and 0.12s. Settling time of HGWOSCA, GHO, CS, PSOGS, PSO and P&O is 0.24s, 0.35s, 0.55s, 0.35s, 0.45s and 0.12s. The overall comparative analysis of all techniques in case 1 is presented in Figure 4.15.
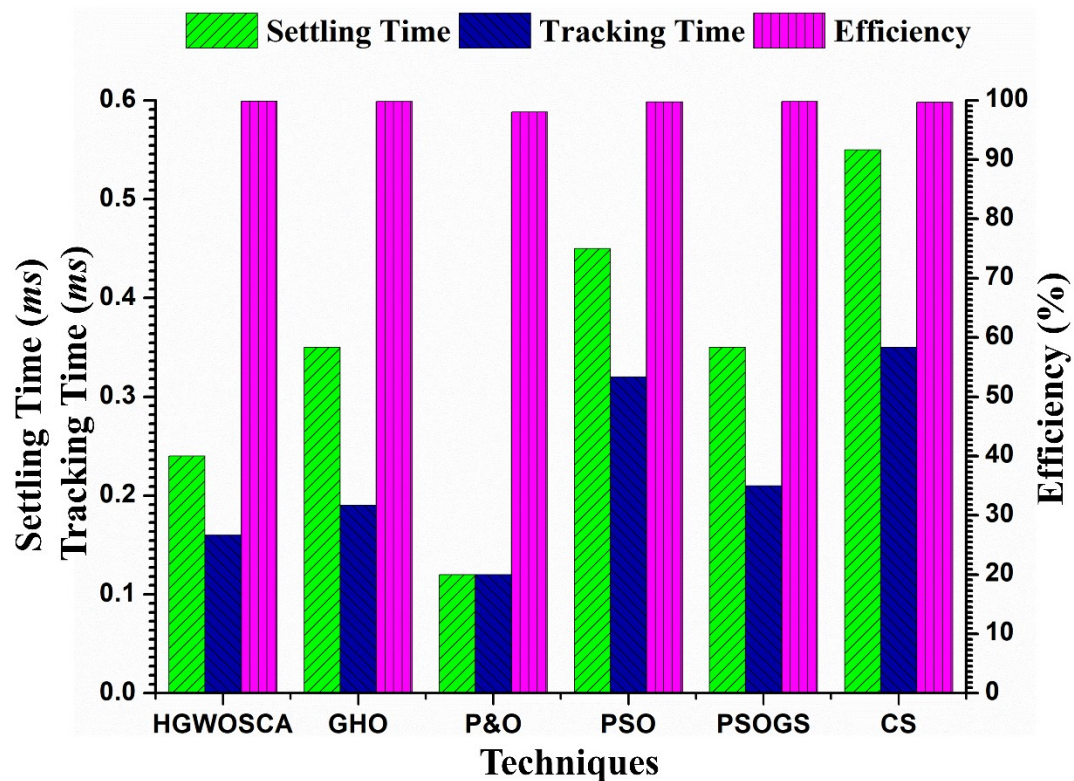
FIGURE 4.15: Comparative analysis of evaluation parameters for case 1

4.3 Case 2: PS Condition

4.3.1 Test Scenario Case 2

In this case, GMPP is at 335W. Irradiance pattern is shown in Table 4.2, whereas P-V curve is presented in Figure 4.16 with center skewed GMPP and the maximum power is 335 W. The irradiance pattern on all 4 panels is shown in Figure 4.17. The irradiance on every panel is constant for 1 s and created a partial shading condition. In this PV curve for case 2, there are 4 peaks which have 3 local maxima's and 1 global maxima. The GMPP is center skewed which means he PV curve have GMPP in the center and have LM at the right and left side of the peak. Conventional MPPT techniques i.e. perturb and observe is unable to track GMPP and stuck at the LMPP that why the P&O technique is not included in the comparison.
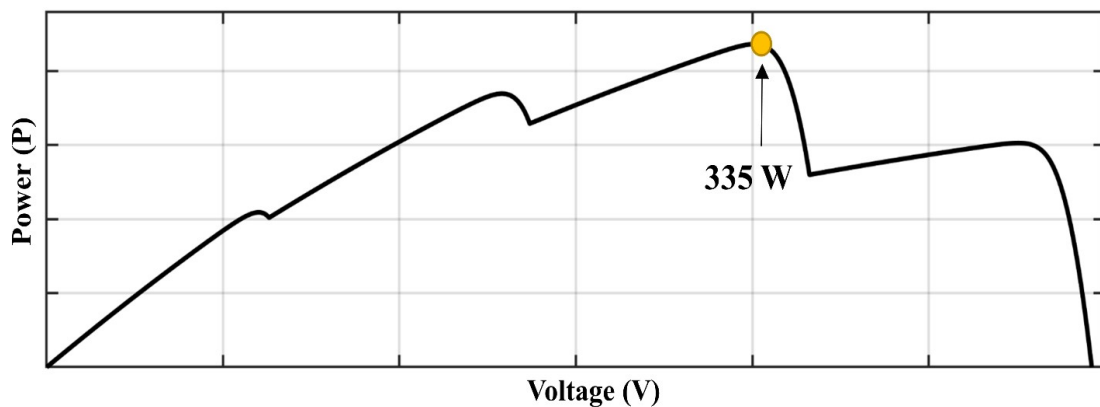
FIGURE 4.16: PV Curve for the partial shading condition in case 2 with center skewed global maxima

4.3.2 Case 2 Results

HGWOSCA has the capability of distinguishing among exploration and exploitation phases, which cause effective tracking of GMPP under partial shading conditions. The HGWOSCA tracks the global maxima in less time with high efficiency. Figure 4.18(a) shows the tracking of power under case 2 by HGWOSCA and Figure
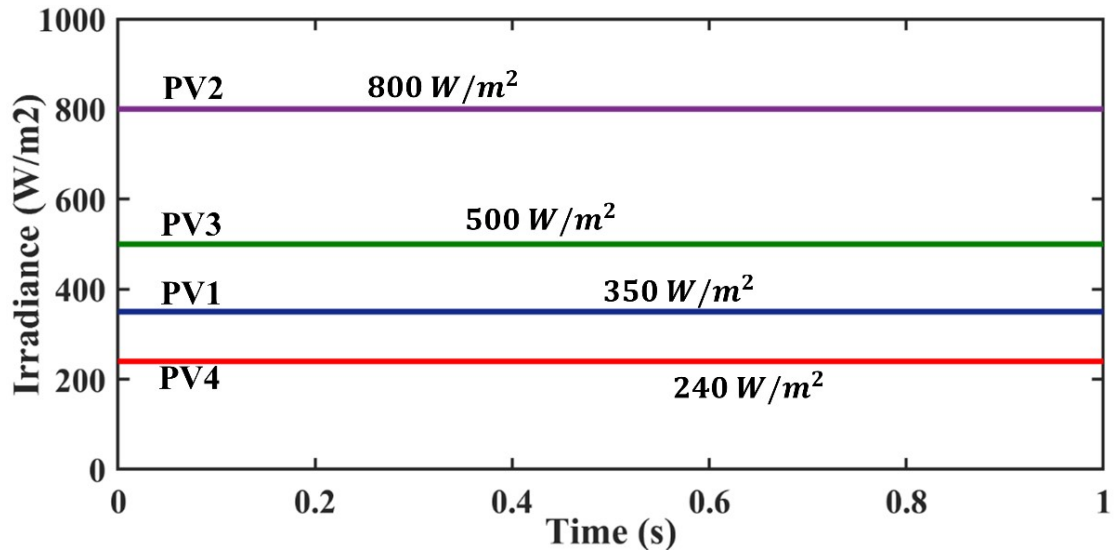
FIGURE 4.17: Irradiance Values on all panels in case 2

4.18()b) shows the variation of duty cycle for case 2. The evaluation parameter achieved by the HGWOSCA shown in Figure 4.19.

Integration of Sine-Cosine algorithm in GWO makes exploration capability very high, which helps to locate the GM very efficiently. Over the iterations, the parameter "a" decreases, which works as exploitation, phase and reduces the movement of the particles. Over the iterations, the particles will start converging to the global maxima and settles at GM. The maximum power in case 2 is 335 W and the power tracked by the HGWOSCA is 334.7 W which shows the high efficiency of the HGWOSCA under partial shading conditions.

The evaluation parameter of HGWOSCA for case 2 is shown in Figure 4.19 which shows that the tracking and settling time of HGWOSCA is 0.15 s and 0.22 s respectively. The efficiency achieved is upto 99.91 %.

GHO have the capability to effectively track GM under partial shading conditions but the oscillations after tracking of GM are the main problems, which cause the low efficiency. Power tracked by the GHO under case 2 is shown in Figure 4.20(a) and duty cycle variation by GHO under case 2 is shown in Figure 4.20(b).

Parameter "c" in GHO causes oscillations, which reduces the efficiency. The effective tuning of parameter "c" is the biggest problem in GHO, that has to be
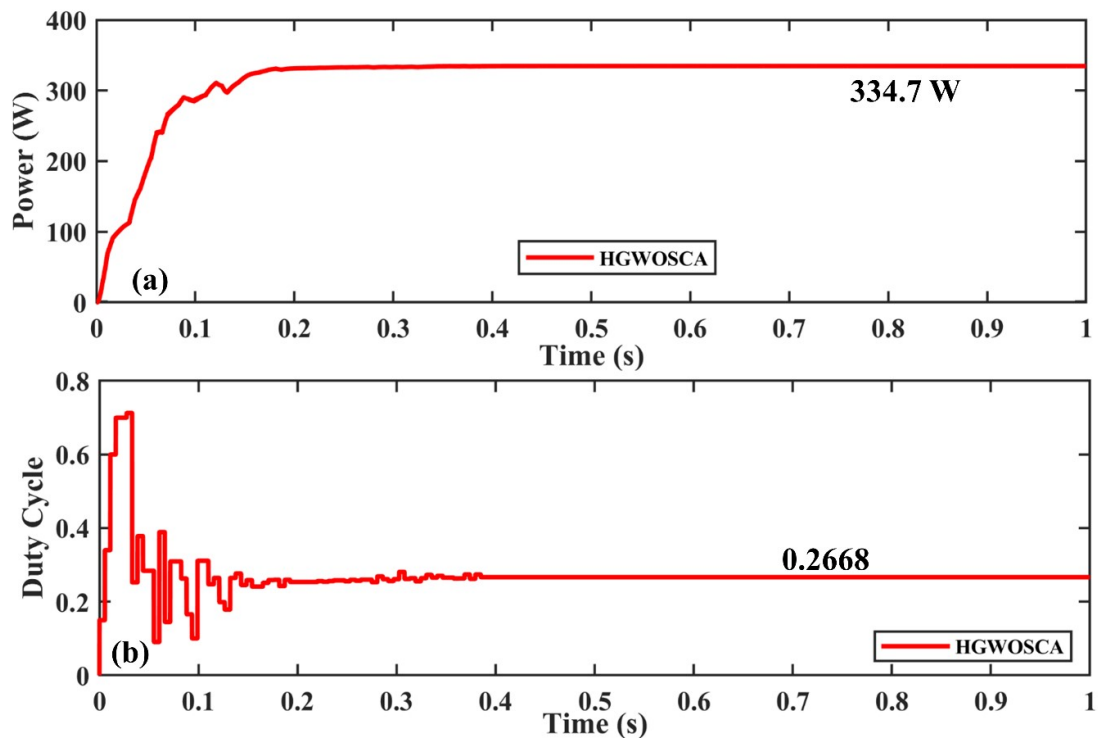
FIGURE 4.18: (a) Power Tracking of HGWOSCA in Case 2 under PSC (b)
Duty Cycle Variation of HGWOSCA in Case 2 under PSC
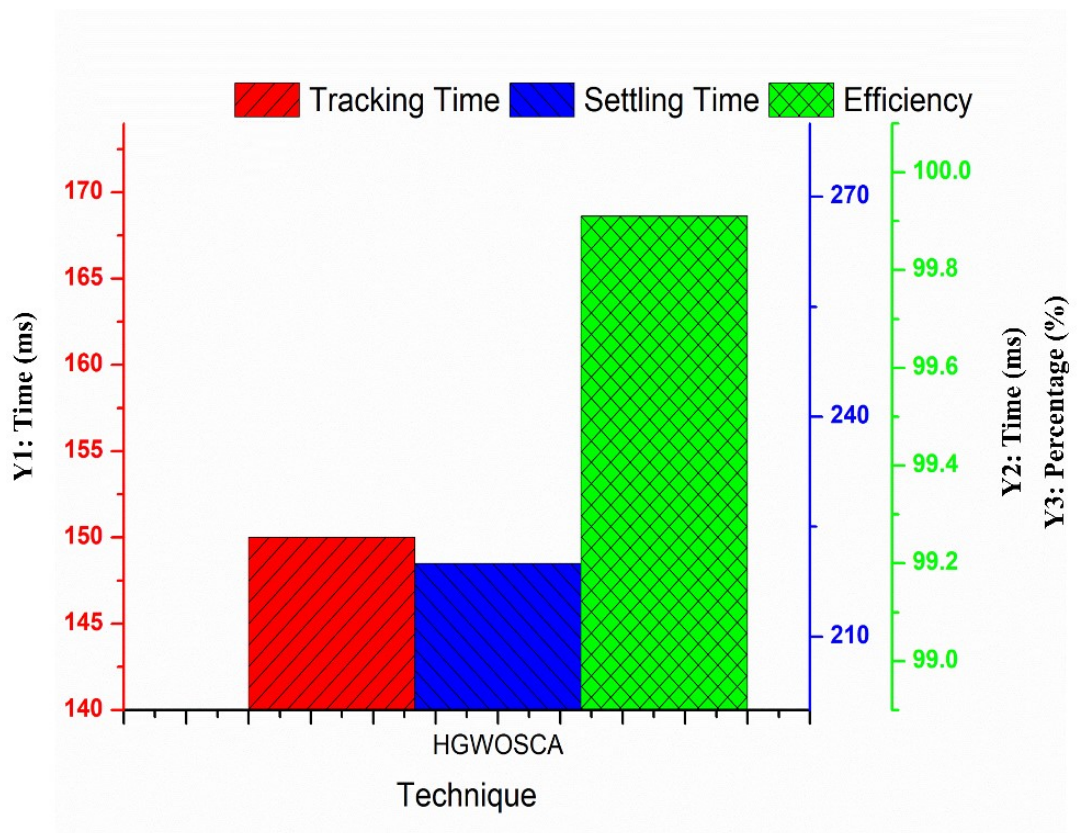
FIGURE 4.19: Evaluation parameter of HGWOSCA for case 2

done very carefully for effective tracking. The power tracked by the GHO is 334.6 W, which is low as compared to HGWOSCA. The tracking time of the GHO is 0.16 seconds and the settling time of the GHO is 0.51 seconds. The tracking and settling time are high as compared to HGWOSCA, which causes the low efficiency of the GHO as compared to HGWOSCA. The evaluation parameters achieved by GHO are presented in Figure 4.21.

The extraction of the energy is also an important parameter, which depends upon the extraction of power over the time. Therefore, high power extraction leads to high-energy extraction from the PV system.
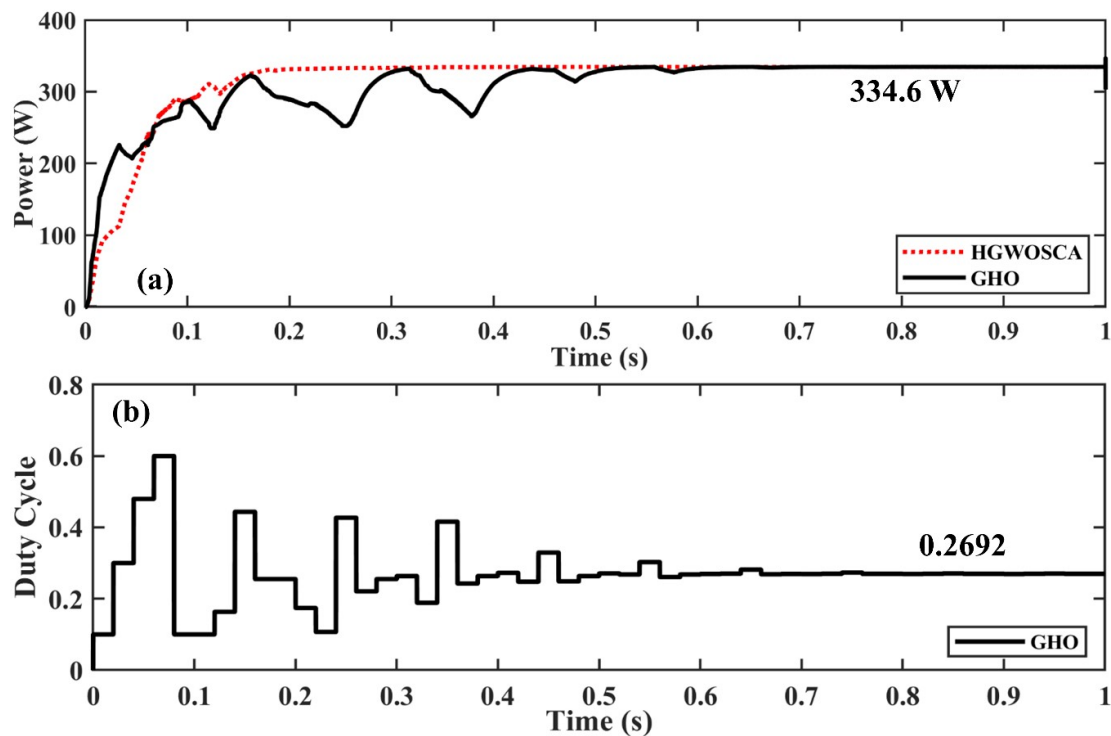
FIGURE 4.20: (a) Power Tracking of GHO in Case 2 under PSC (b) Duty Cycle Variation of GHO in Case 2 under PSC

Particle swarm optimization with gravitational search (PSOGS) is the another technique which is implemented for the MPPT application. The PSOGS have low oscillations as compared to GHO but have low tracking efficiency due to restricted movement of the particle due to gravitational effect. The power tracked by PSOGS is shown in Figure 4.22(a) and the duty cycle variation of PSOGS under partial shading condition is shown in Figure 4.22(b).
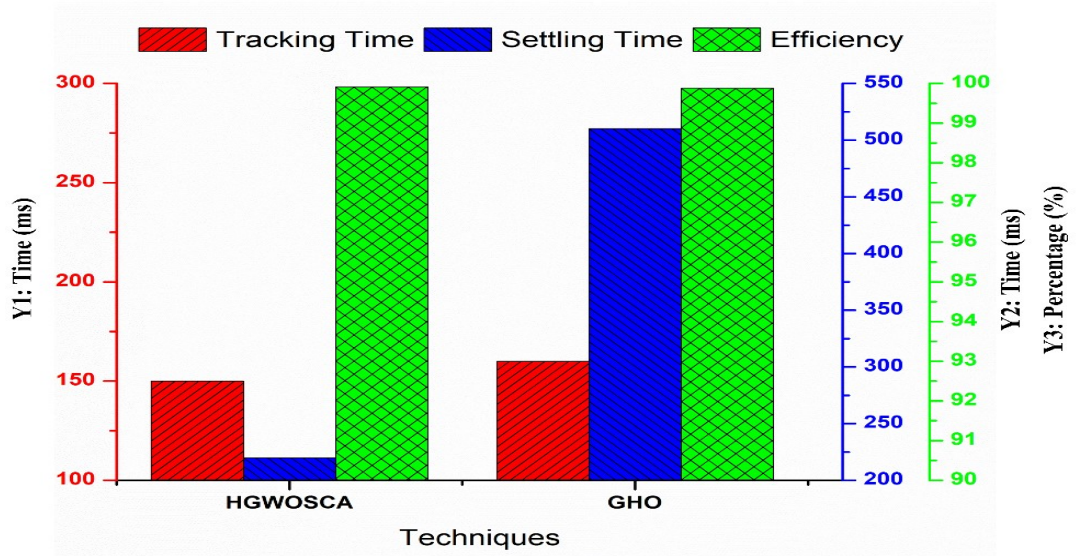
FIGURE 4.21: Evaluation parameter of GHO for case 2
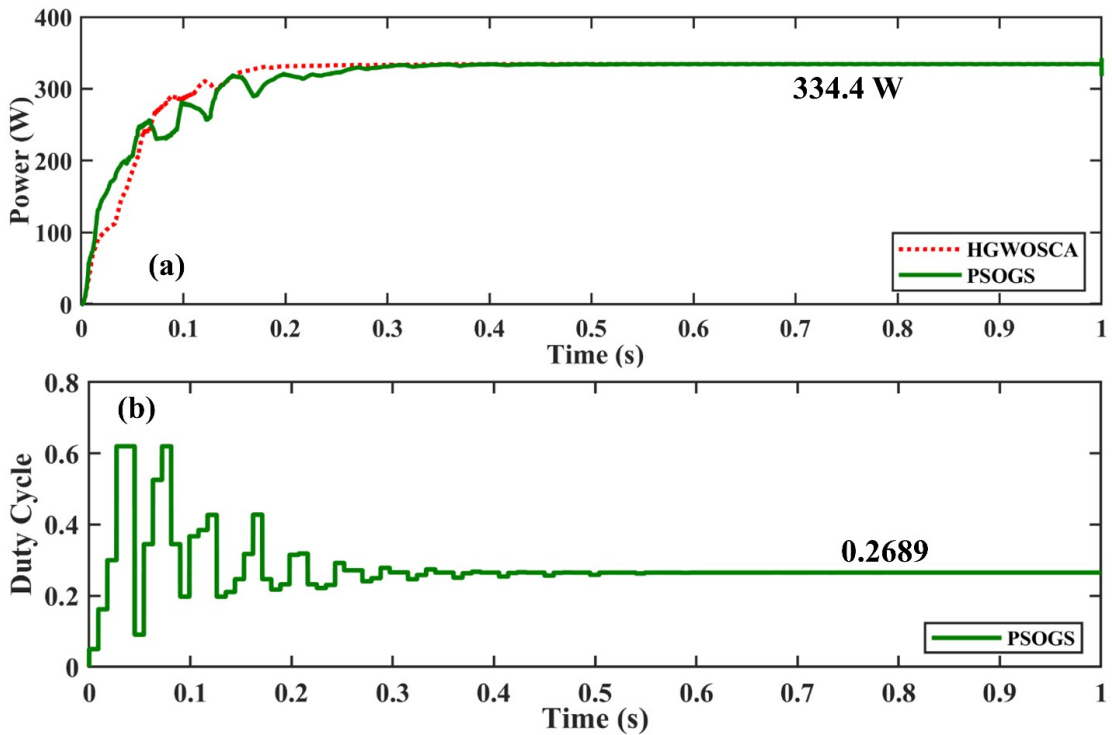
FIGURE 4.22: (a) Power Tracking of PSOGS in Case 2 under PSC (b) Duty
Cycle Variation of PSOGS in Case 2 under PSC

Under partial shading condition random assignment of particles position occurs
and the particle updation occurs due to PSOGS algorithm but the oscillations are
very low. The average power tracked by the PSOGS is 334.4 W, which is less than
GHO and HGWOSCA. The tracking time and settling time are 0.27 seconds and
0.55 seconds respectively. The oscillations of PSOGS after tracking of GM is very

low due to high exploitation behavior.

Tracking time, settling time, and efficiency achieved by PSOGS is shown in Figure 4.23. The efficiency achieved by PSOGS is 99.82 % which is less than HGWOSCA.
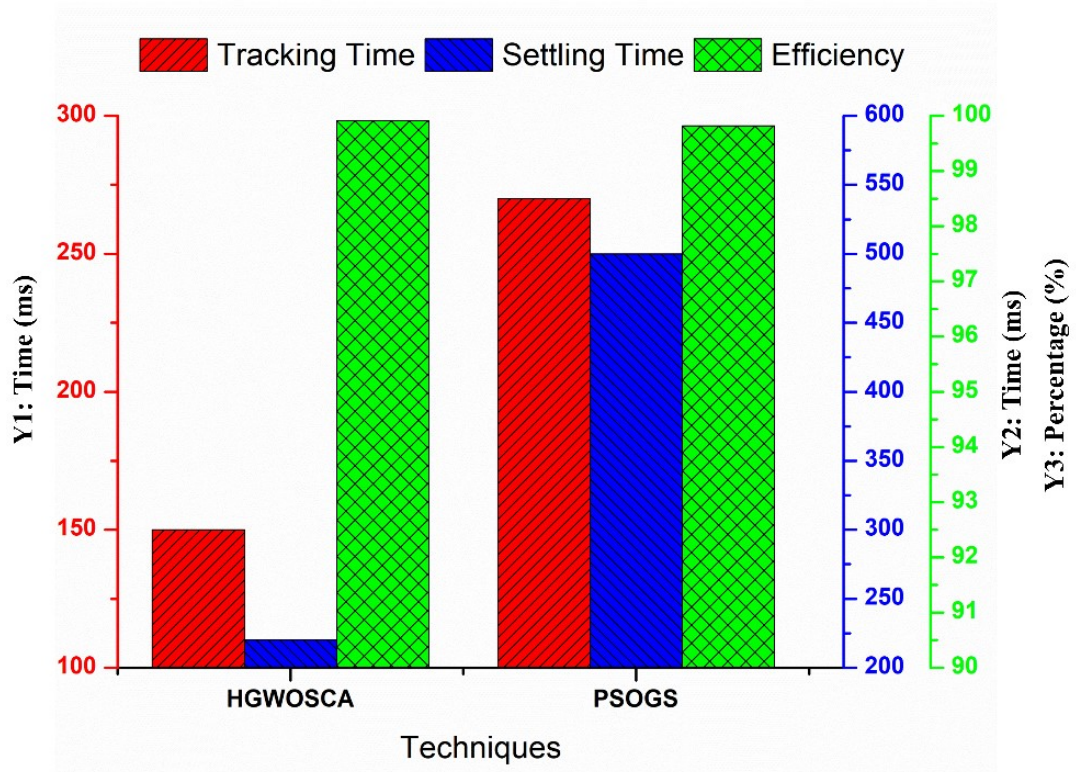
FIGURE 4.23: Evaluation parameter of PSOGS for case 2

Levy flight function is one of the random walks, which are used in optimization algorithm. Cuckoo search uses the levy flight function for updation of particles position. Due to this levy flight function the particles are moving even after the exploitation phase. Due to this oscillations can be observed after tracking of GM and the efficiency of the CS based MPPT technique reduced.

Power tracking capability of CSA is shown in Figure 4.24(a) and the variation of the duty cycle is shown in Figure 4.24(b). The power tracked by the CSA is 334.5 W which is less as compared to GHO, HGWOSCA and PSOGS. The average time taken to track and settle at GM is 0.30 seconds and 0.64 seconds respectively. The high settling time validates that the CSA uses the levy flight function for updation of particles position.

The traking time, settling time and efficiency achieved by CSA is shown in Figure 4.25. The efficiency achieved is 99.85 % which is less as compared to HGWOSCA and GHO.

FIGURE 4.24: (a) Power Tracking of CSA in Case 2 under PSC (b) Duty Cycle Variation of CSA in Case 2 under PSC
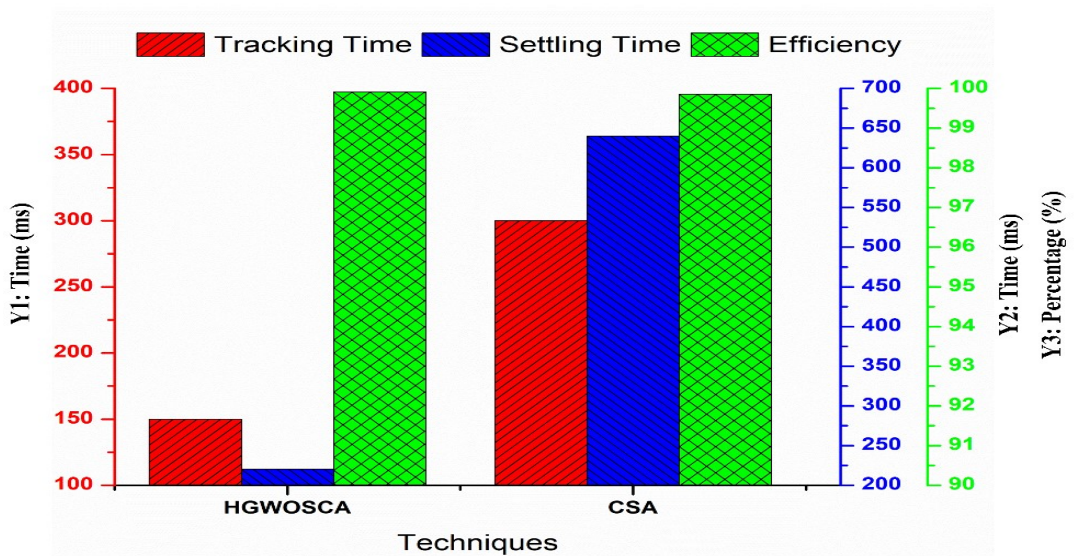
FIGURE 4.25: Evaluation parameter of CSA for case 2

Particle swarm optimization uses the behavior of birds flock to locate the global maxima in the optimization problem. The position updation of the particles in

PSO depends upon the velocity vector used which has random numbers embedded. The parameters C1 and C2 are also required to tune for the specified applications. PSO is one of the first swarm optimization algorithms presented that's why it is used for the comparison.

Particle swarm optimization algorithm shows high oscillations due to random numbers in velocity vector and the weight factor is used to control the movement of particles. Figure 4.26(a) shows the power tracking of PSO under case 2 and Figure 4.26(b) shows duty cycle variation of PSO for case 2. The tracking time and settling time achieved by PSO is 0.30 s and 0.75 s respectively. The efficiency achieved by PSO is 99.85 %. These evaluation parameters are shown in Figure 4.27.

PSO, PSOGS, GS, CS and GHO have randomness which causes more oscillations. PSO and CS both track GMPP at 334.5 however with the toll of high settling time of 0.75s and 0.64s respectively which causes power loss and decrease efficiency.
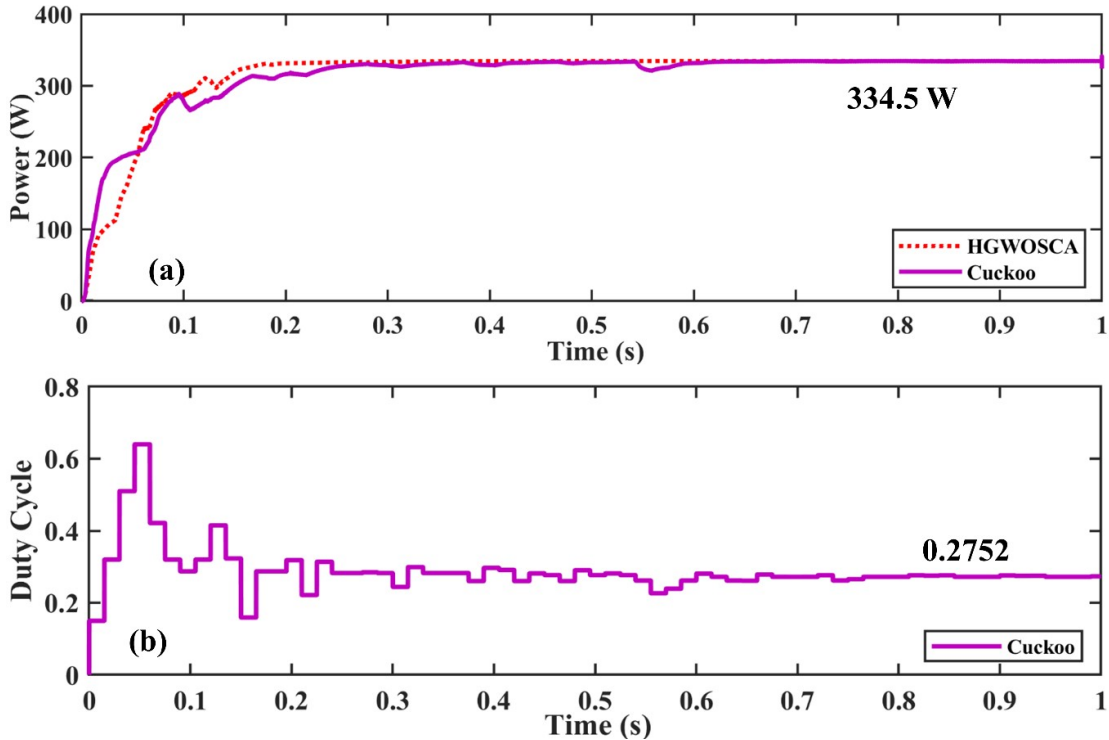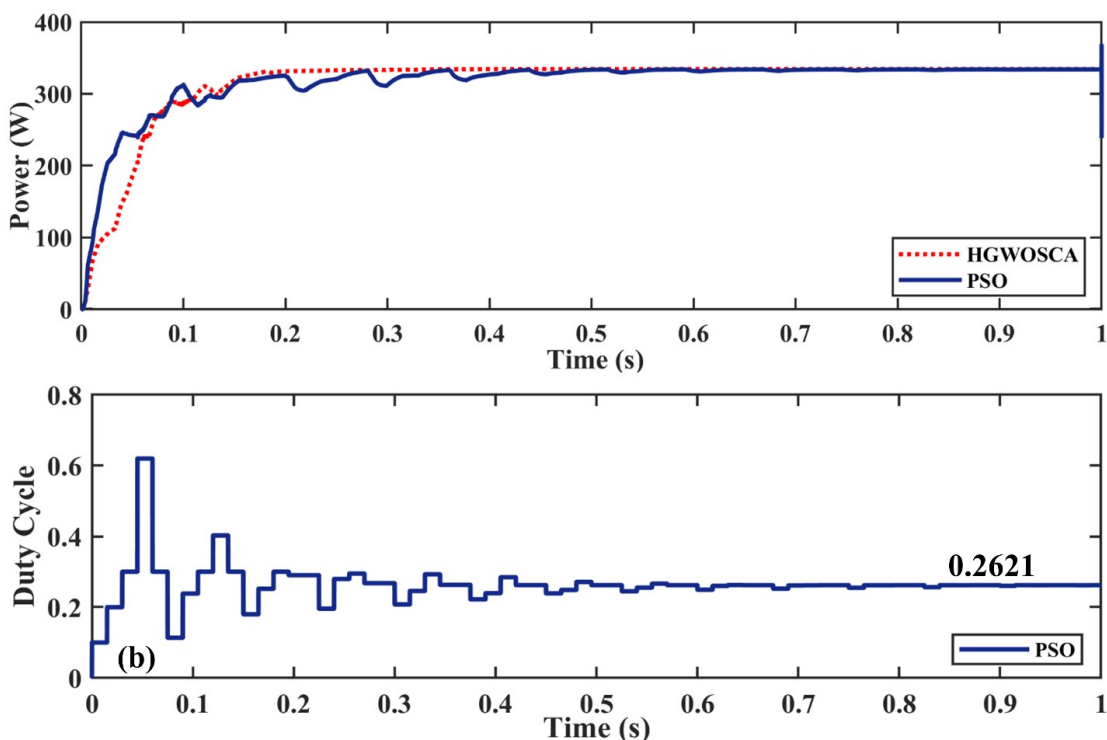

FIGURE 4.26: (a) Power Tracking of PSO in Case 2 under PSC (b) Duty Cycle Variation of PSO in Case 2 under PSC
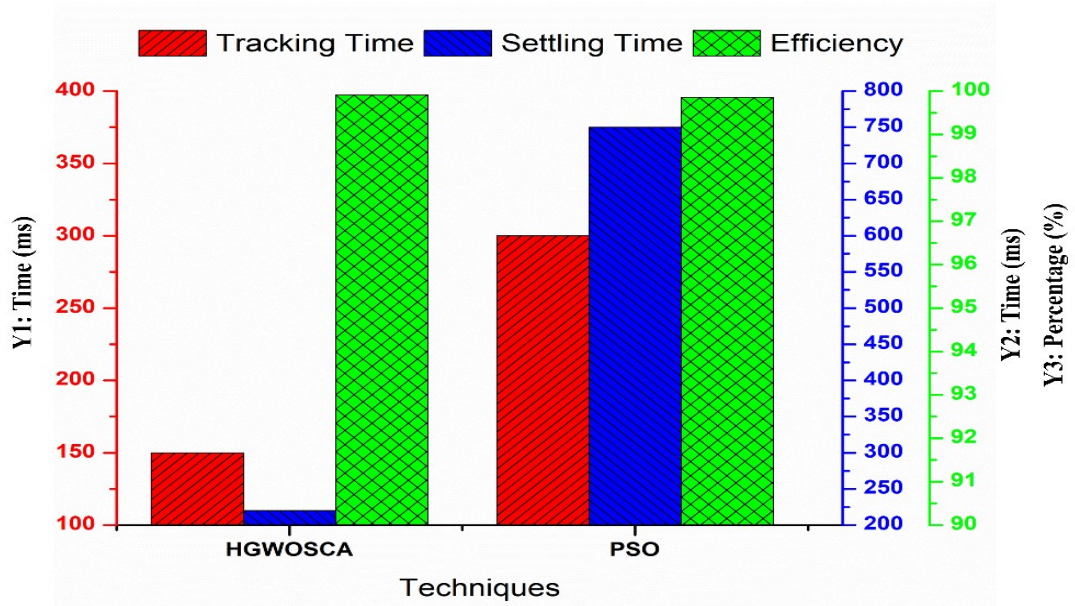
FIGURE 4.27: Evaluation parameter of PSO for case 2 in comparison with proposed technique

4.3.3 Comparative Analysis of Case 2

GMPP is located at 335W and power tracked by HGWOSCA, GHO, PSOGS, CS and PSO is 334.7W, 334.6W, 334.4W, 334.5W with efficiency of 99.91%, 99.88%, 99.82%, 99.85% and 99.85% respectively. It is quite evident that the efficiency of HGWOSCA is better. Fast tracking of GMPP and settling time shows the robustness of MPPT techniques.

Experimental simulations show that it takes HGWOSCA 0.15s, GHO 0.16s, PSO and CSA 0.27s, and PSOGS 0.3s to track GMPP and settles at 0.22s, 0.51s, 0.5s, 0.75s and 0.64s respectively. Comparative analysis of the evaluation parameters is shown in Figure 4.28. Pertub and Observe are stuck in local maxima and achieve a comparatively low efficiency of 71.46 %. The tracking and settling time of P&O can not be defined because it does not track the GMPP. So, the comparison is only made with efficiency.
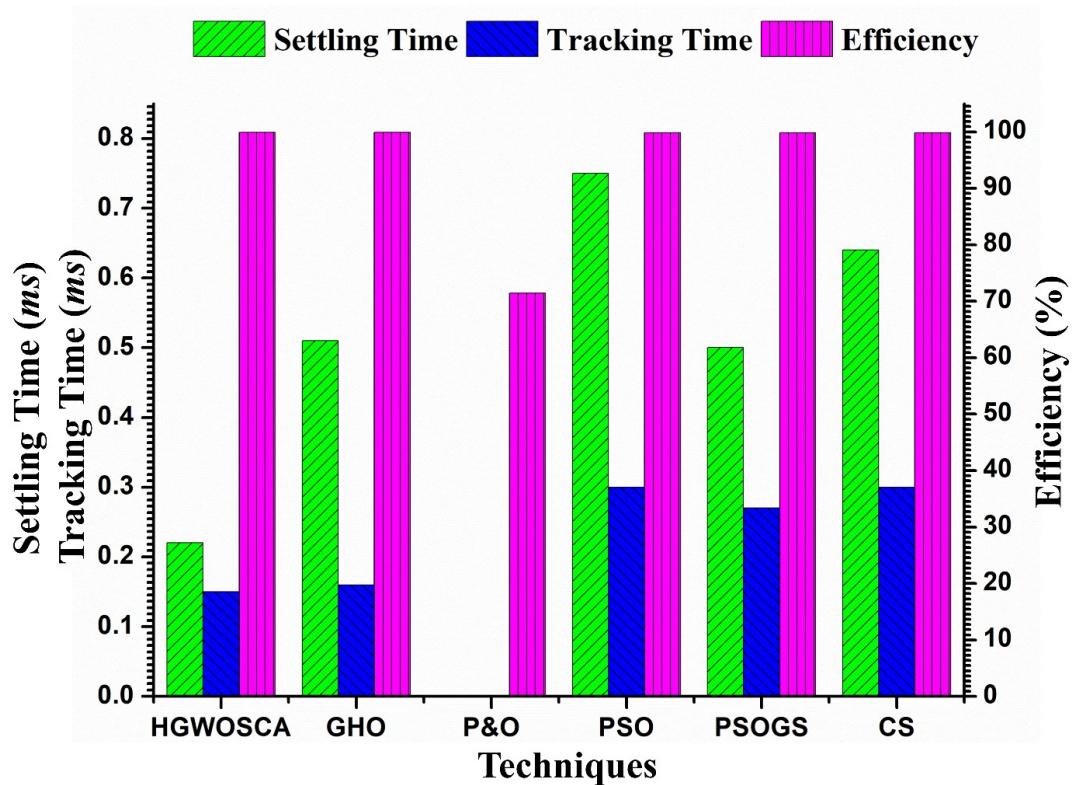
FIGURE 4.28: Comparative analysis of evaluation parameter for case 2

4.4   Case 3: PS Condition

4.4.1   Test Scenario of Case 3

Irradiance under PS given in Table 4.2 and P-V characteristics curve is represented in Figure 4.29 with left skewed GMPP which is located at 702 W and other peaks are local maxima's. The irradiance pattern on all 4 panels in case 3 is shown in Figure 4.30 which is constant on every panel for 1 second.

In this PV curve for case 3, there are 4 peaks which have 3 local maxima's and 1 global maxima. The GMPP is center skewed which means the PV curve have GMPP in the center and has LM at the right and left side of the peak. Conventional MPPT techniques i.e. perturb and observe is unable to track GMPP and stuck at the LMPP that why the P&O technique is not included in the comparison.
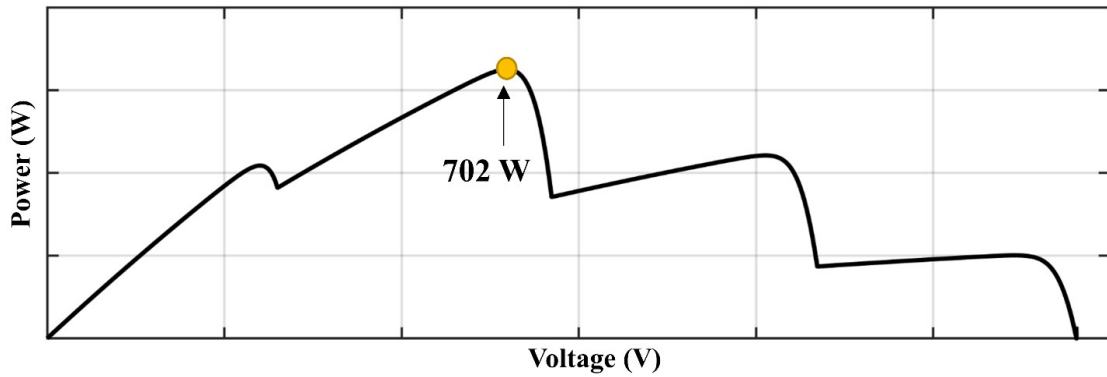
FIGURE 4.29: PV Curve for the partial shading condition in case 3 with left-skewed global maxima
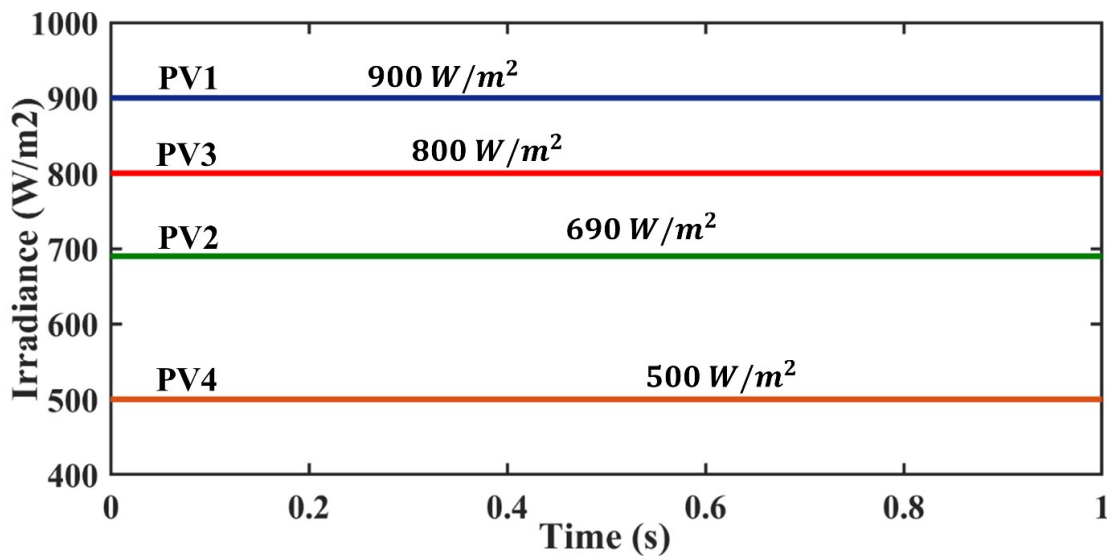
FIGURE 4.30: Irradiance values of all panels in case 3

4.5   Results of Case 3

The HGWOSCA tracks the global maxima in less time with high efficiency. Figure 4.31(a) shows the tracking of power under case 3 by HGWOSCA and Figure 4.31(b) shows the variation of duty cycle for case 3. The evaluation parameter achieved by the HGWOSCA is shown in Figure 4.32.

The maximum power in case 3 is 702 W and the power tracked by the HGWOSCA is 701.5 W which shows the high efficiency of the HGWOSCA under partial shading conditions. The evaluation parameter of HGWOSCA for case 3 is shown in Figure 4.32 which shows that the tracking and settling time of HGWOSCA is 0.16 s and 0.23 s respectively. The efficiency achieved is upto 99.92 %.

FIGURE 4.31: (a) Power Tracking of HGWOSCA in Case 3 under PSC (b) Duty Cycle Variation of HGWOSCA in Case 3 under PSC
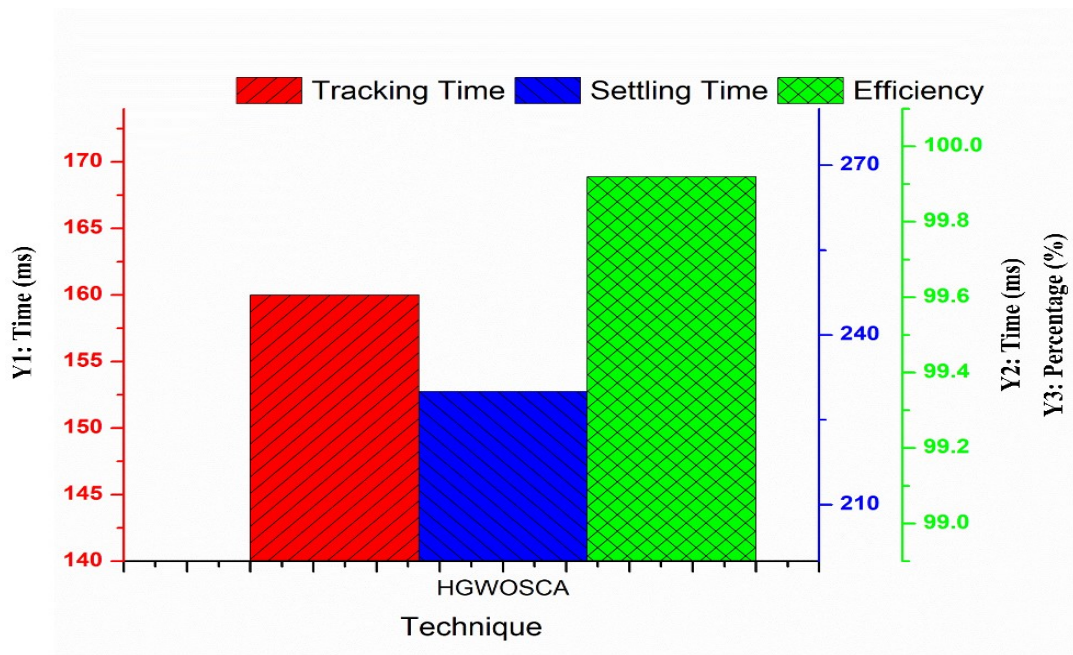
FIGURE 4.32: Evaluation parameter of HGWOSCA for case 3

GHO has the capability to effectively track GM under partial shading conditions but the oscillations after tracking of GM are the main problems, which cause the
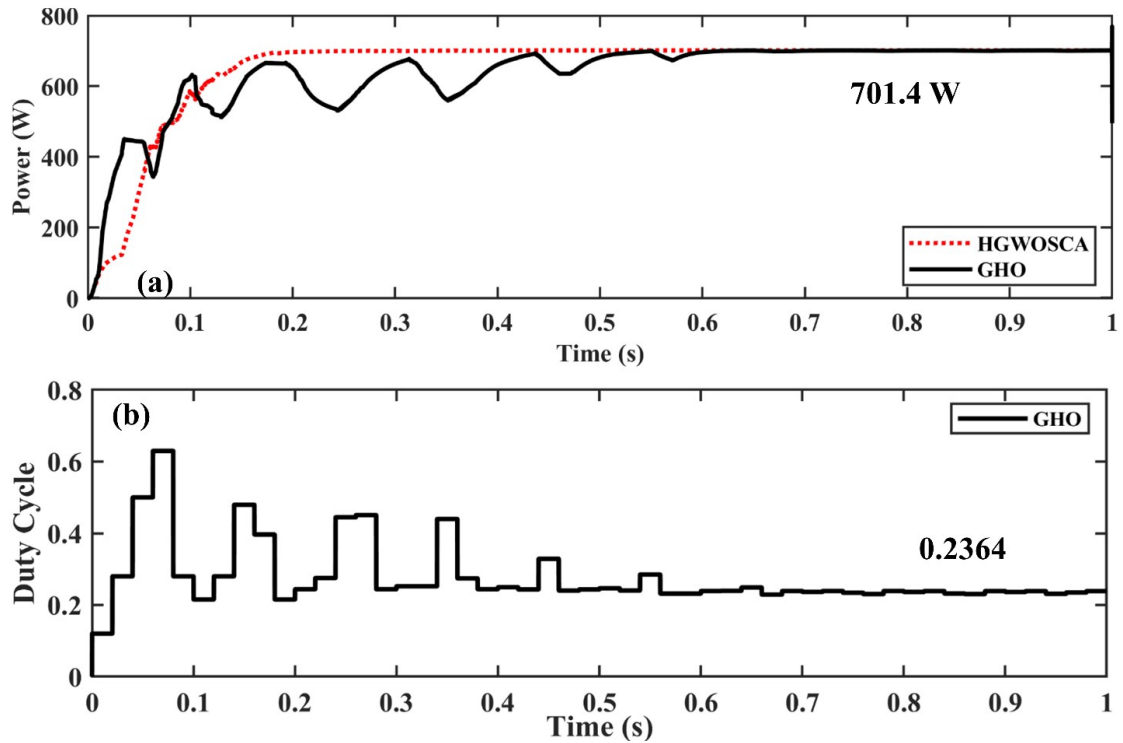
FIGURE 4.33: (a) Power Tracking of GHO in Case 3 under PSC (b) Duty Cycle Variation of GHO in Case 3 under PSC

low efficiency. Power tracked by the GHO under case 3 is shown in Figure 4.33(a) and duty cycle variation by GHO under case 3 is shown in Figure 4.33(b).

Parameter "c" in GHO causes oscillations, which reduces the efficiency. The effective tuning of parameter "c" is the biggest problem in GHO, which has to be done very carefully for effective tracking. The power tracked by the GHO is 701.4 W, which is low as compared to HGWOSCA. The tracking time of the GHO is 0.18 seconds and the settling time of the GHO is 0.60 seconds.

The tracking and settling time are high as compared to HGWOSCA, which causes the low efficiency of the GHO as compared to HGWOSCA. The evaluation parameters achieved by GHO are presented in Figure 4.34.

Particle swarm optimization with gravitational search (PSOGS) is another technique that is implemented for the MPPT application. The PSOGS have low oscillations as compared to GHO but have low tracking efficiency due to restricted movement of the particle due to gravitational effect. The power tracked by PSOGS
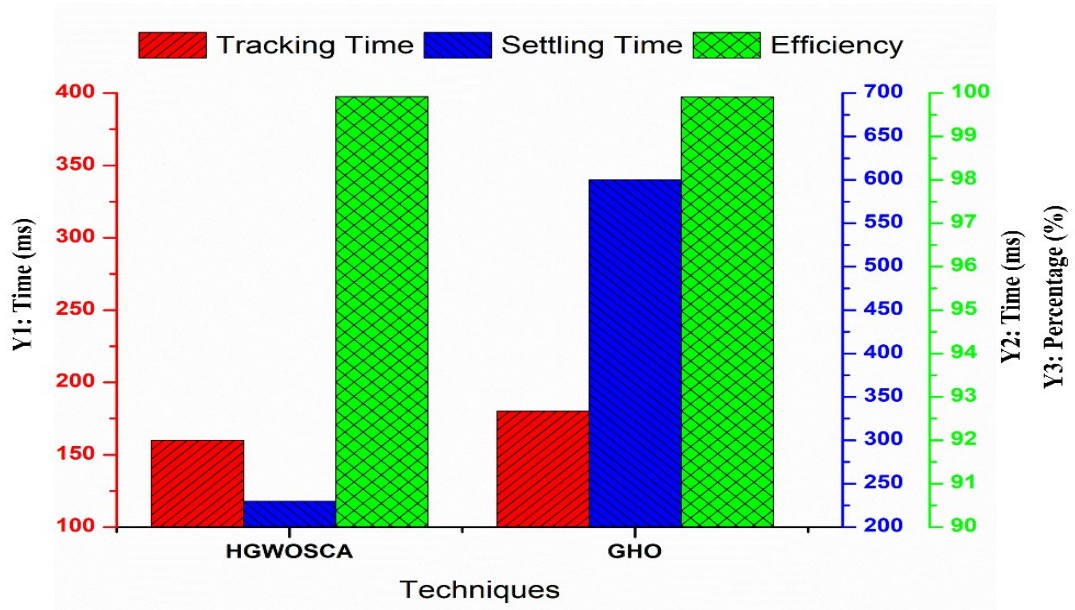
FIGURE 4.34: Evaluation parameter of GHO for case 3

is shown in Figure 4.35(a) and the duty cycle variation of PSOGS under varying irradiance condition is shown in Figure 4.35(b).

Under partial shading condition random assignment of particles position occurs and the particle updation occurs due to PSOGS algorithm but the oscillations are very low. The average power tracked by the PSOGS is 701 W, which is less than GHO and HGWOSCA. The tracking time and settling time are 0.26 seconds and 0.70 seconds respectively. The oscillations of PSOGS after tracking of GM is very low due to high exploitation behavior.

The evaluation parameters of PSOGS are shown in Figure 4.36 which shows that the efficiency achieved by the PSOGS is 99.85 % which is less as compared to GHO and HGWOSCA. Therefore, PSOGS is not suitable for MPPT application under partial shading conditions.

Levy flight function is one of the random walks, which are used in the optimization algorithm. Cuckoo search uses the levy flight function for updation of particles position. Due to this levy flight function the particles are moving even after the
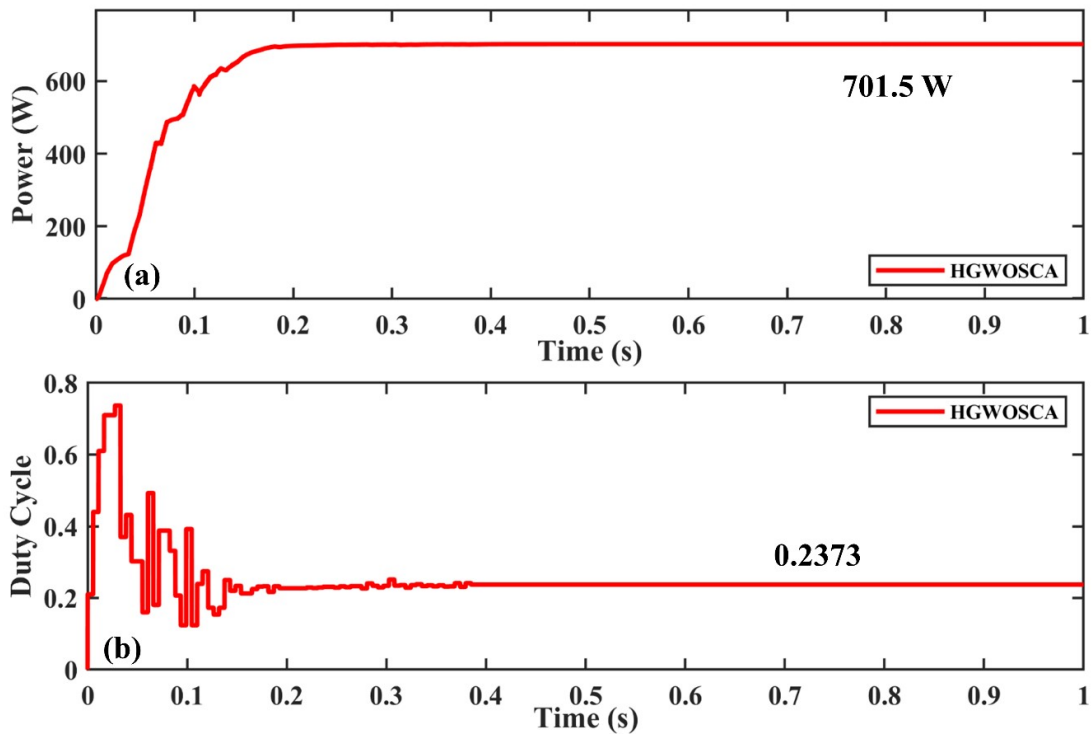
FIGURE 4.35: (a) Power Tracking of PSOGS in Case 3 under PSC (b) Duty
Cycle Variation of PSOGS in Case 3 under PSC
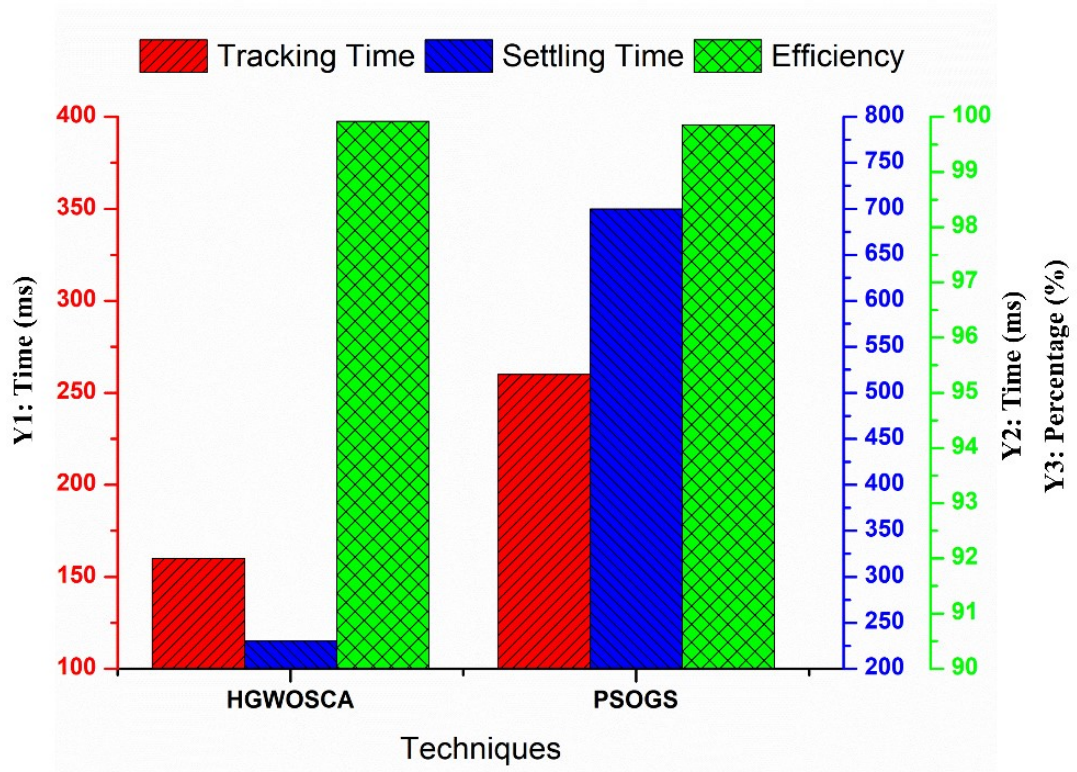
FIGURE 4.36: Evaluation parameter of PSOGS for case 3 in comparison with
the proposed technique which shows the effective performance of HGWOSCA
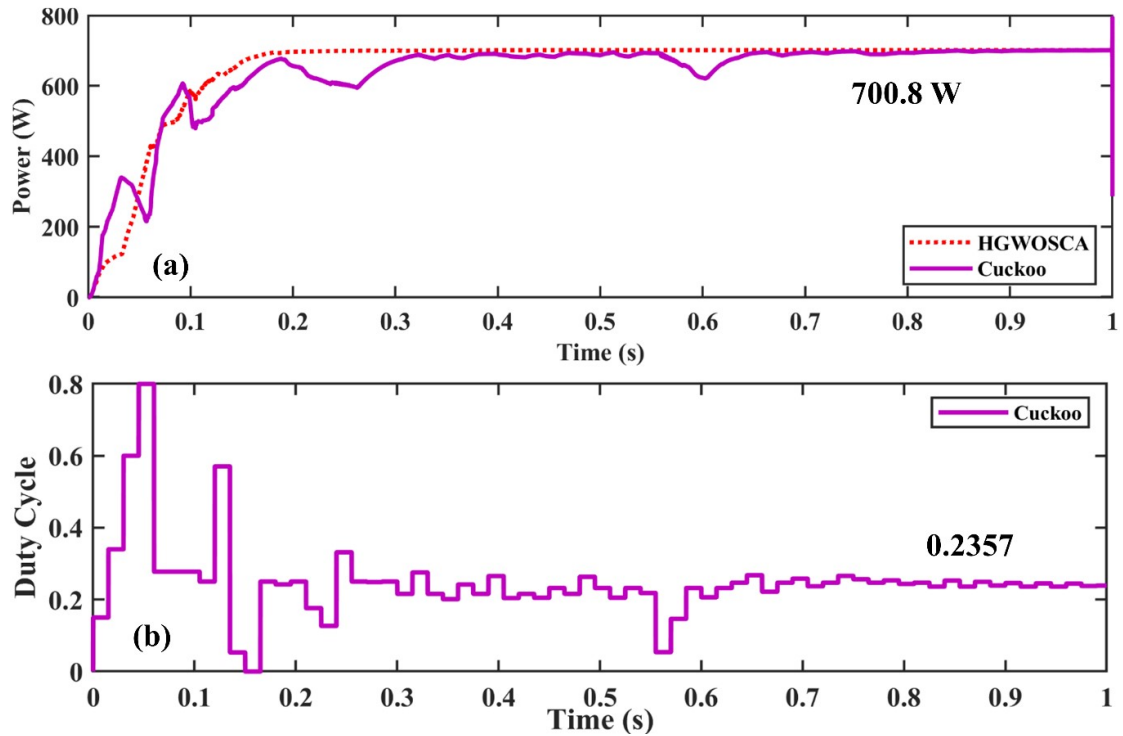
FIGURE 4.37: (a) Power Tracking of CSA in Case 3 under Partial shading condition (b) Duty Cycle Variation of CSA in Case 3 under partial shading condition

exploitation phase. Due to this oscillations can be observed after tracking of GM and the efficiency of the CS based MPPT technique reduced.

Power tracking capability of CSA is shown in Figure 4.37(a) and the variation of the duty cycle is shown in Figure 4.37(b). The average power tracked by the CSA is 700.8 W which is less as compared to GHO, HGWOSCA and PSOGS. The average time taken to track and settle at GM is 0.31 seconds and 0.72 seconds respectively. The high settling time validates that the CSA uses the levy flight function for updation of particle's position.

The evaluation parameter achieved by CSA MPPT technique is shown in Figure 4.38 which shows that the efficiency achieved by CSA is 99.82 %. The efficiency achieved is very low as compared to HGWOSCA, GHO and PSOGS.

Particle swarm optimization uses the behavior of birds flock to locate the global maxima in the optimization problem. The position updation of the particles in
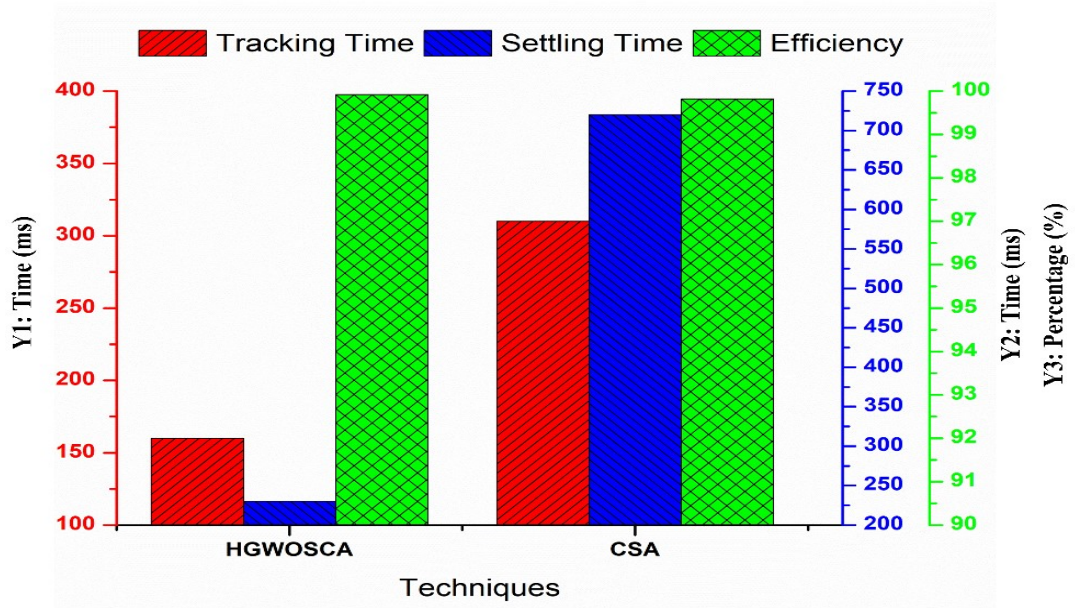
FIGURE 4.38: Evaluation parameter of CSA for case 3 comparison with proposed technique

PSO depends upon the velocity vector used which has random numbers embedded. The parameters C1 and C2 are also required to tune for the specified applications. PSO is one of the first swarm optimization algorithms presented that's why it is used for the comparison. The position updation of the particles in PSO depends upon the velocity vector.

Particle swarm optimization algorithm shows high oscillations due to random numbers in velocity vector and the weight factor is used to control the movement of particles. Figure 4.39(a) shows the power tracking of PSO under case 3 and Figure 4.39(b) shows duty cycle variation of PSO for case 3. The tracking time and settling time achieved by PSO is 0.49 s and 0.90 s respectively. The efficiency achieved by PSO is 98.57 %.

The tracking time, settling time, and efficiency achieved by PSO is shown in Figure 4.40. The achieved efficiency is very low as compared to other MPPT tehniques while the tracking and settling time is also very high. SO, PSO is not a good option for MPPT application.
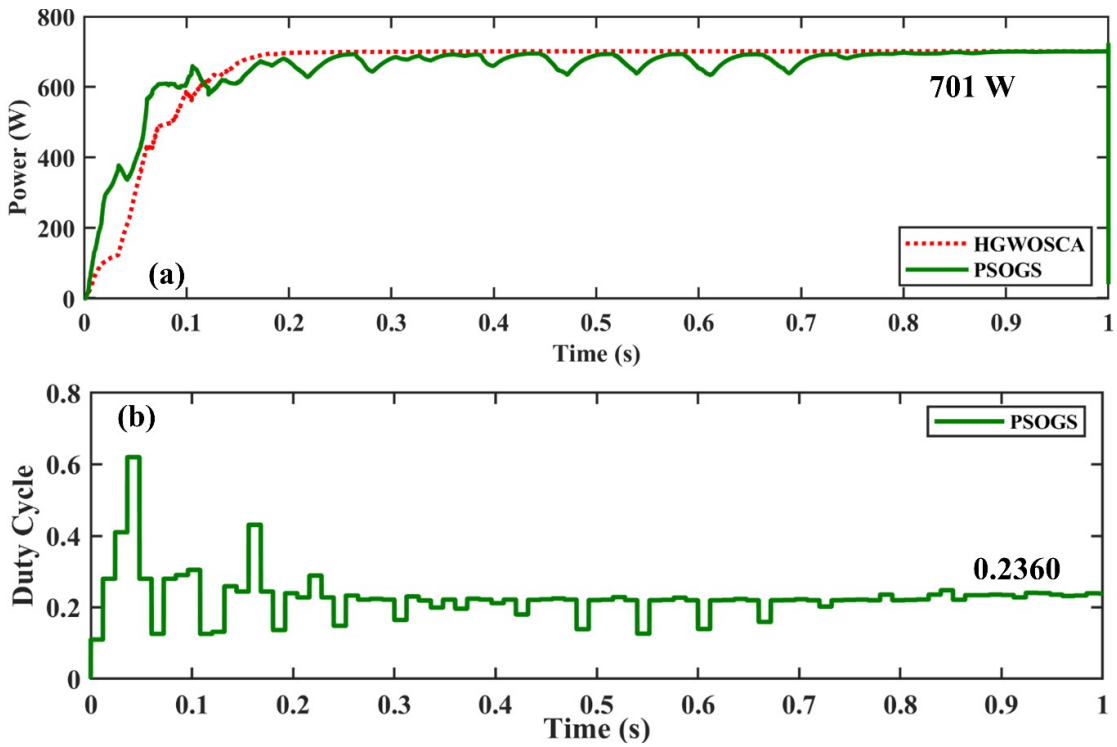
FIGURE 4.39: (a) Power Tracking of PSO in Case 3 under PSC (b) Duty Cycle
Variation of PSO in Case 3 under PSC
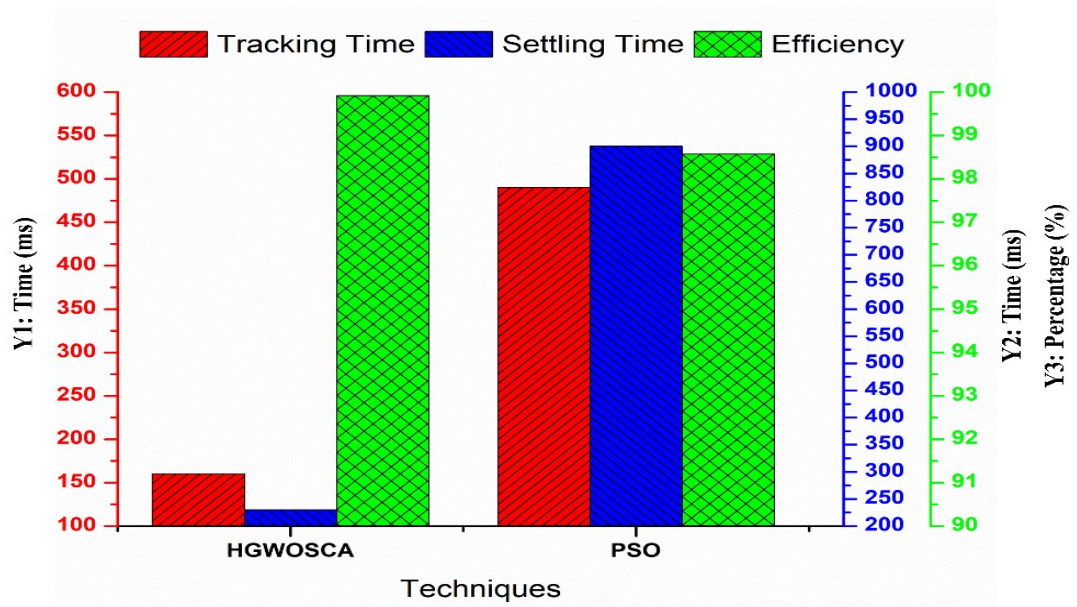
FIGURE 4.40: Evaluation parameter of PSO for case 3

4.5.1 Comparative Analysis of Case 3

Tracking time of HGWOSCA, GHO, PSOGS, CS and PSO is 0.16s, 0.18s, 0.26s,
0.315s and 0.49s respectively whereas their settling time is 0.2s, 0.6s, 0.7s, 0.715s

and 0.9s respectively. HGWOSCA tracks 20ms faster than GHO and also settles 340ms faster which proves the robustness and higher tracking efficiency of HGWOSCA as compared to other techniques.

HGWOSCA has zero power oscillations around GM which plays a vital role in increasing efficiency. Duty cycle in Figures Shows the convergences of HGWOSCA in fewer iterations along with its large exploration phase which effectively tracks GMPP. Under the mentioned PS, the power tracked by HGWOSCA, GHO, PSOGS, CS and PSO is 701.5W, 701.4W, 701W, 700.8W and 692W. Their efficiency is 99.9%, 99.84%, 99.82%, 99.82% and 98.58% respectively.
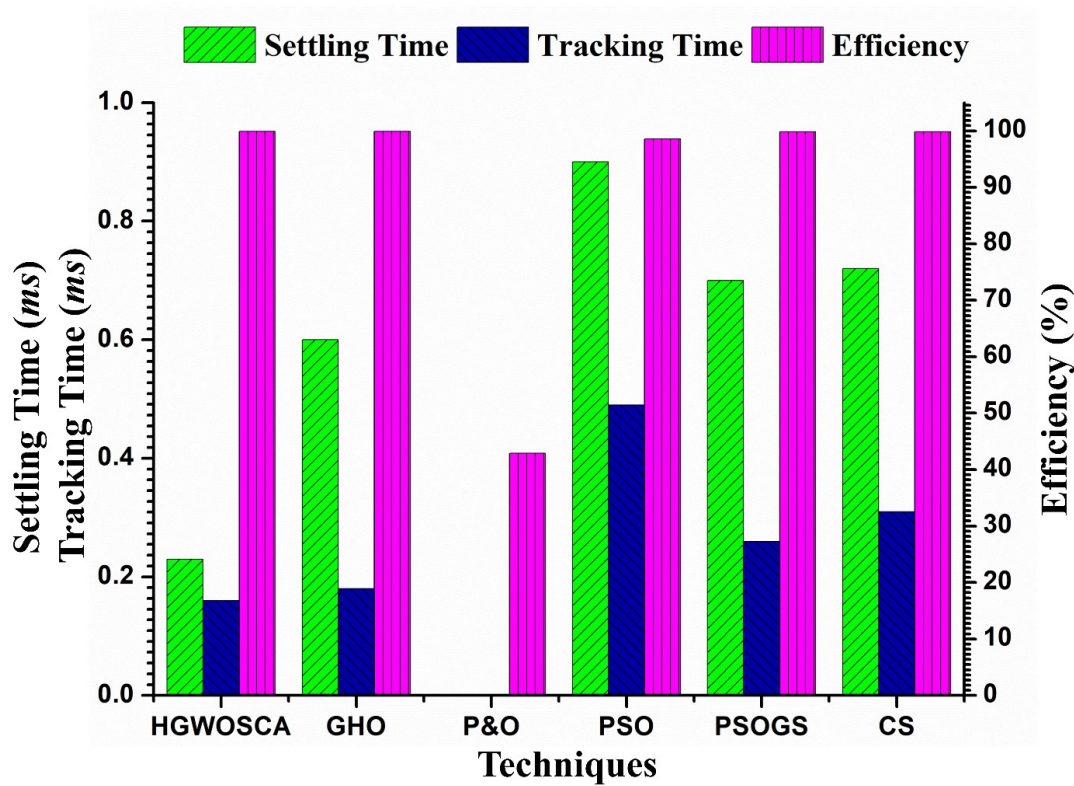
FIGURE 4.41: Comparative analysis of evaluation parameters for case 3

4.6   Case 4: CPS Condition

4.6.1   Test Scenario of Case 4

In case 4, complex partial shading is presented with 8 PV modules connected in series. The irradiance levels for case 4 is presented in Table 4.3. The power tracked by HGWOSCA, GHO, PSOGS, PSO and CS is 921 W, 920.6 W, 910.6 W, 894.1 W and 851.9 W respectively with efficiency of 99.96%, 99.81%, 86.11%, 98.57% and 98.64%.
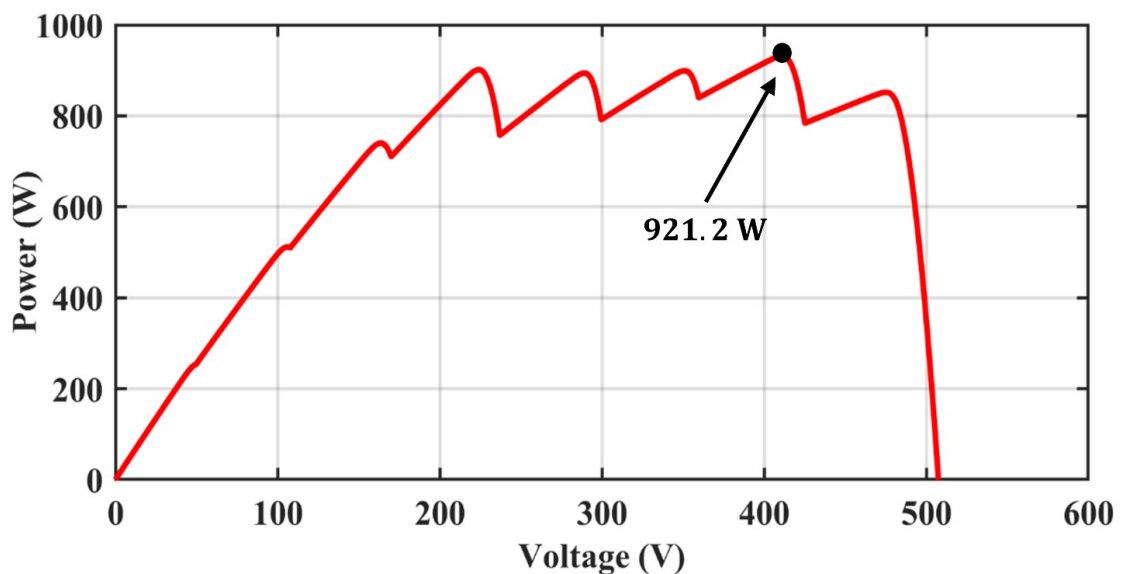
FIGURE 4.42: CPS Condition PV curve

CPS condition is shown and it can be seen that there are two clusters. Cluster-1 exists in left half plane of P-V curve which contains three MPPs. From left - right LM power is 738.3W, 901.4 W and 892.6 W which is the head maxima of cluster 1 whereas, in cluster 2, there are three MPPs.

TABLE 4.3: Irradiance pattern for case 4

Case	Irradiance Si		Pmax
Case 4	PV1:0.46	PV5:0.68	921.2 W
	PV2:0.31	PV6:0.77	
	PV3:0.54	PV7:0.85	
	PV4:0.40	PV8:0.90	

4.6.2 Results of Case 4

The HGWOSCA tracks the global maxima in less time with high efficiency. Figure 4.43(a) shows the tracking of power under case 3 by HGWOSCA and Figure 4.43(b) shows the variation of the duty cycle for case 4. The evaluation parameter achieved by the HGWOSCA is shown in Figure 4.44.

The maximum power in case 4 is 921.2 W and the power tracked by the HG-WOSCA is 921 W which shows the high efficiency of the HGWOSCA under complex partial shading conditions. The evaluation parameter of HGWOSCA for case 4 is shown in Figure 4.44 which shows that the tracking and settling time of HG-WOSCA is 0.17 s and 0.26 s respectively. The efficiency achieved is upto 99.97 %.
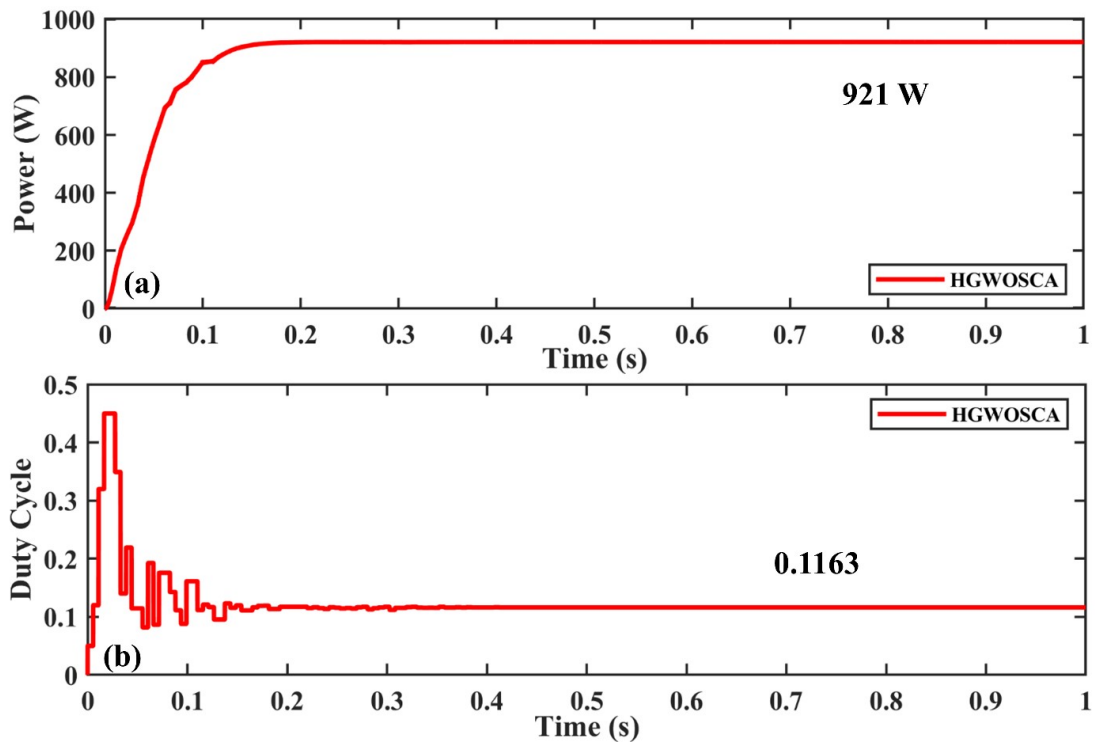
FIGURE 4.43: (a) Power Tracking of HGWOSCA in Case 4 under CPS (b) Duty Cycle Variation of HGWOSCA in Case 4 under CPS

In this PV curve for case 4, there are 12 peaks that have 2 clusters and every cluster has cluster head maxima which is the GM of every cluster. However, the average power of 1 cluster is higher than the other cluster. The conventional techniques are unable to track GMPP but even the swarm intelligence-based MPPT techniques
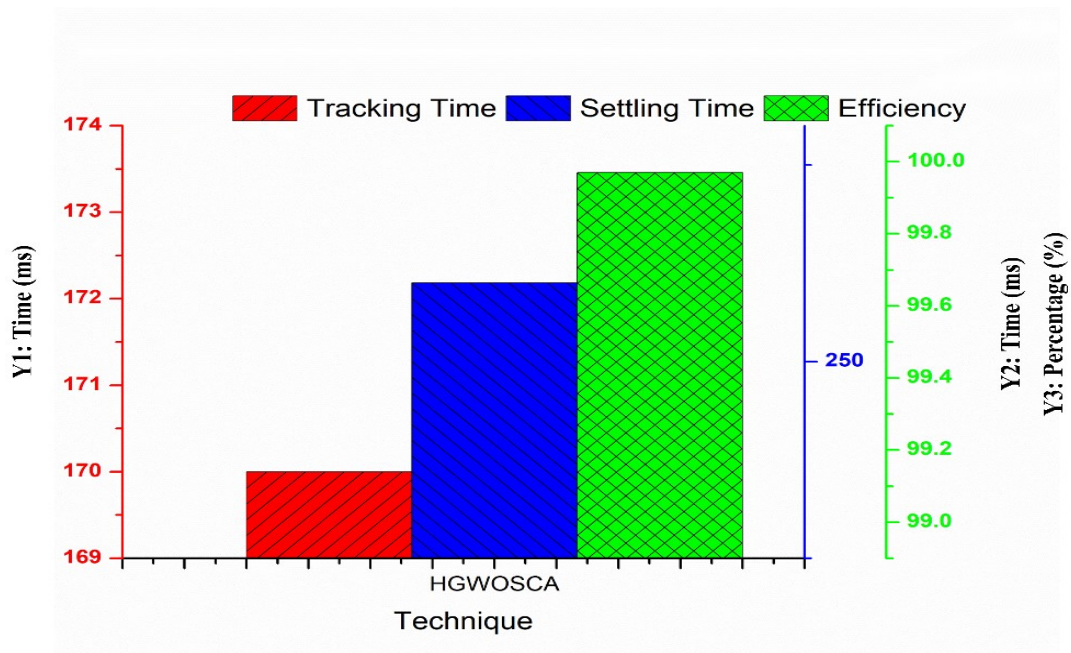
FIGURE 4.44: Evaluation parameter of HGWOSCA for case 4

like PSO, CSA are also unable to differentiate between the GMPP and LMPP in CPS conditions.

Power tracked by HGWOSCA is shown in Figure 4.43(a) and the duty cycle variation is shown in Figure 4.43(b). The power tracked by GHO is presented in Figure 4.45(a) and duty cycle variation is is presented in Figure 4.45(b). HGWOSCA shows higher efficiency as compared to GHO and has low tracking and settling time which shows that under CPS HGWOSCA performs better as compared to GHO.

Parameter "c" in GHO causess oscillations, which reduces the efficiency. The effective tuning of parameter "c" is the biggest problem in GHO, which has to be done very carefully for effective tracking. The power tracked by the GHO is 920.6 W, which is low as compared to HGWOSCA. The tracking time of the GHO is 0.35 seconds and the settling time of the GHO is 0.61 seconds. The evaluation parameter of GHO for case 4 is shown in Figure 4.46.

Particle swarm optimization with gravitational search (PSOGS) is another technique that is implemented for the MPPT application. The PSOGS have low oscillations as compared to GHO but have low tracking efficiency due to restricted movement of the particle due to gravitational effect. The power tracked by PSOGS
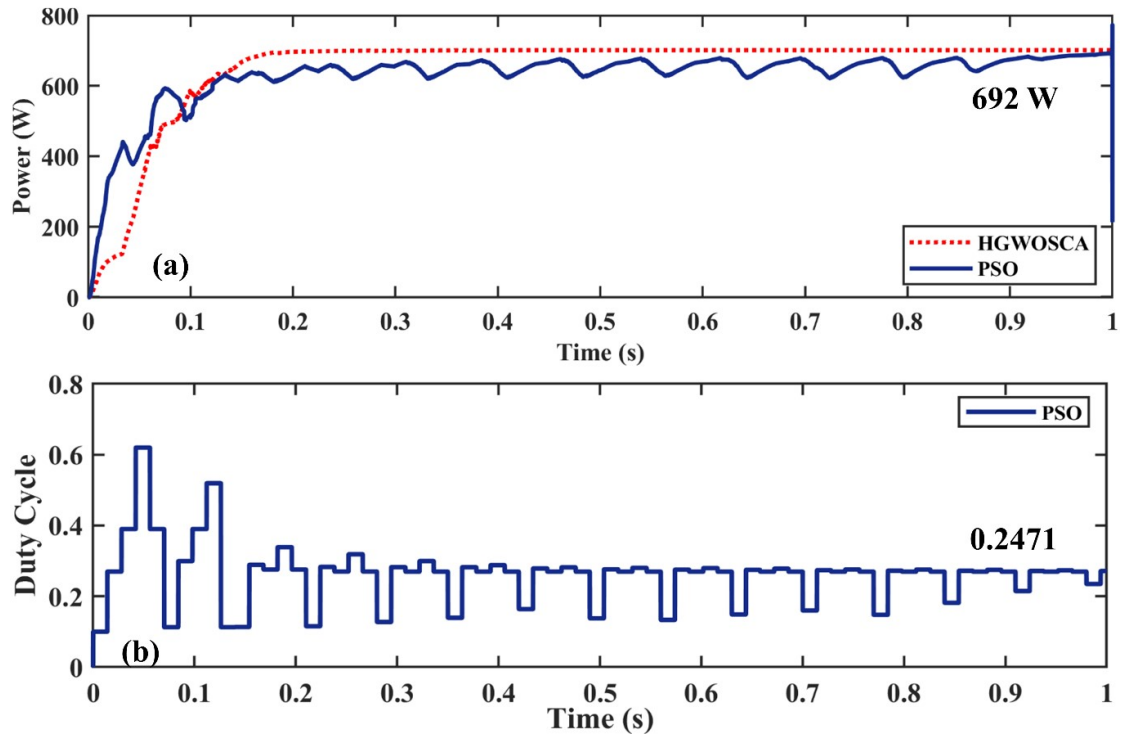
FIGURE 4.45: (a) Power Tracking of GHO in Case 4 under CPS (b) Duty Cycle Variation of GHO in Case 4 under CPS
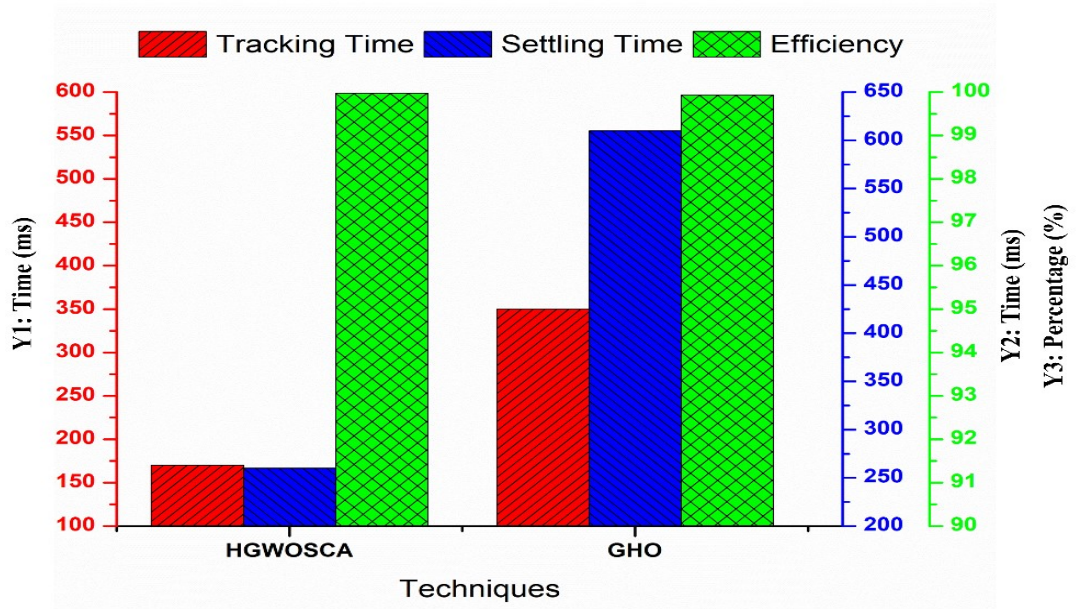
FIGURE 4.46: Evaluation parameter of GHO for case 4 in comparison with HGWOSCA

is shown in Figure 4.47(a) and the duty cycle variation of PSOGS under varying irradiance condition is shown in Figure 4.47(b).

Under partial shading condition random assignment of particles position occurs
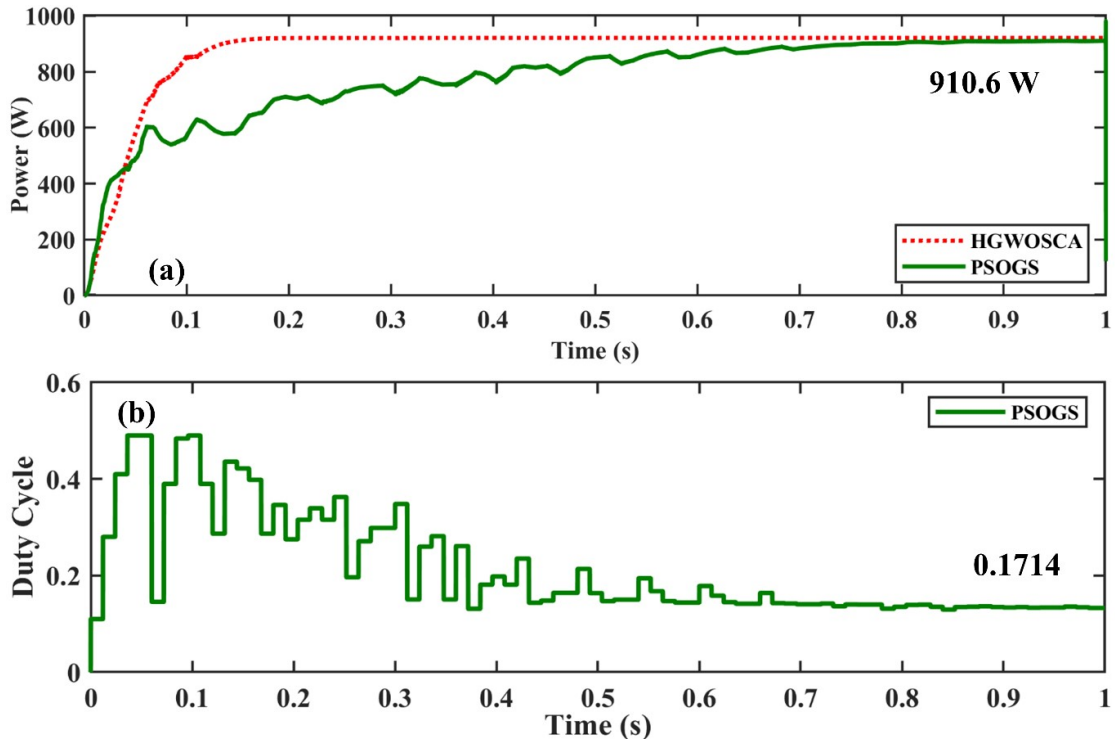
FIGURE 4.47: (a) Power Tracking of PSOGS in Case 4 under CPS (b) Duty
Cycle Variation of PSOGS in Case 4 under CPS

and the particle updation occurs due to PSOGS algorithm but the oscillations are
very low. The average power tracked by the PSOGS is 910.6 W, which is less than
GHO and HGWOSCA. The tracking time and settling time are 0.47 seconds and
0.71 seconds respectively. The oscillations of PSOGS after tracking of GM is very
low due to high exploitation behavior. The evaluation parameter of PSOGS for
case 4 is shown in Figure 4.48.

Levy flight function is one of the random walks, which are used in optimization
algorithm. Cuckoo search uses the levy flight function for updation of particles
position. Due to this levy flight function the particles are moving even after the
exploitation phase. Due to this oscillations can be observed after tracking of GM
and the efficiency of the CS based MPPT technique is reduced.

Power tracking capability of CSA is shown in Figure 4.49(a) and the variation
of the duty cycle is shown in Figure 4.49(b). The average power tracked by the
CSA is 851.9 W which is less as compared to GHO, HGWOSCA and PSOGS. The
average time taken to track and settle at GM is 0.29 seconds and 0.50 seconds
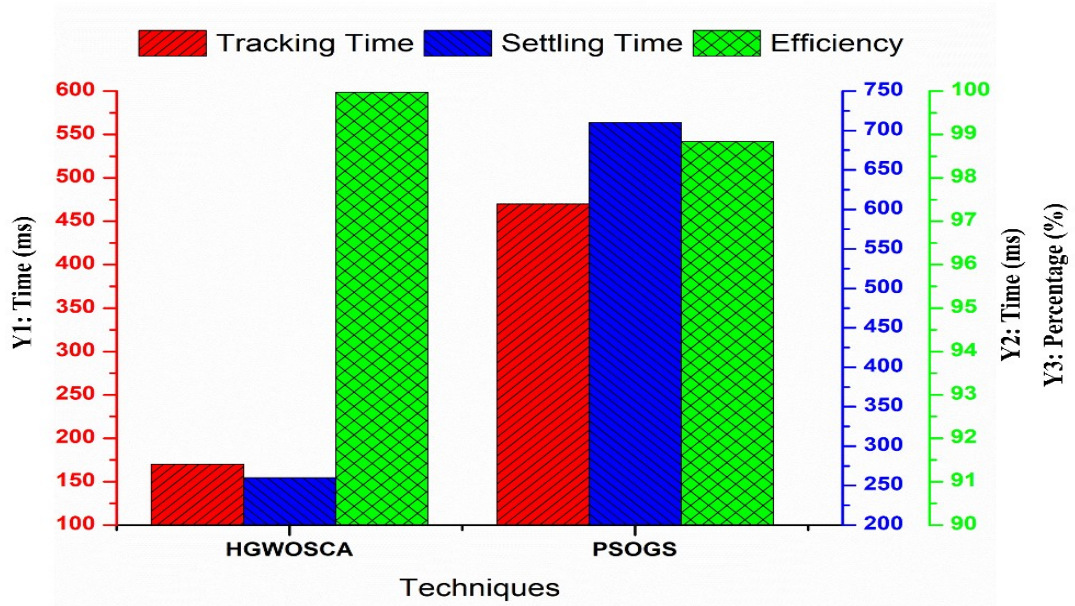
FIGURE 4.48: Evaluation parameter of PSOGS for case 4

respectively. The high settling time validates that the CSA uses the levy flight function for updation of particles position.

The evaluation parameters achieved by the CSA MPPT technique are shown in Figure 4.50 which shows that the efficiency achieved by CSA is 93.25 %. The efficiency achieved is very low as compared to HGWOSCA, GHO and PSOGS.

Particle swarm optimization uses the behavior of birds flock to locate the global maxima in the optimization problem. The position updation of the particles in PSO depends upon the velocity vector used which have random numbers embedded. The parameters C1 and C2 are also required to tune for the specified applications. PSO is one of the first swarm optimization algorithms presented that's why it is used for the comparison.

Particle swarm optimization algorithm shows high oscillations due to random numbers in velocity vector and the weight factor is used to control the movement of particles. Figure 4.51(a) shows the power tracking of PSO under case 4 and Figure 4.51(b) shows duty cycle variation of PSO for case 4. The tracking time and settling time achieved by PSO is 0.37 s and 0.59 s respectively. The efficiency achieved by PSO is 97.05 %.
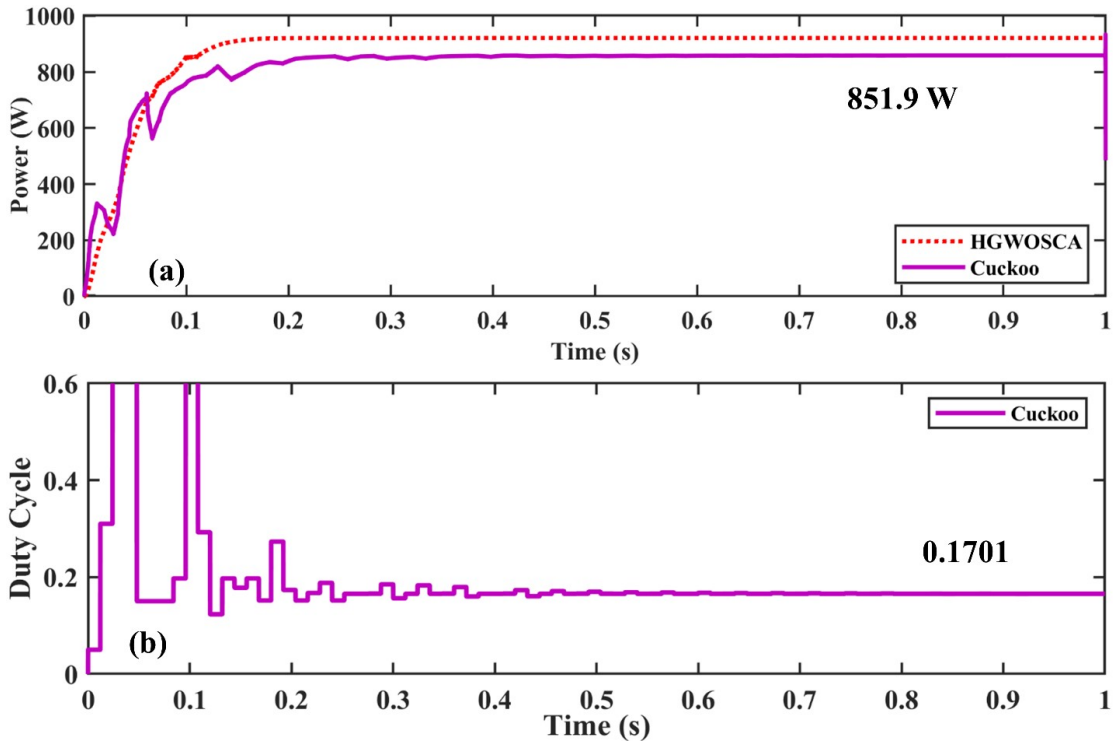
FIGURE 4.49: (a) Power Tracking of CSA in Case 4 under CPS (b) Duty Cycle Variation of CSA in Case 4 under CPS
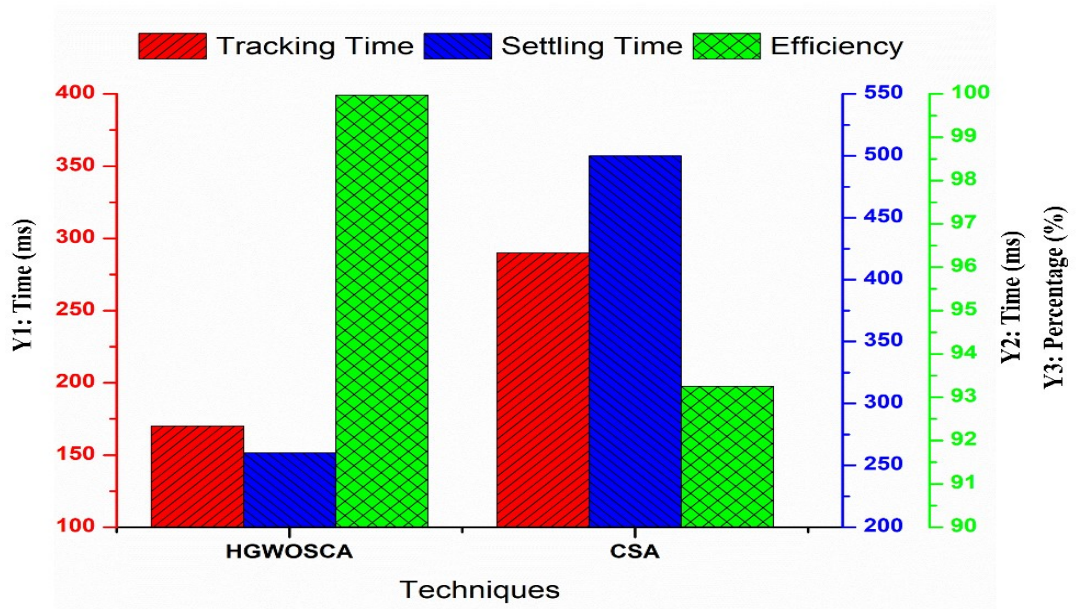
FIGURE 4.50: Evaluation parameter of CSA for case 4

The tracking time, settling time and efficiency achieved by PSO is shown in Figure 4.52. The achieved efficiency is very low as compared to other MPPT techniques while the tracking and settling time is also very high. SO, PSO is not a good option for MPPT application.
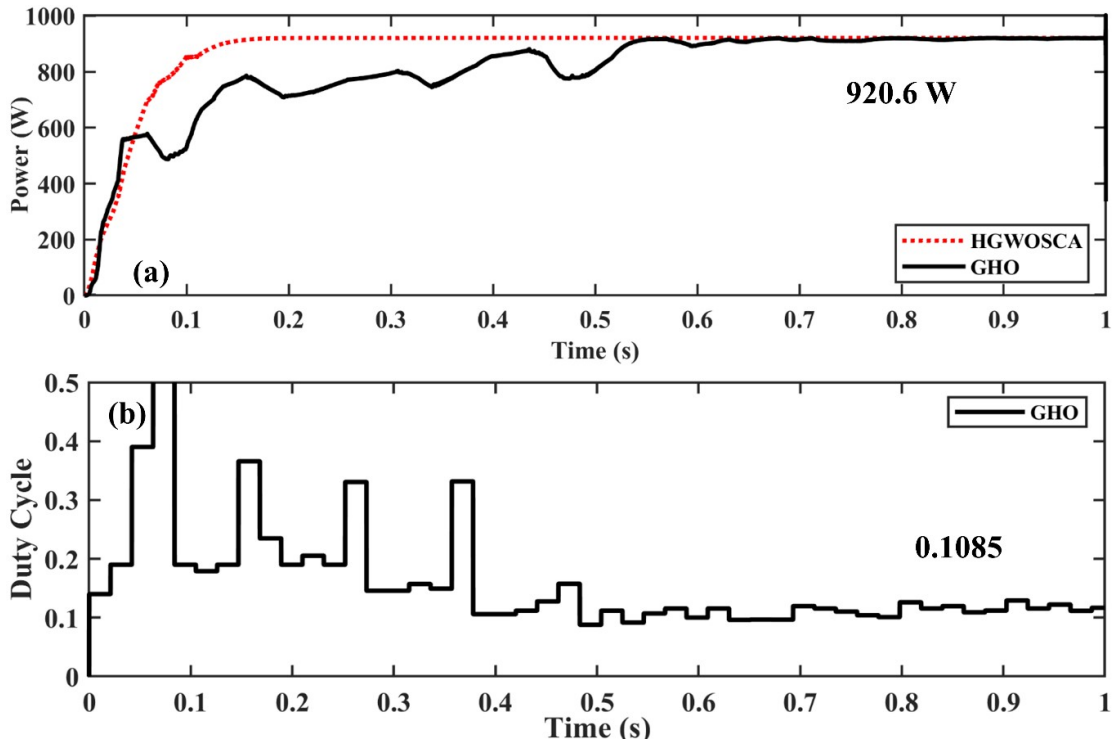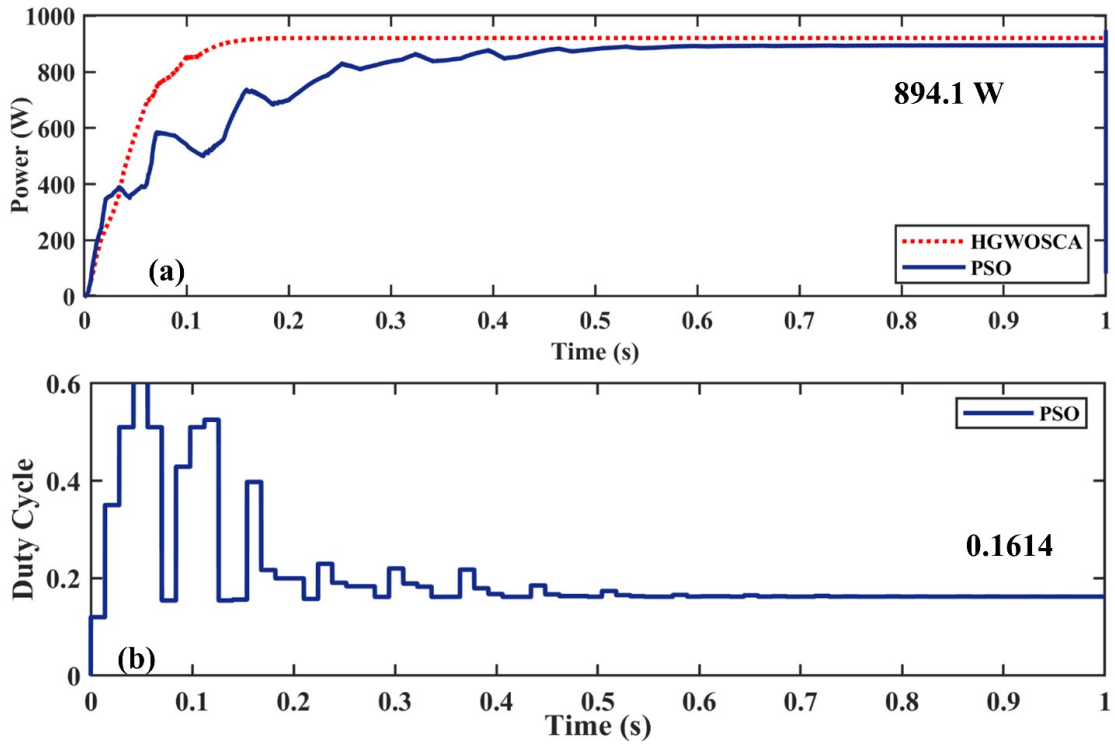
FIGURE 4.51: (a) Power Tracking of PSO in Case 4 under CPS (b) Duty Cycle Variation of PSO in Case 4 under CPS
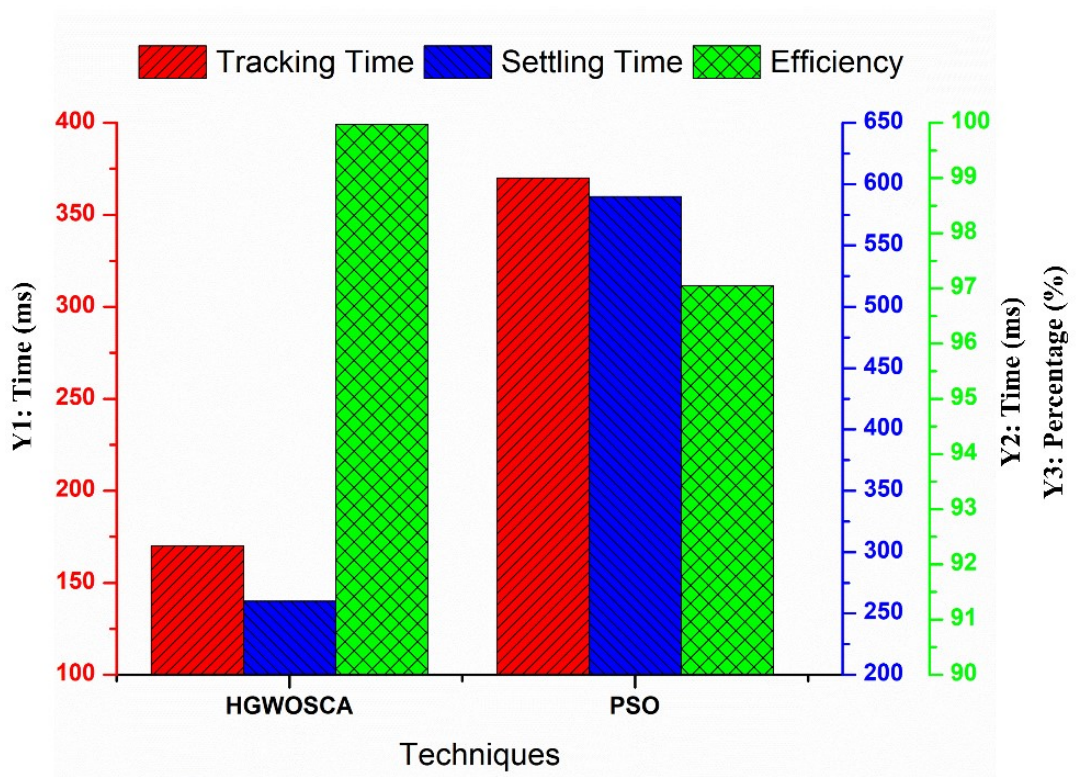
FIGURE 4.52: Evaluation parameter of PSO for case 4

4.6.3   Comparative Analysis of Case 4

Tracking time of GM of HGWOSCA, GHO, PSOGS, CS and PSO is 0.17s, 0.23s, 0.41s, 0.41s and 0.38s. CS and PSOGS have equal tracking time but since PSOGS is stuck within local maxima, it causes great loss of power.

Comparative analysis shows that HGWOSCA has a settling time of 0.25s, which is 440ms less as compared to GHO. Performance comparison of these techniques in the form of ranking can be represented as HGWOSCA > GHO > PSO > CS > PSOGS > P&O. The efficiency achieved by HGWOSCA, GHO, PSOGS, CSA and PSO is 99.97%, 99.93%, 98.84%, 93.25%, and 97.05% respectively. Performance comparison of these techniques in the form of ranking can be represented as HGWOSCA > GHO > PSOGS > PSO > CS > P&O. Settling time of GM of HGWOSCA, GHO, PSOGS, CS and PSO is 0.26s, 0.60s, 0.71s, 0.50s and 0.59s. The comparative analysis of the evaluation parameter for all MPPT techniques in case 4 is shown in Figure 4.53.
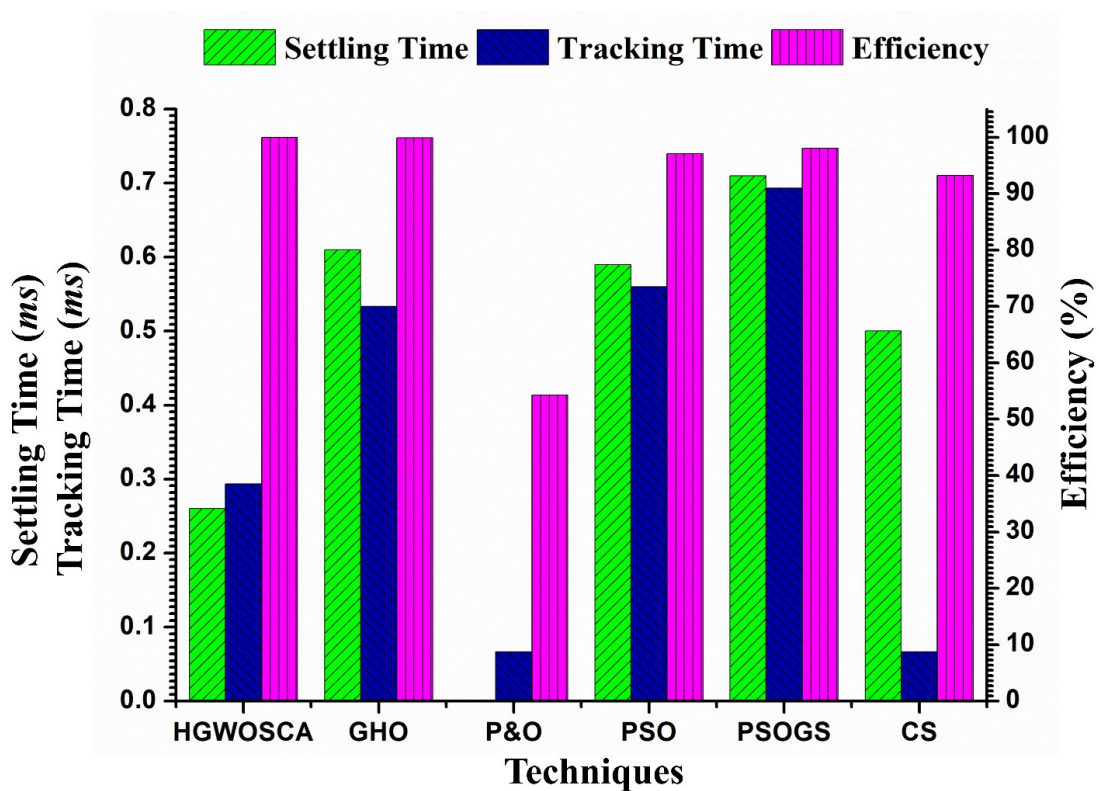
FIGURE 4.53: Comparative analysis of evaluation parameter for case 4

4.7 MPPT Rating

In this section, MPPT rating is calculated using Equation 4.1 as presented. The factors used are the number of tuning parameters, number of random numbers, the requirement of iter_max for termination, average tracking time, average efficiency, modification required in hardware for implementation, and the response of variation in irradiance. These parameters are needed to be calculated for MPPT rating.

$$MPPT_rating = (Total achieved rating)/7 \qquad (4.1)$$

MPPT rating is presented in Table 4.4 in which "1" shows the best and "4" shows the worst. The conditions developed are presented below:

- For one tuning parameter, the rating is 1, two tuning parameter rating is 2, three tuning parameter rating is 3, and four tuning parameter rating is 4 and above for the number of parameters, a rating is 4.

- If the number of random numbers needed is zero then the rating is 1, for one number of random numbers rating is 2, for three random numbers rating is 3 and for greater than three random variables the rating is 4.

- If the termination criteria iter_max is met, then the rating is 2, and if it is not, then the rating is 1.

- If the average tracking time is between 0-500ms then the rating is 1. If it is between 500-750ms the rating is 2. If it is between 750-1000ms then it is 3 and for a rating greater than 1000ms, it will be 4.

- In a similar fashion, if the efficiency is between 99.5%-100%, the rating would be 1. For 99%-99.5%, it would be 2. For 98.5%-99%, it would be 3 and for efficiency of less than 98.5%, the rating would be 4.

- If hardware modification is required for the implementation of MPPT then the rating would be 2 and if not, then it would be 1.

- If the response to irradiance variation is less than 0.25s then the rating would be 1, between 0.25s-.5s, the rating would be 2, between 0.5s-.75s, the rating would be 3, and for more than 0.75s, the rating would be 4.

As depicted in Table 4.4, the HGWOSCA has the best MPPT rating of 1.142, which suggests that IMFO can track GM at a much faster rate. Only one tuning parameter is required for HGWOSCA in order to implement MPPT, which makes it simple. Oscillations are also reduced because there is only one random number involved in HGWOSCA.

The notations used in Table 4.4 are No. of tuning parameters: NTP, No. of random numbers: NRN, Average tracking time: ATT, Average Efficiency: AE, Modification required in hardware: MH, Response Time RT, Termination criteria: TC

TABLE 4.4: Comparison of MPPT techniques for MPPT rating

Tech	NTP	NRN	TC	ATT (s)	AE (%)	MH	RT (s)	Rating
HGWOSCA	1 (1)	1 (1)	No (1)	0.3411 (1)	99.89 (1)	No (1)	Fast (2)	1.142
GHO	3 (3)	1 (1)	Yes (2)	0.3761 (1)	99.84 (1)	Yes (2)	Very slow (4)	2
PSOGS	3 (3)	2 (3)	Yes (2)	0.5512 (2)	99.79 (1)	No (1)	Slow (3)	2.142
CS	1 (1)	2 (3)	No (1)	0.7212 (2)	99.73 (1)	No (1)	Slow (3)	1.714
PSO	3 (3)	2 (3)	No (1)	0.7408 (2)	99.62 (1)	No (1)	Very slow (4)	2.142

4.8 Efficiency and Performance Evaluation

Based on statistical analysis, the performance evaluation of HGWOSCA with other competing techniques helps to understand common characteristics. We know that conventional P&O is a comparatively faster and simple to implement technique
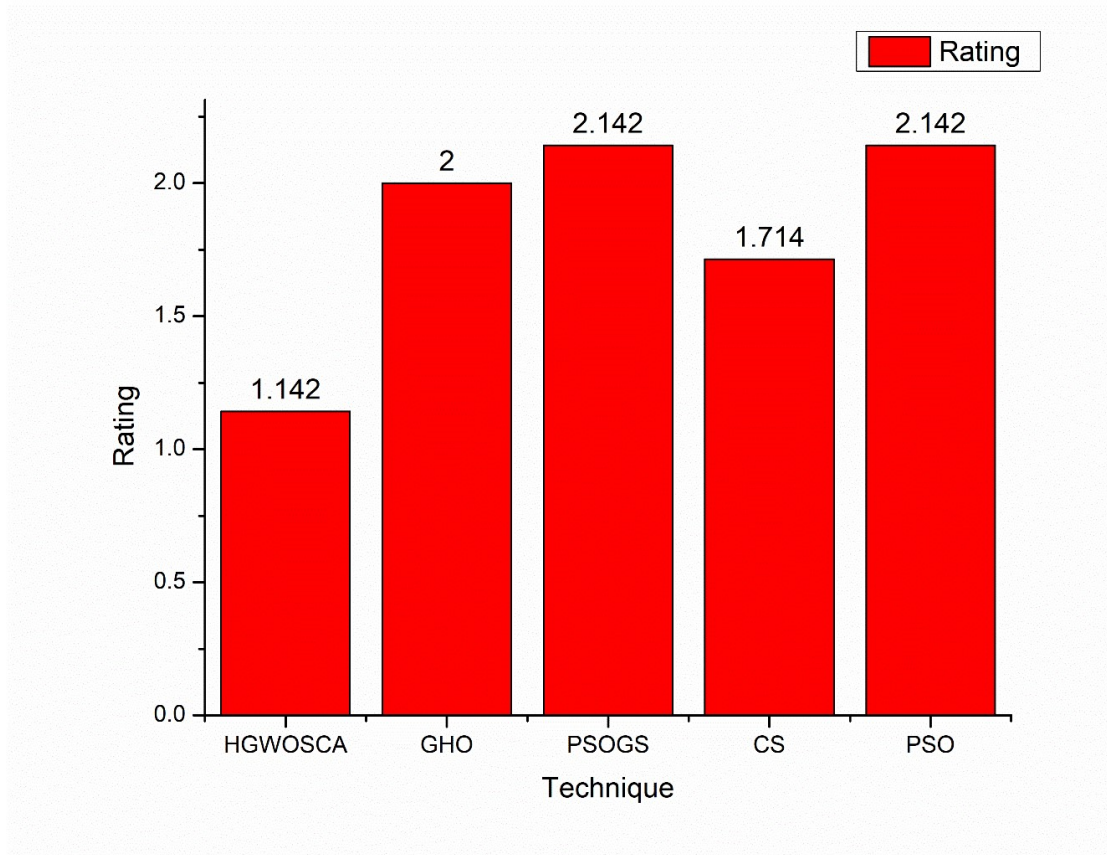
FIGURE 4.54: Comparison of MPPT rating of competing techniques

because of gradient based control, however significant power loss due to oscillations under varying irradiances and trapping of LM makes P&O a non-desirable technique.

On the other hand another technique, under PS, PSO has 100% efficiency in locating GMPP but it offers a low power efficiency of 97%-98%. As seen in case 4, CS causes large fluctuations, which are not very desirable.

CS offers a high efficiency of up to 94%-99% but it takes almost up to 840ms for CS to track GM. HGWOSCA tackles these shortcomings by overshooting its minimum and its efficiency is as good as 99% under all operating conditions. Table 4.5 shows these results.

- HGWOSCA excellent tracking ability can be confirmed from case 1 which shows that HGWOSCA performs better in the transient phase whereas in case 2 and case 3, the power convergence efficiency of other techniques is slightly low and GM is located successfully by bio-inspired techniques.

- Steady state power is reduced in case of PSOGS, which attenuates the power losses related to PSO.

- Case 4 and 5 shows that HGWOSCA can tackle CPS. In PSO and other comparative techniques, their performances are compromised due to the fact that random initialization is used even though they have located the GMPP. HGWOSCA's statistical analysis is presented in Figure 4.55.

- Robustness and sensitivity of all techniques inspected by mean, standard deviation (SD), relative error (RE) by Equation 4.2, mean absolute error (MAE) by Equation 4.3 and root means square error (RMSE) by Equation 4.4 [87].

$$Error_R E = (P_{pvi} - P_{pv})/P_{pv}x100\% \tag{4.2}$$

$$Error_R E = (P_{pvi} - P_{pv})/n \tag{4.3}$$

$$Error_R E = sqrt((P_{pvi} - P_{pv})^2/n) \tag{4.4}$$

Where Ppvi represents the power at STC, Ppvi the power tracked and n represents the number of samples.

Statistical analysis of the competing techniques is presented in Figure 4.55 which shows that HGWOSCA has low RMSE, MAE, and high success rate (SR). The effective tracking and settling capability of HGWOSCA at GPP makes it suitable for the implementation of MPPT technique.
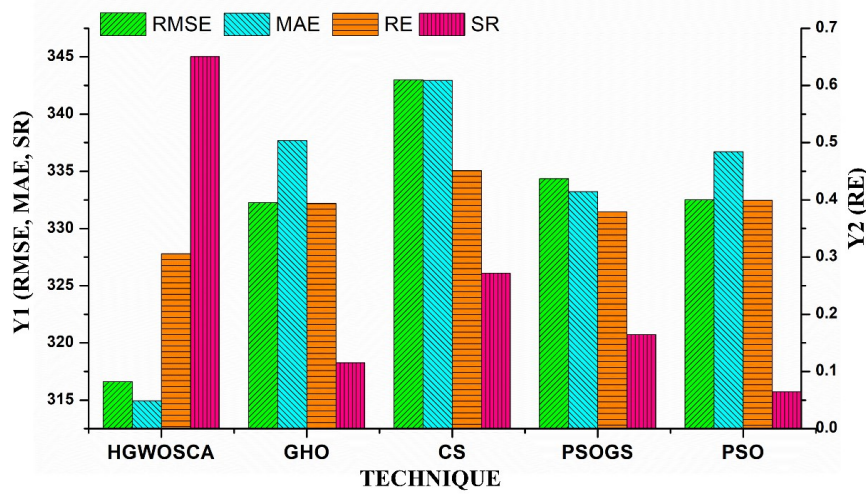
FIGURE 4.55: Statistical analysis comparison of competing MPPT techniques

TABLE 4.5: The electrical characteristics of TDC-M20-36 PV array module [18].

Description	TDC-M20-36
Power at MPP	20 W
Maximum Voltage	18.76 V
Maximum Current	1.07 A
Current due to short circuit	1.17 A
Voltage due to open circuit	22.7 V

4.9 Hardware Setup

In this section, experimental validation of proposed MPPT techniques is presented. MPPT techniques are implemented on low cost microcontroller use to control the duty cycle of boost converter which is interfaced with the PV emulator. The specifications of the PV module and components used for the experimental validation is presented in Table 4.4.

In this experimental setup, the irradiance is changed from 950 W/m2 to 550 W/m2. The test scenario for the experimental setup is presented in Figure 4.57.

Experimental setup is shown in Figure 4.56. The specifications of the setup are presented below:

- ATmega 328 microcontroller is interfaced with MATLAB for data acquisition of voltage and current sensor.

- MOSFET with low ON resistance is selected for higher efficiency and high switching frequency Schottky diode is selected for the boost converter design.

- The detailed experimental setup is presented in Figure 4.58.

- Figure 4.59 shows the power tracked by PSO under fast varying irradiance which validates that PSO takes 300ms to track the GM and 450ms to settles at GM. While in comparison with PSO, HGWOSCA tracks the higher power in 170ms.

- HGWOSCA settles at GM in less than 250ms causing less power loss. It validates that HGWOSCA achieves high efficiency, with less tracking and settling time.

- Proposed techniques show very low oscillations at the GM causing low power loss at GM.
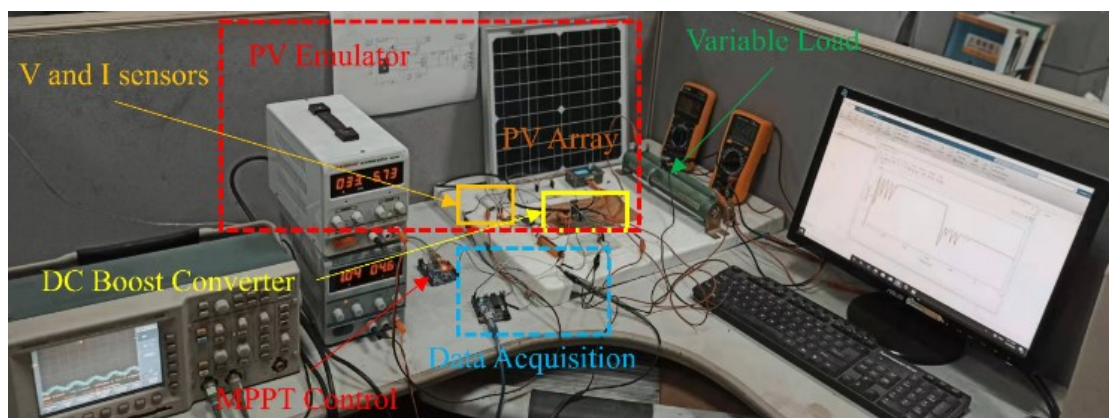
FIGURE 4.56: Experimental Setup for implementation of maximum power point tracking control

Cost-effective implementation of the MPPT technique is an important aspect but it depends upon the mathematical complexity of the technique. The competing technique like grasshopper optimization algorithm (GHO) has complex random walks like Levy flight and other complex functions which are very difficult to implement on the low-cost microcontroller.
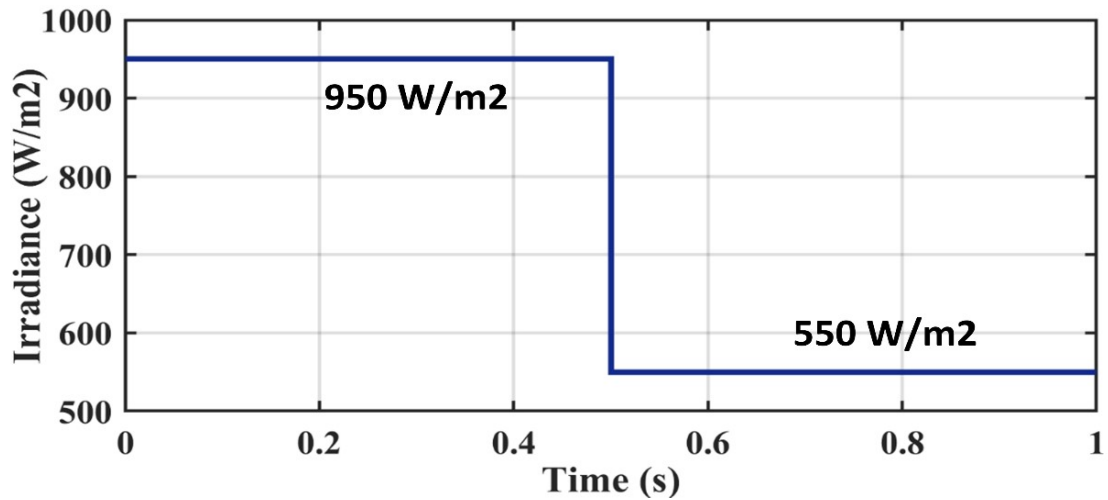
FIGURE 4.57: Test scenario for Experimental Setup
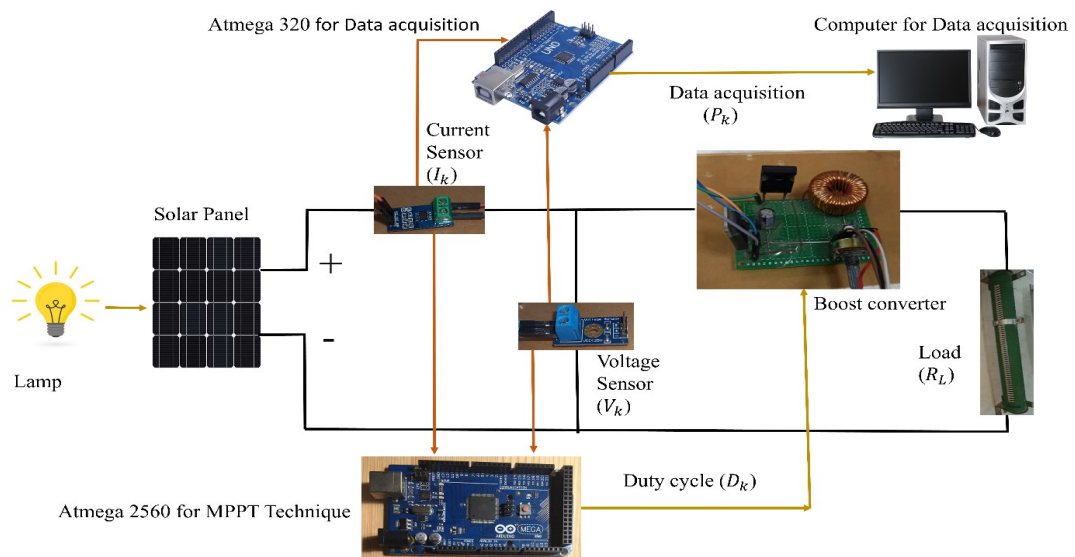
FIGURE 4.58: Implmentation of the experimental setup

The microcontroller required for GHO is STM32 controller whose price is 3000 PKR, as HGWOSCA has very less complex functions and can be implemented on Arduino NANO development board, whose price is 1100 PKR.

Therefore 3 times reduction in implementation cost can be observed. The experimental validation was also done using a low-cost PV emulator.
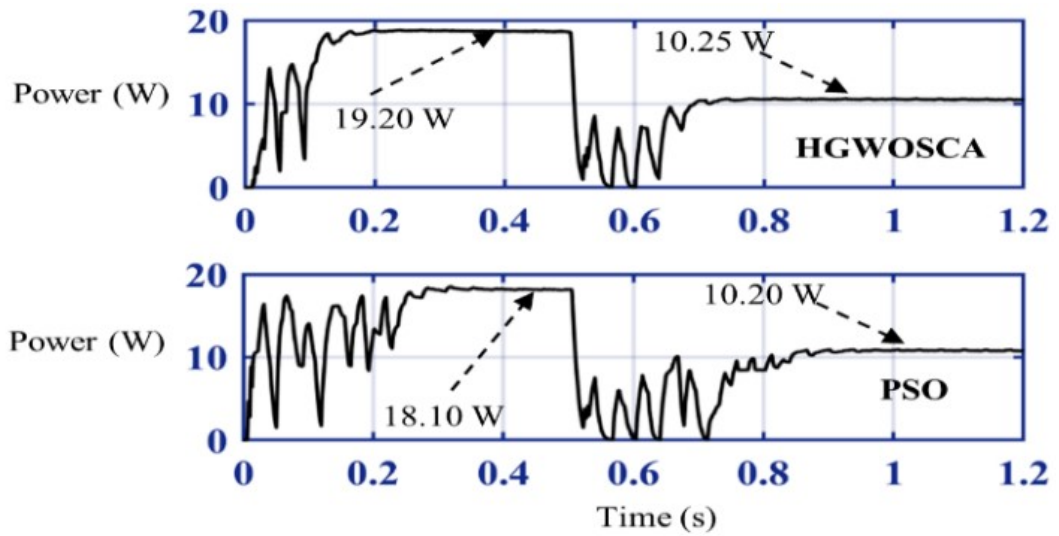
FIGURE 4.59: Experimental Results of Power Tracked by HGWOSCA and PSO
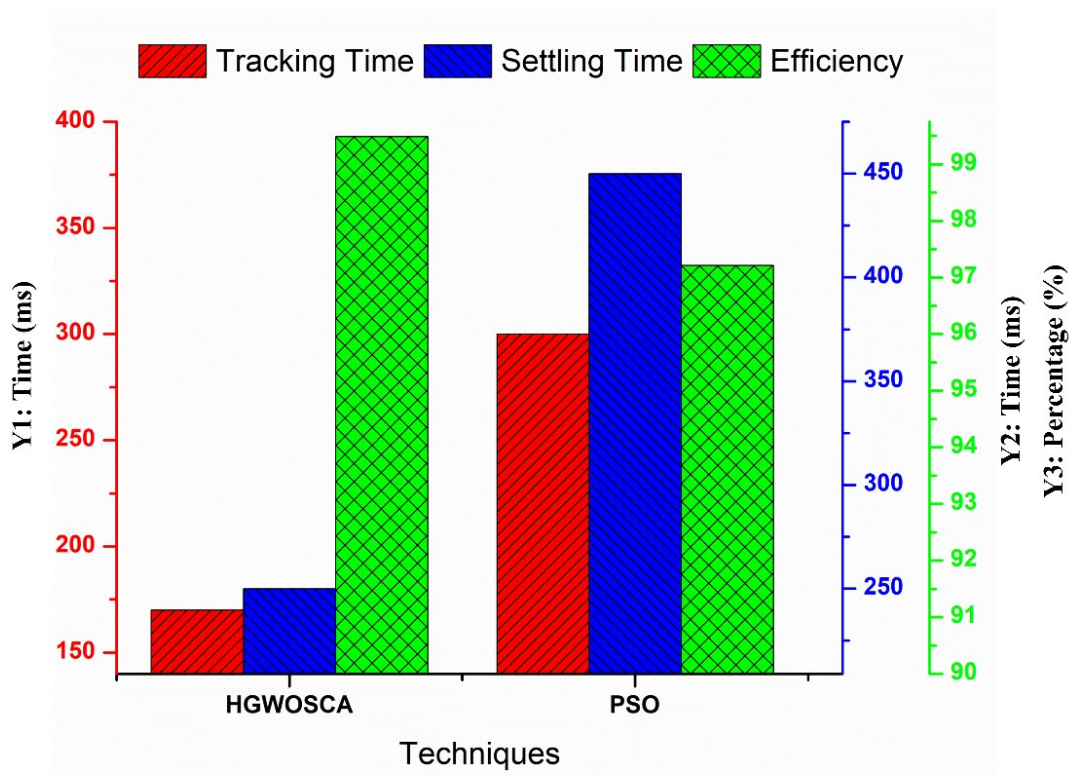
FIGURE 4.60: Evaluation Parameter for Experimental Setup

Figure 4.59 shows that HGWOSCA tracks higher power as compared to PSO and also required less time to settle at GMPP. The higher efficiency and less tracking time validate that the HGWOSCA MPPT technique is very effective for

implementation in real-time applications or the PV system. So, we can used that technique for MPPT control in real time applications for the PV system.

TABLE 4.6: Quantitative comparison of HGWOSCA with GHO, P&O, PSO, PSOGS and CS

Tech.	Case No.	Tracking Time (s)	Settling Time (s)	GM Located	Power at GM	Power Tracked (W)	Effie (%)
HGWOSCA	Case 1	0.16	0.24	Yes	1282	1280	99.84
	Case 2	0.15	0.22	Yes	335	334.7	99.91
	Case 3	0.16	0.23	Yes	702	701.5	99.92
	Case 4	0.17	0.26	Yes	921.2	921	99.97
	Case 1	0.19	0.35	Yes	1282	1279.9	99.82
	Case 2	0.16	0.51	Yes	335	334.6	99.88
GHO	Case 3	0.18	0.6	Yes	702	701.4	99.91
	Case 4	0.35	0.61	Yes	921.2	920.6	99.93
	Case 1	0.12	0.12	Yes	1282	1257	98.04
	Case 2	LM	LM	No	335	239.4	71.46
P & O	Case 3	LM	LM	No	702	301.5	42.91
	Case 4	LM	LM	No	921.2	500.1	54.28
	Case 1	0.32	0.45	Yes	1282	1278.5	99.72
	Case 2	0.3	0.75	Yes	335	334.5	99.85
PSO	Case 3	0.49	0.9	Yes	702	692	98.57
	Case 4	0.37	0.59	No	921.2	894.1	97.05
	Case 1	0.21	0.35	Yes	1282	1279.7	99.82
	Case 2	0.27	0.5	Yes	335	334.4	99.82
PSOGS	Case 3	0.26	0.7	Yes	702	701	99.85
	Case 4	0.47	0.71	Yes	921.2	910.6	98.84
	Case 1	0.35	0.55	Yes	1282	1278	99.68
	Case 2	0.3	0.64	Yes	335	334.5	99.85
CS	Case 3	0.31	0.72	Yes	702	700.8	99.82
	Case 4	0.29	0.5	No	921.2	859.1	93.25

4.10 Chapter Summary

In this chapter, the proposed MPPT technique is tested under different scenarios which include fast varying irradiance, partial shading conditions, and complex partial shading conditions. The comparison of the proposed technique is made between GHO, CSA, PSO, and PSOGS. The MPPT rating is calculated which verifies the superior performance of HGWOSCA. The proposed technique is also validated experimentally. Statistical analysis is carried out to check the performance of the proposed techniques.

Chapter 5

Conclusion and Future Work

In this chapter, a complete dissertation is summarized and future work is specified. The aim is to facilitate the research directions of interesting readers in the field of MPPT control of PV systems using SI techniques. Chapter 1 provided the introduction of renewable energy, utility, and future trends. Among various renewable resources, the importance of solar energy in the form of photovoltaic is established using technical data and projections. In chapter 2 a general review of the PV System is developed. Its components are briefly introduced and the effects of irradiance and temperature on the performance of the PV systems are studied. Chapters 2 also discuss about the MPPT techniques used in the literature and Chapter 3 present the contributions of the author in the field of MPPT of PV systems. In chapter 4 the performance of proposed MPPT technique is validated by simulating four different scenarios.

5.1   Contributions

The author contributed the following research work in this thesis

1. The importance of renewable energy is established and its significance is highlighted. The effects of PS are conceptualized for a better understanding of large-scale PV system power generation.

2. Extensive literature review is presented in which conventional, mahine learning based and swarm intelligence based MPPT techniques are discussed.

3. In this work author developed soft computing-based MPPT technique for a comprehensive comparison. A novel Swarm intelligence-based HGWOSCA MPPT control is implemented on the PV system, which produced better results as compared to particle swarm optimization (PSO), particle swarm optimization (PSOGS), grasshopper optimization (GHO), and cuckoo search algorithm (CSA) based MPPT techniques.

4. The outcomes verify that the proposed system has superior performance for tracking GM and reducing oscillations around MPP. Tracking efficiency of up to 99.9% and negligible oscillations are notable contributions in this field.

5. Proposed work is also implemented on Experimental Setup for the real-time validation of the MPPT control technique whose results also validates that the proposed MPPT technique can be implemented on the low-cost microcontroller and can be used in real-time applications

5.2 Future Work

This thesis initiated the work in the field of MPPT of PV systems under PS and CPS conditions by using the novel implementation of swarm intelligence-based techniques. The expertise and learning obtained by research work in this field highlighted several drawbacks and advantages in the field of PV systems MPPT control. Specifically, field studies, complex partial shading, and hardware components require much work to be done. There is a need to develop a standard environment, better counter checks and comprehensive models of such systems. Some future research directions are listed below

Complex partial shading will be studied further which shifts the entire GMPP region vigorously. It needs to be addressed as the operating point of the MPPT controller suddenly loses efficiency. CPS is yet another weather condition in which multiple closely associated LM appear in a cluster. This situation lowered the

efficiency and created a trade-off between computational power needed, time to track GMPP and cost-effectiveness of MPPT controllers. The proposed technique will also be implemented and integrated with the DC microgrid.

Bibliography

[1] Q. Ma, Z. Jia, L. Meng, J. Zhang, H. Zhang, W. Huang, J. Yuan, F. Gao, Y. Wan, Z. Zhang *et al.*, "Promoting charge separation resulting in ternary organic solar cells efficiency over 17.5%," *Nano Energy*, vol. 78, p. 105272, 2020.

[2] A. F. Mirza, M. Mansoor, Q. Ling, B. Yin, and M. Y. Javed, "A salp-swarm optimization based mppt technique for harvesting maximum energy from pv systems under partial shading conditions," *Energy Conversion and Management*, vol. 209, p. 112625, 2020.

[3] H. K. Mehta, H. Warke, K. Kukadiya, and A. K. Panchal, "Accurate expressions for single-diode-model solar cell parameterization," *IEEE Journal of Photovoltaics*, vol. 9, no. 3, pp. 803–810, 2019.

[4] D. Allam, D. Yousri, and M. Eteiba, "Parameters extraction of the three diode model for the multi-crystalline solar cell/module using moth-flame optimization algorithm," *Energy Conversion and Management*, vol. 123, pp. 535–548, 2016.

[5] G. Ciulla, V. L. Brano, V. Di Dio, and G. Cipriani, "A comparison of different one-diode models for the representation of i–v characteristic of a pv cell," *Renewable and Sustainable Energy Reviews*, vol. 32, pp. 684–696, 2014.

[6] M. Zagrouba, A. Sellami, M. Bouaïcha, and M. Ksouri, "Identification of pv solar cells and modules parameters using the genetic algorithms: Application to maximum power extraction," *Solar energy*, vol. 84, no. 5, pp. 860–866, 2010.

[7] A. F. Mirza, Q. Ling, M. Y. Javed, and M. Mansoor, "Novel mppt techniques for photovoltaic systems under uniform irradiance and partial shading," *Solar Energy*, vol. 184, pp. 628–648, 2019.

[8] M. H. Zafar, U. A. Khan, and N. M. Khan, "Hybrid grey wolf optimizer sine cosine algorithm based maximum power point tracking control of pv systems under uniform irradiance and partial shading condition," in *2021 4th International Conference on Energy Conservation and Efficiency (ICECE)*. IEEE, 2021, pp. 1–6.

[9] Y.-Y. Hong, A. A. Beltran Jr, and A. C. Paglinawan, "A robust design of maximum power point tracking using taguchi method for stand-alone pv system," *Applied energy*, vol. 211, pp. 50–63, 2018.

[10] B. R. Jogi, A. A. Kadle *et al.*, "A dc-dc buck converter for standalone solar dc microgrid system using perturb and observe mppt algorithm," in *2019 Global Conference for Advancement in Technology (GCAT)*. IEEE, 2019, pp. 1–5.

[11] E. Kabalci, G. Gokkus, and A. Gorgun, "Design and implementation of a pi-mppt based buck-boost converter," in *2015 7th International Conference on Electronics, Computers and Artificial Intelligence (ECAI)*. IEEE, 2015, pp. SG–23.

[12] A. Safari and S. Mekhilef, "Simulation and hardware implementation of incremental conductance mppt with direct control method using cuk converter," *IEEE transactions on industrial electronics*, vol. 58, no. 4, pp. 1154–1161, 2010.

[13] R. Bollipo, S. Mikkili, and P. Bonthagorla, "Hybrid optimization intelligent and classical pv mppt techniques," *CSEE Journal of Power and Energy Systems, Early Access*, 2019.

[14] A. M. Zador, "A critique of pure learning and what artificial neural networks can learn from animal brains," *Nature communications*, vol. 10, no. 1, pp. 1–7, 2019.

[15] A. Badis, M. N. Mansouri, and M. H. Boujmil, "A genetic algorithm optimized mppt controller for a pv system with dc-dc boost converter," in *2017 International Conference on Engineering & MIS (ICEMIS)*. IEEE, 2017, pp. 1–6.

[16] S. Z. Mirjalili, S. Mirjalili, S. Saremi, H. Faris, and I. Aljarah, "Grasshopper optimization algorithm for multi-objective optimization problems," *Applied Intelligence*, vol. 48, no. 4, pp. 805–820, 2018.

[17] S. Mirjalili, S. M. Mirjalili, and A. Lewis, "Grey wolf optimizer," *Advances in engineering software*, vol. 69, pp. 46–61, 2014.

[18] A. Chalh, A. El Hammoumi, S. Motahhir, A. El Ghzizal, U. Subramaniam, and A. Derouich, "Trusted simulation using proteus model for a pv system: Test case of an improved hc mppt algorithm," *Energies*, vol. 13, no. 8, p. 1943, 2020.

[19] M. Aneke and M. Wang, "Energy storage technologies and real life applications–a state of the art review," *Applied Energy*, vol. 179, pp. 350–377, 2016.

[20] N. Panwar, S. Kaushik, and S. Kothari, "Role of renewable energy sources in environmental protection: A review," *Renewable and sustainable energy reviews*, vol. 15, no. 3, pp. 1513–1524, 2011.

[21] W. Burns, "Loss and damage and the 21st conference of the parties to the united nations framework convention on climate change," *ILSA J. Int'l & Comp. L.*, vol. 22, p. 415, 2015.

[22] N. Aste, C. Del Pero, and F. Leonforte, "Pv technologies performance comparison in temperate climates," *Solar Energy*, vol. 109, pp. 1–10, 2014.

[23] P. Colter, B. Hagar, and S. Bedair, "Tunnel junctions for iii-v multijunction solar cells review," *Crystals*, vol. 8, no. 12, p. 445, 2018.

[24] S. Sugumar, D. P. Winston, and M. Pravin, "A novel on-time partial shading detection technique for electrical reconfiguration in solar pv system," *Solar Energy*, vol. 225, pp. 1009–1025, 2021.

[25] A. Amir, A. Amir, J. Selvaraj, N. A. Rahim, and A. M. Abusorrah, "Conventional and modified mppt techniques with direct control and dual scaled adaptive step-size," *Solar Energy*, vol. 157, pp. 1017–1031, 2017.

[26] C. H. Basha and C. Rani, "Performance analysis of mppt techniques for dynamic irradiation condition of solar pv," *International Journal of Fuzzy Systems*, vol. 22, no. 8, pp. 2577–2598, 2020.

[27] M. S. Nkambule, A. N. Hasan, A. Ali, J. Hong, and Z. W. Geem, "Comprehensive evaluation of machine learning mppt algorithms for a pv system under different weather conditions," *Journal of Electrical Engineering & Technology*, vol. 16, no. 1, pp. 411–427, 2021.

[28] S. H. Hanzaei, S. A. Gorji, and M. Ektesabi, "A scheme-based review of mppt techniques with respect to input variables including solar irradiance and pv arrays' temperature," *IEEE Access*, vol. 8, pp. 182 229–182 239, 2020.

[29] Z. Salam, J. Ahmed, and B. S. Merugu, "The application of soft computing methods for mppt of pv system: A technological and status review," *Applied energy*, vol. 107, pp. 135–148, 2013.

[30] G. Dileep and S. Singh, "Application of soft computing techniques for maximum power point tracking of spv system," *Solar Energy*, vol. 141, pp. 182–202, 2017.

[31] A. Ali, K. Almutairi, M. Z. Malik, K. Irshad, V. Tirth, S. Algarni, M. Zahir, S. Islam, M. Shafiullah, N. K. Shukla *et al.*, "Review of online and soft computing maximum power point tracking techniques under non-uniform solar irradiation conditions," *Energies*, vol. 13, no. 12, p. 3256, 2020.

[32] F. Ghani, G. Rosengarten, M. Duke, and J. Carson, "The numerical calculation of single-diode solar-cell modelling parameters," *Renewable Energy*, vol. 72, pp. 105–112, 2014.

[33] X. Gao, Y. Cui, J. Hu, G. Xu, and Y. Yu, "Lambert w-function based exact representation for double diode model of solar cells: Comparison on fitness

and parameter extraction," *Energy conversion and management*, vol. 127, pp. 443–460, 2016.

[34] V. Khanna, B. Das, D. Bisht, P. Singh *et al.*, "A three diode model for industrial solar cells and estimation of solar cell parameters using pso algorithm," *Renewable Energy*, vol. 78, pp. 105–113, 2015.

[35] H. Kawamura, K. Naka, N. Yonekura, S. Yamanaka, H. Kawamura, H. Ohno, and K. Naito, "Simulation of i–v characteristics of a pv module with shaded pv cells," *Solar Energy Materials and Solar Cells*, vol. 75, no. 3-4, pp. 613–621, 2003.

[36] J. Ahmed and Z. Salam, "An improved method to predict the position of maximum power point during partial shading for pv arrays," *IEEE Transactions on Industrial Informatics*, vol. 11, no. 6, pp. 1378–1387, 2015.

[37] M. Mansoor, A. F. Mirza, and Q. Ling, "Harris hawk optimization-based mppt control for pv systems under partial shading conditions," *Journal of Cleaner Production*, vol. 274, p. 122857, 2020.

[38] H. Labar and M. S. Kelaiaia, "Real time partial shading detection and global maximum power point tracking applied to outdoor pv panel boost converter," *Energy Conversion and Management*, vol. 171, pp. 1246–1254, 2018.

[39] S. Jana, N. Kumar, R. Mishra, D. Sen, and T. K. Saha, "Development and implementation of modified mppt algorithm for boost converter-based pv system under input and load deviation," *International Transactions on Electrical Energy Systems*, vol. 30, no. 2, p. e12190, 2020.

[40] S. E. Babaa, G. El Murr, F. Mohamed, S. Pamuri *et al.*, "Overview of boost converters for photovoltaic systems," *Journal of Power and Energy Engineering*, vol. 6, no. 04, p. 16, 2018.

[41] P. Shaw, "Modelling and analysis of an analogue mppt-based pv battery charging system utilising dc–dc boost converter," *IET Renewable Power Generation*, vol. 13, no. 11, pp. 1958–1967, 2019.

[42] R. Ayop and C. W. Tan, "Design of boost converter based on maximum power point resistance for photovoltaic applications," *Solar Energy*, vol. 160, pp. 322–335, 2018.

[43] Z. Li, Y. Yuan, and H.-N. Wang, "Fuzzy adaptive time-delay feedback controlling chaos in buck converter," in *2020 Chinese Control And Decision Conference (CCDC)*. IEEE, 2020, pp. 4732–4737.

[44] M. Saoudi, A. El-Sayed, and H. Metwally, "Design and implementation of closed-loop control system for buck converter using different techniques," *IEEE Aerospace and Electronic Systems Magazine*, vol. 32, no. 3, pp. 30–39, 2017.

[45] M. R. Banaei and H. Ajdar Faeghi Bonab, "High-efficiency transformerless buck–boost dc–dc converter," *International Journal of Circuit Theory and Applications*, vol. 45, no. 8, pp. 1129–1150, 2017.

[46] R. K. Subroto, L. Ardhenta, and K.-L. Lian, "Observer based adaptive pi sliding mode controller for cuk converter," in *2019 6th International Conference on Instrumentation, Control, and Automation (ICA)*. IEEE, 2019, pp. 82–87.

[47] H. A. Sher, A. F. Murtaza, A. Noman, K. E. Addoweesh, K. Al-Haddad, and M. Chiaberge, "A new sensorless hybrid mppt algorithm based on fractional short-circuit current measurement and p&o mppt," *IEEE Transactions on sustainable energy*, vol. 6, no. 4, pp. 1426–1434, 2015.

[48] D. Baimel, S. Tapuchi, Y. Levron, and J. Belikov, "Improved fractional open circuit voltage mppt methods for pv systems," *Electronics*, vol. 8, no. 3, p. 321, 2019.

[49] M. Abdel-Salam, M.-T. El-Mohandes, and M. Goda, "An improved perturb-and-observe based mppt method for pv systems under varying irradiation levels," *Solar Energy*, vol. 171, pp. 547–561, 2018.

[50] S. Necaibia, M. S. Kelaiaia, H. Labar, A. Necaibia, and E. D. Castronuovo, "Enhanced auto-scaling incremental conductance mppt method, implemented

on low-cost microcontroller and sepic converter," *Solar Energy*, vol. 180, pp. 152–168, 2019.

[51] M. S. Bouakkaz, A. Boukadoum, O. Boudebbouz, I. Attoui, N. Boutasseta, and A. Bouraiou, "Fuzzy logic based adaptive step hill climbing mppt algorithm for pv energy generation systems," in *2020 International Conference on Computing and Information Technology (ICCIT-1441)*. IEEE, 2020, pp. 1–5.

[52] U. Chauhan, A. Rani, B. Kumar *et al.*, "A modified incremental conductance maximum power point technique for standalone pv system," in *2020 7th International Conference on Signal Processing and Integrated Networks (SPIN)*. IEEE, 2020, pp. 61–64.

[53] X. Yue, D. Geng, Q. Chen, Y. Zheng, G. Gao, and L. Xu, "2-d lookup table based mppt: Another choice of improving the generating capacity of a wave power system," *Renewable Energy*, vol. 179, pp. 625–640, 2021.

[54] Ž. Zečević and M. Rolevski, "Neural network approach to mppt control and irradiance estimation," *Applied Sciences*, vol. 10, no. 15, p. 5051, 2020.

[55] Y. Li, S. Samad, F. W. Ahmed, S. S. Abdulkareem, S. Hao, and A. Rezvani, "Analysis and enhancement of pv efficiency with hybrid msfla–flc mppt method under different environmental conditions," *Journal of Cleaner Production*, vol. 271, p. 122195, 2020.

[56] Z. M. Ali, N. V. Quynh, S. Dadfar, and H. Nakamura, "Variable step size perturb and observe mppt controller by applying θ-modified krill herd algorithm-sliding mode controller under partially shaded conditions," *Journal of Cleaner Production*, vol. 271, p. 122243, 2020.

[57] K. P. Panda, A. Anand, P. R. Bana, and G. Panda, "Novel pwm control with modified pso-mppt algorithm for reduced switch mli based standalone pv system," *International Journal of Emerging Electric Power Systems*, vol. 19, no. 5, 2018.

[58] F.-S. Pai and P.-S. Tseng, "An efficient gwo mppt for a pv system using impedance information acceleration," *International Journal of Electronics*, vol. 106, no. 4, pp. 648–661, 2019.

[59] M. Ebrahim, A. Osama, K. M. Kotb, and F. Bendary, "Whale inspired algorithm based mppt controllers for grid-connected solar photovoltaic system," *Energy Procedia*, vol. 162, pp. 77–86, 2019.

[60] D. A. Nugraha, K.-L. Lian *et al.*, "A novel mppt method based on cuckoo search algorithm and golden section search algorithm for partially shaded pv system," *Canadian Journal of Electrical and Computer Engineering*, vol. 42, no. 3, pp. 173–182, 2019.

[61] M. Mansoor, A. F. Mirza, Q. Ling, and M. Y. Javed, "Novel grass hopper optimization based mppt of pv systems for complex partial shading conditions," *Solar Energy*, vol. 198, pp. 499–518, 2020.

[62] F. D. Murdianto, A. R. Nansur, and A. S. L. Hermawan, "Modeling and simulation of mppt coupled inductor sepie converter using flower pollination algorithm (fpa) method in dc mierogrid system," in *2017 International Electronics Symposium on Engineering Technology and Applications (IES-ETA)*. IEEE, 2017, pp. 7–13.

[63] M. Lasheen, A. K. A. Rahman, M. Abdel-Salam, and S. Ookawara, "Adaptive reference voltage-based mppt technique for pv applications," *IET Renewable Power Generation*, vol. 11, no. 5, pp. 715–722, 2017.

[64] A. Voulodimos, N. Doulamis, A. Doulamis, and E. Protopapadakis, "Deep learning for computer vision: A brief review," *Computational intelligence and neuroscience*, vol. 2018, 2018.

[65] U. Hasson, S. A. Nastase, and A. Goldstein, "Direct fit to nature: An evolutionary perspective on biological and artificial neural networks," *Neuron*, vol. 105, no. 3, pp. 416–434, 2020.

[66] D. Stursa and P. Dolezel, "Comparison of relu and linear saturated activation functions in neural network for universal approximation," in *2019 22nd International Conference on Process Control (PC19)*. IEEE, 2019, pp. 146–151.

[67] A. U. Rehman, L. Khan, Q. Khan, and F. W. Karam, "Grnn based higher order sliding mode mppt control paradigms for standalone pv system," in *2019 15th International Conference on Emerging Technologies (ICET)*. IEEE, 2019, pp. 1–6.

[68] S. Balraj and A. Ganesan, "Performance analysis of bldc generator power maximization using pi and fuzzy logic controller."

[69] M. Aly and H. Rezk, "A mppt based on optimized flc using manta ray foraging optimization algorithm for thermo-electric generation systems," *International Journal of Energy Research*, 2021.

[70] W. Mu, Y. Wang, H. Sun, and G. Liu, "Double-loop sliding mode controller with an ocean current observer for the trajectory tracking of rov," *Journal of Marine Science and Engineering*, vol. 9, no. 9, p. 1000, 2021.

[71] R. B. Bollipo, S. Mikkili, and P. K. Bonthagorla, "Critical review on pv mppt techniques: classical, intelligent and optimisation," *IET Renewable Power Generation*, vol. 14, no. 9, pp. 1433–1452, 2020.

[72] C. Cartis and L. Roberts, "A derivative-free gauss–newton method," *Mathematical Programming Computation*, vol. 11, no. 4, pp. 631–674, 2019.

[73] F. Marini and B. Walczak, "Particle swarm optimization (pso). a tutorial," *Chemometrics and Intelligent Laboratory Systems*, vol. 149, pp. 153–165, 2015.

[74] W. Hayder, E. Ogliari, A. Dolara, A. Abid, M. Ben Hamed, and L. Sbita, "Improved pso: a comparative study in mppt algorithm for pv system control under partial shading conditions," *Energies*, vol. 13, no. 8, p. 2035, 2020.

[75] N. Priyadarshi, M. S. Bhaskar, S. Padmanaban, F. Blaabjerg, and F. Azam, "New cuk–sepic converter based photovoltaic power system with hybrid gsa–pso algorithm employing mppt for water pumping applications," *IET Power Electronics*, vol. 13, no. 13, pp. 2824–2830, 2020.

[76] A. H. Gandomi, X.-S. Yang, and A. H. Alavi, "Cuckoo search algorithm: a metaheuristic approach to solve structural optimization problems," *Engineering with computers*, vol. 29, no. 1, pp. 17–35, 2013.

[77] M. Prabukumar, L. Agilandeeswari, and K. Ganesan, "An intelligent lung cancer diagnosis system using cuckoo search optimization and support vector machine classifier," *Journal of Ambient Intelligence and Humanized Computing*, vol. 10, no. 1, pp. 267–293, 2019.

[78] X.-N. Wang, Y.-J. Feng, and Z.-R. Feng, "Ant colony optimization for image segmentation," in *2005 international conference on machine learning and cybernetics*, vol. 9. IEEE, 2005, pp. 5355–5360.

[79] K. Sundareswaran, V. Vigneshkumar, P. Sankar, S. P. Simon, P. S. R. Nayak, and S. Palani, "Development of an improved p&o algorithm assisted through a colony of foraging ants for mppt in pv system," *IEEE transactions on industrial informatics*, vol. 12, no. 1, pp. 187–200, 2015.

[80] D. Karaboga and B. Akay, "A comparative study of artificial bee colony algorithm," *Applied mathematics and computation*, vol. 214, no. 1, pp. 108–132, 2009.

[81] S. Padmanaban, N. Priyadarshi, M. S. Bhaskar, J. B. Holm-Nielsen, V. K. Ramachandaramurthy, and E. Hossain, "A hybrid anfis-abc based mppt controller for pv system with anti-islanding grid protection: Experimental realization," *IEEE Access*, vol. 7, pp. 103 377–103 389, 2019.

[82] F. C. NK and S. D. K. Viswanatha, "Routing algorithm using mobile agents and genetic algorithm," *International Journal of Computer and Electrical Engineering*, vol. 1, no. 3, pp. 1793–8163, 2009.

[83] A. A. Kulaksız and R. Akkaya, "A genetic algorithm optimized ann-based mppt algorithm for a stand-alone pv system with induction motor drive," *Solar Energy*, vol. 86, no. 9, pp. 2366–2375, 2012.

[84] S. Mirjalili, "Sca: a sine cosine algorithm for solving optimization problems," *Knowledge-based systems*, vol. 96, pp. 120–133, 2016.

[85] S. Padmanaban, N. Priyadarshi, J. B. Holm-Nielsen, M. S. Bhaskar, F. Azam, A. K. Sharma, and E. Hossain, "A novel modified sine-cosine optimized mppt algorithm for grid integrated pv system under real operating conditions," *Ieee Access*, vol. 7, pp. 10 467–10 477, 2019.

[86] I. Shams, S. Mekhilef, and K. S. Tey, "Improved-team-game-optimization-algorithm-based solar mppt with fast convergence speed and fast response to load variations," *IEEE Transactions on Industrial Electronics*, vol. 68, no. 8, pp. 7093–7103, 2020.

[87] M. H. Zafar, U. A. Khan, and N. M. Khan, "A sparrow search optimization algorithm based mppt control of pv system to harvest energy under uniform and non-uniform irradiance," in *2021 International Conference on Emerging Power Technologies (ICEPT)*. IEEE, 2021, pp. 1–6.